INSIGHTS OF CHEMICAL, CULTURAL AND GENETIC EXPLORATION FOR SOYBEAN SUDDEN DEATH SYNDROME MANAGEMENT, AND FUSARIUM VIRGULIFORME

By

Amy Marie Baetsen-Young

A DISSERTATION

Submitted to
Michigan State University
in partial fulfillment of the requirements
for the degree of

Plant Pathology – Doctor of Philosophy

2019

ABSTRACT

INSIGHTS OF CHEMICAL, CULTURAL AND GENETIC EXPLORATION FOR SOYBEAN SUDDEN DEATH SYNDROME MANAGEMENT, AND FUSARIUM VIRGULIFORME

By

Amy Marie Baetsen-Young

Soybean sudden death syndrome, caused by *Fusarium virguliforme*, is a key limitation in reaching soybean (*Glycine max*) yield potential, stemming from limited disease management through cultural practices and partial host resistance. The research within this thesis reveals the economic potential of fungicide seed treatment SDS fluopyram to alleviate yield loss, provides insights into field management of *F. virguliforme* and highlights transcriptomic plasticity of diverse host-fungal interactions. Previously, farm level studies have found the fungicide seed treatment of fluopyram profitable, yet the benefit across an aggregate level of soybean production at risk to SDS yield loss is unknown. To estimate economic benefits of fluopyram adoption in SDS at risk acres, in the light of U.S public research and outreach costs, an economic surplus approach was applied to calculate *ex ante* net benefits from 2018 to 2032. Through this framework of fluopyram adoption for alleviation of SDS associated yield losses, we estimated a net benefit of $5,829 million over 15 years, considering public seed treatment research costs from 2014 to present and future extension communication. While chemical seed treatments aid disease management of SDS, the ability of this pathogen to colonize asymptomatic hosts may increase the prevalence of *F. virguliforme*. Thus, the impact of cultural tactics upon *F. virguliforme* colonization of an asymptomatic host, and the ability of this colonization to alter subsequent SDS symptoms when rotated to soybean were explored. The exploration of tillage, and residue management across four U.S. states provided clarity to variable reports, revealing that no-tillage inconsistently enhances *F.*

virguliforme colonization of corn and soybean roots, while corn residue did not alter pathogen colonization. Alternatively, an asymptomatic host provides a unique application to discover genetic factors facilitating soybean sudden death syndrome through investigation host-fungal interactions. Exploring this plant disease through a comparative orthologous mRNA-Seq on soybean and corn hosts under colonization of *F. virguliforme* uncovered transcriptional responses enabling a robust defense response in corn, and delayed immune induction within soybean permitting pathogenic colonization and susceptibility. To colonize both hosts, *F. virguliforme* exhibited a massive transcriptional rewiring of an infection program. Transcriptomic responses suggest, *F. virguliforme* is less suited for colonization of monocots by delayed colonization, and lower induction of CAZymes and effector proteins. Integration of the data generated through the mRNA-Seq experiments, including a micro-like RNA-Seq analysis of soybean host during colonization by *F. virguliforme* revealed an intimate communication between the plant and fungal pathogen; we posit that a micro-like RNA cross-talk potentially regulates host susceptibility. Overall, several hypotheses were generated surrounding hemibiotrophic enhancement of host senescence, and fungal ecological plasticity through transcriptomic reprogramming, which will deliver transparency upon a currently difficult and enigmatic syndrome.

I would like to dedicate this dissertation to my husband Stephen Young, who has encouraged and supported me to chase my dreams no matter the distance.

ACKNOWLEDGMENTS

I would like to acknowledge my advisor, Dr. Brad Day for providing me with academic freedom and guidance throughout the last four years.

I would also like to thank my committee members, Dr. Shinhan Shiu, Dr. Scott Swinton, and Dr. Martin Chilvers, for their support and advice throughout my dissertation research. I would also thank Dr. Jennifer Wai for teaching me the ways of genomics and Dr. Kevin Childs for bioinformatics support and collaboration. Also, I must thank Adam Byrne and Janette Jacobs for collaboration and support during my field studies. Finally, I would like to thank Drs. Daren Muller, Kiersten Wise, Yuba Kandel, Grazieli Araldi Da Silva, Damon Smith for collaboration, support and incorporation in to the field crops pathology community.

I would like to thank Michigan State University for supporting me through a Plant Science Fellowship, C. S. Mott Foundation and for research support through Project GREEN. I would also like to thank the Plant Resilience Institute for in part funding this research.

I would like to thank all of my lab mates who have supported me throughout the years including Alex Corrion, Yi-Ju Lu, Pai Li, Miranda Haus, Saroopa Samaradivakara, Masaki Shimono, and Judy Chen. Finally, I would also like to thank the members of the fourth floor Molecular Plant Sciences, for entertaining my thoughts and providing a delightful work atmosphere.

TABLE OF CONTENTS

LIST OF TABLES

LIST OF FIGURES

CHAPTER 1

Literature Review

Introduction

Soybean is a leading annual crop, accounting for 35% of global harvestable acreage planted for oil crops (Thoenes, 2015). The sub-products of meal and oil from this crop are highly valuable, in large part stemming from wide use for food consumption and animal feed. Soybean production is primarily highly geographically concentrated in Argentina, Brazil, China, and the United States (Thoenes, 2015). For example, in the U.S. in 2018, soybean was the most planted crop, at 88 million acres planted (NASS, 2018). Within increased acreage, comes the potential for increased exposure to diseases to incur yield losses. Soybean cyst nematode (*Heterodera glycines*) was the most destructive pathogen from 2010 to 2014, causing between 90 to 112 million bushels of soybean to be lost annually (Allen, 2017). The top three fungal diseases within soybean from 2010-2014 included seedling diseases of *Rhizoctonia* spp., *Fusarium* spp., *Phomopsis* spp. and, or *Pythium* spp., an Oomycete; soybean sudden death syndrome caused by *Fusarium virguliforme;* and charcoal rot caused by *Macrophomina phaseolina* caused an average of 134.2 million blushes of soybean production lost annually in the U.S. (Allen et al., 2017). These yield losses highlight the need for successful management strategies to enable soybean production to reach maximum yield potential.

Soybean Sudden Death Syndrome

Soybean sudden death syndrome (SDS) is a devastating disease with an estimated impact of >$330 million dollars in the U. S. (Koenning et al., 2010). Since the first report in the 1970's

in Arkansas, soybean SDS has quickly spread to nearly all soybean producing states, including Michigan in 2009 (Figure 1). In North America, soybean SDS is caused by the soil borne fungus *Fusarium virguliforme* and *F. brasiliense,* while in South America, an additional two closely related species (e.g., *F. tucumaniae*, and *F. cuneirostrum)* have also been identified as possible casual agents within the *F. solani* species complex 2 (FSSC2) (O'Donnell et al., 2010; Wang et al., 2019b). The *F. solani* species complex (FSSC) has been the most comprehensively studied group of plant pathogens (Coleman, 2015). Within the FSSC, over 60 phylogenetically distinct species have been identified and are thought to arose over the last 55 million years (Ma et al., 2013) which have been further characterized into *formae speciales* (f. sp.) by host specificity (Coleman, 2015).

In the United States, *F. virguliforme* is an asexual hemibiotrophic fungus, infesting soil and crop residues. This fungus infects soybean roots during the early plant developmental stages (Jin et al., 1996) colonizing the xylem tissues, where the pathogen secretes phytotoxins, which then degrade rubisco-1,5-bisphosphate carboxylase oxygenase, initiating programmed cell death of the soybean leaf through an accumulation of oxygen radicals (Brar et al., 2011). The host response creates a characteristic symptom of interveinal leaf scorch associated with SDS (Figure 2). Root infection and leaf scorch leads to a reduction of overall plant biomass, flowering and pod loss, and thus yield. Yield losses of up to 80% have been reported in highly infested fields, but typically yield losses of 5 to 15% are observed (Hershman et al., 1990; Roy,1997). As the plant matures below ground, *F. virguliforme* will degrade soybean root tissue and cause tap and lateral root necrosis, decreasing root biomass. As the plant senesceses, *F. virguliforme* may produce characteristically blue asexual

spore mass (sporodochia) externally on soybean roots, which enables re-infestation of the soil (Roy, 1997).

Development of soybean SDS is affected by environmental and biotic factors. Environmental conditions inducing high disease intensity are cool temperatures and wet compacted soil during planting, and increased soil moisture during early reproductive growth stages (Rupe, 1989; Roy et al., 1997; Scherm and Yang, 1999; Chong et al., 2005). These conditions are thought to favor fungal infection, while slowing plant growth and development. Furthermore, the interaction of soybean cyst nematode (*Heterodera glycines*) with *F. virguliforme* has been observed to synergistically promote SDS severity and incidence (Gao et al., 2006; Westphal et al., 2014), yet the underlying mechanism enhancing this interaction remains unknown. genetic strategies.

SDS Management

At present, no single strategy can fully manage SDS. Partial genetic resistance of soybean cultivars has been developed through quantitative trait loci. However, if disease pressure is high in soybean fields, the partial resistance is broken (Njiti et al., 1996). Tillage is thought to reduce symptom development by decreasing soil moisture and increasing soil temperature (Roy et al., 1997; Vick et al., 2003). An additional strategy for field crop disease management is crop rotation, which reduces pathogen population within soils by planting non-hosts for multiple years (Agrios, 2004). Previous research on corn (*Zea mays* L.), soybean, and wheat (*Triticum aestivum* L.) rotation was found to reduce SDS yield losses

when compared to continuous soybean (Von Qualen et al., 1989; Roy et al., 1997). However, more recent studies have shown corn and other crop rotations have not reduced SDS severity (Hershman, 2003; Xing and Westphal, 2009; Leandro et al., 2018). Therefore, to prevent the development and subsequent yield loss, an integrated pest management approach to control SDS through chemical, cultural, and genetic strategies is needed.

Chemical Management

Because cultural approaches and limited genetic resistance have not consistently mitigated SDS associated yield loss, a fungicidal strategy was recently explored. As initial infection occurs below ground, seed treatment application of SDS-specific fungicide (i.e., fluopyram) was developed; fluopyram targets succinate dehydrogenase (SDH) – complex II of the mitochondrial respiration chain – associated with the mitochondrial electron transport (Keon et al., 1991; Fraaije et al., 2012). In multiple studies, fluopyram was found to reduce soybean foliar symptoms and improve yields under SDS pressure in comparison to commercial base seed treatments of insecticide, fungicide and nematicide (Kandel et al., 2016; Gaspar et al., 2017; Kandel et al., 2018b; Kandel et al., 2018a; Kandel et al., 2019a). These reported yield gains from fluopyram have ranged from 2.8% to 12.0% in fields with a historical SDS pressure (Kandel et al., 2016; Gaspar et al., 2017; Kandel et al., 2018b; Kandel et al., 2018a; Kandel et al., 2019a). While several additional products containing fungicidal activity are registered for foliar application to manage SDS development, recent research has revealed that only fluopyram provided a reduction of root rot and foliar symptoms when compared commercial base for currently registered foliar products (Kandel et al., 2019a).

Cultural Management

In annual row crop production systems, such as soybean, the application of several cultural practices can reduce disease development. Tillage of soil was thought to reduce root infection by *F. virguliforme* from decreasing soil moisture and increasing soil temperature through increased porosity of the soil (Roy et al., 1997; Vick et al., 2003). Yet, recent exploration through long-term tillage and no-till management revealed that alteration of these practices did not impact soybean root and foliar SDS disease severity or yield loss (Kandel et al., 2019a). Additionally, infected soybean roots from no-till fields supported summer level CFUs of *F. virguliforme* through the fallow season, whereas soil did not harbor detectable CFUs of *F. virguliforme* to spring (Luo et al., 2001), suggesting residue, especially in no-till fields may promote disease development. Through inoculated field and greenhouse experiments Navi and Yang (2016) explored this hypothesis that plant residue contributes to *F. virguliforme* populations and found that corn (*Zea mays*) kernel residue increases soil CFUs of *F. virguliforme* at three- and 12-months post treatment establishment. Corn residue colonization by *F. virguliforme*, also indicates corn maybe able to support *F. virguliforme*, and therefore may support this soybean fungal pathogen through crop rotations of corn to soybean. Field studies spanning three decades of research have not resolved if corn is an asymptomatic host of F*. virguliforme* (Von Qualen et al., 1989; Roy et al., 1997 Hershman, 2003; Xing and Westphal, 2009; Leandro et al., 2018). Similarily, greenhouse studies have found root colonization by *F. virguliforme*, however, contrasting conclusions regarding the asymptomatic host status of corn (Kolander et al., 2012; Kobayashi-Leonel et al., 2017). Therefore, inconsistencies persist within the research community regarding whether corn is

an asymptomatic host of *F. virguliforme* and if crop rotation of corn and soybean enhances or reduces the severity of SDS.

Genetic Management

Host resistance to *F. virguliforme* would prevent pathogen colonization and SDS symptom development. However, over 80 quantitative trait loci (QTL) and many single nucleotide polymorphisms (SNPs) have been discovered in association with phenotypic resistance to SDS, suggesting genetic resistance to SDS highly complex (Chang et al., 2018). The diverse methodology applied to decipher QTL and SNPs has further complicated resolution of genetic loci, as several techniques apply laboratory screening germplasm in a manner distinct from field trials. In total, these methods often do not take into consideration the biotic and abiotic factors enabling disease development, which in turn promote the discovery of loci tied to foliar resistance, and not root resistance to *F. virguliforme* (Chang et al., 2018 and Kazi et al., 2008). Although these traits are tied to reducing above ground symptom development, breeding genetically resistant varieties have produced soybeans with partial resistance to SDS (Kandel et al., 2016; Kandel et al., 2017). More recently, efforts have focused upon root colonization by *F. virguliforme* and root symptom development, as field studies have revealed dis-correlation between root and foliar symptomology development (Wang et al., 2019). Phenotyping below ground root symptoms across a soybean diversity panel discovered 13 putative SDS resistance genes associated with foliar and root rot resistance for SDS (Swaminathan et al., 2018). Future introgression of these loci may assist

with developing cultivars with greater resistance to root and foliar components of SDS than current commercial cultivars.

Exploration of transcriptomic expression tied to disease development and soybean susceptibility have uncovered potential loci that are modulated during infection and root necrosis development, when comparing *F. virguliforme* inoculated and mock inoculated single cultivars (Ngaki et al., 2016). Transgenic overexpression of an ankyrin repeat containing proteins discovered through this transcriptomic approach elevated SDS resistance. This suggests comparative transcriptomics during infection by *F. virguliforme* may yield novel genes tied to susceptibility, which can be employed resistance.

Conclusions

Fusarium virguliforme is a causal agent for soybean sudden death syndrome (SDS), a destructive soil-borne fungal disease. Since the first report in the 1970's in Arkansas, soybean SDS has quickly spread to nearly all soybean producing states, highlighting the need for integrated disease management to mitigate yield losses. Through Chapter 2 of this dissertation, I developed a framework to evaluate economic returns of public research and outreach investment surrounding grower adoption of a *F. virguliforme* seed treatment fungicide: fluopyram. This framework enabled parameterization of economic SDS incidence and grower adoption of fluopyram at national level, to estimate economic impacts of SDS over 15 years and the alleviation of SDS associated yield losses by fluopyram, which has only been researched at the farm gate level prior.

Multiple approaches are likely necessary to manage this complex disease. To this end, I also explored the integration of tillage and corn residue management to alter *F. virguliforme* colonization of soybean roots and an asymptomatic host of corn in Chapter 3. These field studies across the North Central region of the U.S. revealed that corn is an asymptomatic host of *F. virguliforme,* yet this host's residue does not alter *F. virguliforme* root colonization of either soybean or corn. Additionally, manipulating the soil environment through tillage or no-till did not consistently change root colonization of soybean and corn, suggesting implications of tillage management upon *F. virguliforme* root colonization is soil- or site-specific.

The development of SDS starts within the genetic capacity of the host to be susceptible, thus a resistant host would prevent F*. virguliforme* infection and lessen the dependency up on fungicide chemistries and cultural management. Through a comparative transcriptomic approach of a symptomatic host and asymptomatic host under *F. virguliforme* colonization in Chapter 4, I revealed transcriptional responses enabling a robust defense response in corn and delayed immune induction within soybean permitting pathogenic colonization and susceptibility. Additionally, as described in Chapter 5, evaluation of the fungal transcriptomic response to two diverged hosts identified that *F. virguliforme* can manipulate its genetic repertoire to enable colonization of hosts with distinct phenotypic outcomes.

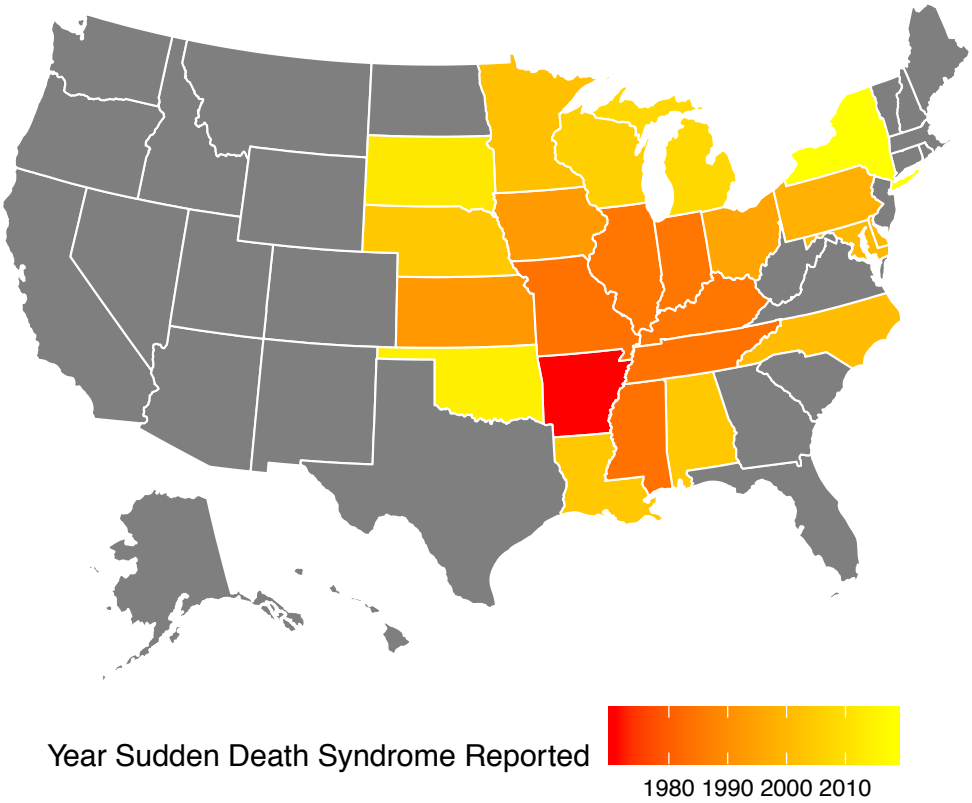

Figure 1. Distribution of soybean sudden death syndrome, since first report in Arkansas in 1971. Transition in color denotes decade change.

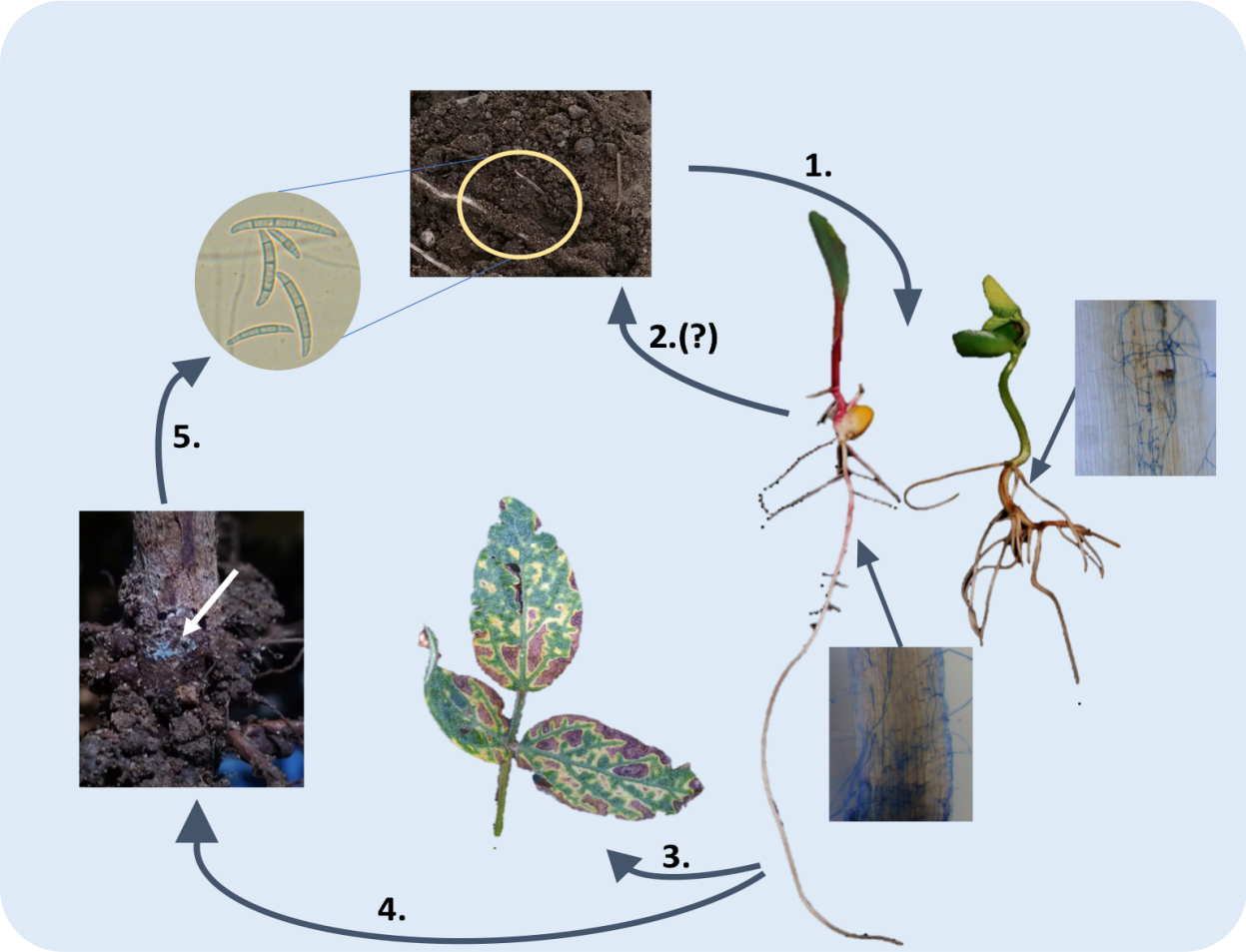

Figure 2. *Fusarium virguliforme* disease cycle. 1. Macroconidia, microconidia and chlamydospores infested within soil, germinate and colonize roots of soybean and corn, causing rot and necrosis in soybean, but is non-symptomatic corn. 2. Colonized corn roots may enable pathogen persistence in the soil. 3. *F. virguliforme* releases toxins within the soybean xylem causing foliar chlorosis and necrosis. 4. Pathogen sporulation on soybean roots, which, 5. re-infests soil with macroconidia, microconidia and chlamydospores.

REFERENCES

REFERENCES

Agrios, G.N. (2004). Plant pathology. (San Diego: Elsevier Academic Press).

Allen, T.W., Bradley, C.A., Sisson, A.J., Byamukama, E., Chilvers, M.I., Coker, C.M., Collins, A.A., Damicone, J.P., Dorrance, A.E., Dufault, N.S., Esker, P.D., Faske, T.R., Giesler, L.J., Grybauskas, A.P., Hershman, D.E., Hollier, C.A., Isakeit, T., Jardine, D.J., Kelly, H.M., Kemerait, R.C., Kleczewski, N.M., Koenning, S.R., Kurle, J.E., Malvick, D.K., Markell, S.G., Mehl, H.L., Mueller, D.S., Mueller, J.D., Mulrooney, R.P., Nelson, B.D., Newman, M.A., Osborne, L., Overstreet, C., Padgett, G.B., Phipps, P.M., Price, P.P., Sikora, E.J., Smith, D.L., Spurlock, T.N., Tande, C.A., Tenuta, A.U., Wise, K.A., and Wrather, J.A. (2017). Soybean yield loss estimates due to diseases in the United States and Ontario, Canada, from 2010 to 2014. Plant Health Prog. **18,** 19-27.

Brar, H.K.B., M.K. (2012). Expression of a single-chain variable-fragment antibody against a *Fusarium virguliforme* toxin peptide enhances tolerance to sudden death syndrome in transgenic soybean plants. Mol. Plant-Microbe Interact. **25,** 817-824.

Chang, H.X., Domier, L.L., Radwan, O., Yendrek, C.R., Hudson, M.E., and Hartman, G.L. (2016). Identification of multiple phytotoxins produced by *Fusarium virguliforme* including a phytotoxic effector (FVNIS1) associated with sudden death syndrome foliar symptoms. Mol Plant-Microbe Interact. **29,** 96-108.

Kazi, S., Shultz, J., Afzal, J., Johnson, J., Njiti, V. N., and Lightfoot, D.A. 2008. Separate loci underlie resistance to root infection and leaf scorch during soybean sudden death syndrome. Theor. Appl. Genet. **116:**967-977.

Chong, S.K., Hildebrand, K.K., Luo, Y., Myers, O., Indorante, S.J., Kazakevicius, A., and Russin, J. (2005). Mapping soybean sudden death syndrome as related to yield and soil/site properties. Soil Till. Res. **84,** 101-107.

Coleman, J.J. (2015) The *Fusarium solani* species complex: ubiquitous pathogens of agricultural importance. Molecular Plant Pathology **17**: 146-158.

Fraaije, B.A., Bayon, C., Atkins, S., Cools, H.J., Lucas, J.A., and Fraaije, M.W. (2012). Risk assessment studies on succinate dehydrogenase inhibitors, the new weapons in the battle to control septoria leaf blotch in wheat. Mol. Plant Pathol. **13,** 263-275.

Gao, X., Jackson, T.A., Hartman, G.L., and Niblack, T.L. (2006). Interactions between the soybean cyst nematode and *Fusarium solani* f. Sp. *Glycines* based on greenhouse factorial experiments. Phytopathol. **96,** 1409-1415.

Gaspar, A.P., Mueller, D.S., Wise, K.A., Chilvers, M.I., Tenuta, A.U., and Conley, S.P. (2017). Response of broad-spectrum and target-specific seed treatments and seeding rate on soybean seed yield, profitability, and economic risk. Crop Sci. **57,** 2251-2263.

Hershman, D.E. (2003). Soybean diseases control series: Are we missing opportunities? Part 2: Soybean sudden death syndrome. In Kentucky Pest News (University of Kentucky.).

Hershman, D.E., Hendrix, J.W., Stuckey, R.E., Bachi, P.R., and Hendson, G. (1990). Influence of planting date and cultivar on soybean sudden death syndrome in Kentucky. Plant Dis. **74,** 761-766.

Jin, H., Hartman, G.L., Nickell, D., and Widholm, J.M. (1996). Phytotoxicity of culture filtrate from *Fusarium solani*, the causal agent of sudden death syndrome of soybean. Plant Dis. **80,** 922-927.

Kandel, Y.R., Leandro, L.F., and Mueller, D.S. (2019a). Effect of tillage and cultivar on plant population, sudden death syndrome, and yield of soybean in Iowa. Plant Heal. Prog**.,** doi:10.1094/PHP-1010-1018-0063-RS.

Kandel, Y.R., Wise, K.A., Bradley, C.A., Chilvers, M.I., Tenuta, A.U., and Mueller, D.S. (2016). Fungicide and cultivar effects on sudden death syndrome and yield of soybean. Plant Dis. **100,** 1339-1350.

Kandel, Y.R., Wise, K.A., Chilvers, M.I., Byrne, A.M., Tenuta, A.U., Faghihi, J., Wiggs, S.N., and Mueller, D.S. (2017). Effect of soybean cyst nematode resistance source and seed treatment on population desities of Heterodera glycines, sudden death syndrome and yeild of soybean. Plant Dis. **101,**1237-2143.

Kandel, Y.R., Mueller, D.S., Legleiter, T., Johnson, W.G., Young, B.G., and Wise, K.A. (2018a). Impact of fluopyram fungicide and preemergence herbicides on soybean injury, population, sudden death syndrome, and yield. Crop Prot. **106,** 103-109.

Kandel, Y.R., Bradley, C.A., Chilvers, M.I., Mathew, F.M., Tenuta, A.U., Smith, D.L., Wise, K.A., and Mueller, D.S. (2019b). Effect of seed treatment and foliar crop protection products on sudden death syndrome and yield of soybean. Plant Dis**.,** PDIS-12-18-2199-RE.

Kandel, Y.R., McCarville, M.T., Adee, E.A., Bond, J.P., Chilvers, M.I., Conley, S.P., Giesler, L.J., Kelly, H.M., Malvick, D.K., Mathew, F.M., Rupe, J.C., Sweets, L.E., Tenuta, A.U., Wise, K.A., and Mueller, D.S. (2018b). Benefits and profitability of fluopyram-amended seed treatments for suppressing sudden death syndrome and protecting soybean yield: A meta-analysis. Plant Dis. **102,** 1093-1100.

Keon, J.P.R., White, G.A., and Hargreaves, J.A. (1991). Isolation, characterization and sequence of a gene conferring resistance to the systemic fungicide carboxin from the maize smut pathogen, *Ustilago maydis*. Curr. Genet. **19,** 475-481.

Kobayashi-Leonel, R., Mueller, D., Harbach, C., Tylka, G., and Leandro, L. (2017). Susceptibility of cover crop plants to *Fusarium virguliforme*, causal agent of soybean sudden death syndrome, and *Heterodera glycines*, the soybean cyst nematode. J. Soil Water Conserv. **72,** 575-583.

Koenning, S.R., and Wrather, J.A. (2010). Suppression of soybean yield potential in the continental united states by plant diseases from 2006 to 2009. Plant Health Prog. **11,** 10.1094/php-2010-1122-1001-rs.

Kolander, T.M., Bienapfl, J.E., Kurle, J.E., and Malvick, D.K. (2012). Symptomatic and asymptomatic host range of *Fusarium virguliforme*, the causal agent of soybean sudden death syndrome. Plant Dis. **96,** 1148-1153.

Leandro, L.F.S., Eggenberger, S., Chen, C., Williams, J., Beattie, G.A., and Liebman, M. (2018). Cropping system diversification reduces severity and incidence of soybean sudden death syndrome caused by *Fusarium virguliforme*. Plant Dis. **102,** 1748-1758.

Luo, Y., Chong, S.K., and Myers, O. (2001). Spatio-temporal analysis of soybean root colonization by *Fusarium solani* f. sp. *glycines* in fields. Plant Dis. **18,** 303-310.

Ma, L.J., Geiser, D.M., Proctor, R.H., Rooney, A.P., O'Donnell, K., Trail, F., Gardiner, M., Manners, J.M., Kazan, K. (2013) *Fusarium* pathogenomics. Ann Rev Microbiol **67**: 399-416.

NASS. (2018). Acreage (Washington, D.C: U.S. Department of Agriculture, National Agricultural Statistics Service).

Navi, S.S., and Yang, X.B. (2016). Impact of crop residue and corn-soybean rotation on survival of *Fusarium virguliforme* a causal agent of sudden death syndrome of soybean. J. Plant Path. Microbiol. **7,** 330.

Ngaki, M.N., Wang, B., Sahu, B.B., Srivastava, S.K., Farooqi, M.S., Kambakam, S., Swaminathan, S., and Bhattacharyya, M.K. (2016). Tanscriptomic study of the soybean-*Fusarium virguliforme* interaction revealed a novel ankyrin-repeat containing defense gene, expression of whose during infection led to enhanced resistance to the fungal pathogen in transgenic soybean plants. PLoS ONE **11,** e0163106.

Njiti, V.N., Shenaut, M.A., Suttner, R.J., Schmidt, M.E., and Gibson, P.T. (1996). Soybean response to sudden death syndrome: Inheritance influenced by cyst nematode resistance in pyramid × douglas progenies. Crop Sci. **36,** 1165-1170.

O'Donnell, K., Sink, S., Mercedes Scandiani, M., Luque, A., Colletto, A., Biasoli, M., Lenzi, L., Salas, L., González, V., Ploper, L.D., Formento, N., Pioli, R.N., Aoki, T., Yang, X.B., and Sarver, B.A.J. (2010). Soybean sudden death syndrome species diversity within North and South America revealed by multilocus genotyping. Phytopathol. **100,** 58-71**.**

Roy, K.W., Rupe, J.C., Hershman, D.E., and Abney, T.S. (1997). Sudden death syndrome of soybean. Plant Dis. **81,** 1100-1111.

Rupe, J.C. (1989). Frequency and pathogenicity of *Fusarium solani* recovered from soybeans with sudden death syndrome. Plant Dis. **73,** 581-584.

Scherm, H., and Yang, X.B. (1999). Risk assessment for sudden death syndrome of soybean in the north-central united states. Agri. Sys. **59,** 301-310.

Swaminathan, S., Das, A., Assefa, T., Knight, J.M., Da Silva, A.F., Carvalho, J.P.S., Hartman, G.L., Huang, X., Landro, L.F., Cianzo, S.R., and Bhattacharyya, M.K. (2018). Genome wide association study identifies novel single nucleotide polymorphic loci and candidate genes involved in soybean sudden death syndrom resistance. PLoS One. 14:e0212071.

Theones, P. (2015). Soybean international commodity profile. In: Competitive commercial agriculture in sub-saharan Africa (CCAA) study, FAO, UN. 1-25.

Vick, C.M., Bond, J.P., Chong, S.K., and Russin, J.S. (2003). Response of soybean sudden death syndrome to tillage and cultivar. Can. J. Plant Pathol. **28,** 77-83.

Von Qualen, R.H., Abney, T.S., Huber, D.M., and Schreiber, M.M. (1989). Effects of rotation, tillage, and fumigation on premature dying of soybeans. Plant Dis. **73,** 740-744.

Wang, J., Jacobs, J.L., Roth, M.G., and Chilvers, M.I. (2019a). Temporal dynamics of *Fusarium virguliforme* colonization of soybean roots. Plant Dis. **103,** 19-27.

Wang, J., Sang, H., Jacobs, J.L., Oudman, K., A., Hanson, L.E., and Chilvers, M.I. (2019b). Soybean sudden death syndrome causal agent *Fusarium brasiliense* present in michigan. Plant Dis. 10.1094/PDIS-1008-1018-1332-RE.

Wang, T., Hao, Y., Zhu, M., Yu, S., Ran, W., Xue, C., Ling, N., and Shen, Q. (2019). Characterizing differences in microbial community composition and function between *Fusarium* wilt diseased and healthy soils under watermelon cultivation. Plant Soil **438,** 421-433.

Westphal, A., Li, C., Xing, L., McKay, A., and Malvick, D. (2014). Contributions of *fusarium Virguliforme* and *Heterodera glycines* to the disease complex of sudden death syndrome of soybean. PLoS One **9,** e99529.

Xing, L., and Westphal, A. (2009). Effects of crop rotation of soybean with corn on severity of sudden death syndrome and population densities of *Heterodera glycines* in naturally infested soil. Field Crops Res. **112,** 107-117.

CHAPTER 2

Economic Impact of Fluopyram-Amended Seed Treatments to Reduce Soybean Yield Loss Associated with Sudden Death Syndrome

This chapter is unpublished, with intention to submit to *Plant Disease*.

Baetsen-Young, A.M., Chilvers, M.I., Swinton, S.M. 20XX. Economic Impact of Fluopyram-Amended Seed Treatments to Reduce Soybean Yield Loss Associated with Sudden Death Syndrome.

Abstract

Soybean sudden death syndrome (SDS), caused by *F. virguliforme*, is a key limitation in reaching soybean yield potential, stemming from limited disease management through cultural practices and partial host resistance. A fungicidal seed treatment was released in 2014 with the active ingredient fluopyram and was the first chemical management strategy to reduce soybean yield loss stemming from sudden death syndrome. While farm level studies have found fluopyram profitable, we were curious if fluopyram would be beneficial nationally if targeted to soybean fields at-risk to SDS yield loss. To estimate economic benefits of fluopyram adoption in SDS at-risk acres, in the light of U.S. public research and outreach from a privately developed product, we applied an economic surplus approach, calculating *ex ante* net benefits from 2018 to 2032. Through this framework of logistic adoption of fluopyram for alleviation of SDS associated yield losses, we estimated a net benefit of $5,829 million over 15 years, considering the costs of public seed treatment research and future extension communication. While the sensitivity analysis indicates that overall net benefits from fluopyram adoption on SDS at-risk acres are highly dependent upon the market price of soybeans, the incidence of SDS, and the adoption path of this seed treatment, the net benefits still exceeded 1.3 billion in the worse-case scenario.

Introduction

Soybean sudden death syndrome (SDS) is an economically damaging disease in the United States (Koenning and Wrather, 2010). Since the first report in the 1970's in Arkansas, soybean SDS has quickly spread to nearly all soybean producing states. In North America, soybean SDS is predominantly caused by the soil borne fungus *Fusarium virguliforme* (O'Donnell et al., 2010). *Fusarium virguliforme* is an asexual hemibiotrophic fungus, infesting soil and crop residues. This fungus infects soybean roots during the early plant developmental stages (Jin et al., 1996), colonizing the xylem tissues, where the pathogen secretes the phytotoxins, initiating programmed cell death of the soybean leaf (Brar, 2012). The host response creates the characteristic symptom of interveinal leaf scorch associated with SDS. Root infection and leaf scorch leads to a reduction of overall plant biomass, flowering and pod loss, and thus yield. Yield losses of up to 80% have been reported in highly infested fields, but typically yield losses of 5 to 15% are observed (Roy et al., 1997; Hershman, 2003).

Currently, no strategy can fully manage SDS. Partial genetic resistance of soybean cultivars has been developed through quantitative trait loci. However, if disease pressure is high in soybean fields, the partial resistance is broken (Njiti et al., 1996). Conditions inducing high disease pressure are thought to be cool temperatures, and wet compacted soil conditions during planting and early developmental stages (Rupe, 1989; Roy et al., 1997; Scherm and Yang, 1999; Chong et al., 2005). Tillage is thought to reduce symptom development by decreasing soil moisture and increasing soil temperature (Roy et al., 1997; Vick et al., 2003).

An additional strategy for field crop disease management is crop rotation, which reduces pathogen population within soils by planting non-hosts for multiple years (Agrios, 2004). Previous research on corn (*Zea mays* L.), soybean, and wheat (*Triticum aestivum* L.) rotation was found to reduce SDS yield losses when compared to continuous soybean (Von Qualen et al., 1989; Roy et al., 1997). However, more recent studies have shown corn and other crop rotations have not reduced SDS severity (Hershman, 2003; Xing and Westphal, 2009; Leandro et al., 2018).

Because cultural approaches and limited genetic resistance have not consistently mitigated SDS associated yield loss, a fungicidal seed treatment was released in 2014 with the active ingredient fluopyram, commercially designated as ILeVO (BASF, Research Triangle Park, NC). Fluopyram is a succinate dehydrogenase inhibitor and was the first chemical management strategy to reduce soybean foliar symptoms and improve yields under SDS pressure in comparison to pre-existing commercial base seed treatments of insecticide, fungicide and nematicide (Kandel et al., 2016; Gaspar et al., 2017; Kandel et al., 2018b; Kandel et al., 2018a; Kandel et al., 2019a). These reported yield gains have ranged from 2.8 to 12.0% in fields with a historical SDS pressure. But the cost of planting seeds treated with fluopyram is also elevated, potentially reducing economic gains for growers. Thus, the profitability of the fluopyram seed treatment and probability of a positive return on investment have been explored, revealing an increasing probability of capturing return on investment with increasing disease pressure; however, profitability decreased with increasing seed costs (Kandel et al., 2018b) or decreasing grain sale price (Gaspar et al., 2017).

Previous studies have also compared costs and benefits of seed treatments of fungicide, insecticide and nematicide activity against a commercial base or untreated controls (Gaspar et al., 2017; Kandel et al., 2018b; Rossman et al., 2018). As with the exploration of fluopyram, these analyses focused on the farm level, calculating profitability and return on investment with fixed soybean prices and quantities. Interestingly, Kandel et al., assessed the impacts of fluopyram seed treatments upon soybean yield under SDS pressure across 200 field trials in 12 U.S. states (2018b). From these trials, a meta-analysis was conducted that found a 7.6% yield increase across the U.S. soybean production region. The parameterization of fluopyram yield benefits under SDS disease pressure across soybean production could enable the aggregate estimation of economic benefits to growers at-risk to SDS associated yield losses.

Previous research into national economic impacts of agricultural damage agents has dealt primarily with insect pests. The ease of scouting insects enabled the development of economic thresholds for management decision making (Stern et al., 1959). Economic evaluations of aggregate returns to public research from the use of insect integrated pest management (IPM) economic thresholds for field crop growers have found favorable returns (Musser et al., 1981; Greene et al., 1985; Norton and Mullen, 1994; Song and Swinton, 2009). Yet, while an increasing proportion of agricultural research and development occurs within the private sector (Alston et al., 1998; Alston et al., 2009; Wang et al., 2013), the economic returns to public validation research have not been explored. We propose to contribute a plant disease study to evaluate economic impact of a privately developed prophylactic application of fluopyram seed treatments as a disease management tactic for SDS.

Material and Methods

Economic Conceptual Framework

An economic surplus approach modeled after Alston et al. (1998) was applied to determine the economic impact of SDS fluopyram research. The widespread adoption of SDS controls may cause changes in soybean quantities that affect market prices, so the management tactic was evaluated as part of U.S. national soybean production. Changes in total economic surplus were computed from effects on revenues above costs for producers (producer surplus) and the willingness to pay of consumers above the initial equilibrium price (consumer surplus).

The fundamental elements expected to change economic surplus can be illustrated using supply and demand curves. As shown in Figure 1A the supply curve (S_T) and demand curve (D) represent the soybean market before the management intervention. The consumer surplus represents the area above the equilibrium price (P_o) and below the demand curve (1) and the producer surplus is the area below the equilibrium price (P_o), but above the supply curve (2). The total economic surplus is the union of areas 1 and 2.

This analysis compares the current U.S. soybean market where fluopyram is gradually being adopted to avert SDS losses to a counterfactual where fluopyram does not become available. If the fluopyram tactic was adopted in SDS affected areas this would increase supply, shifting the supply curve to the right from S_T to S_{1FT}, causing the equilibrium price to fall (P_1), which would occur if the value of reduced SDS associated yield losses were greater than the

increased costs of SDS control (Figure 3B). The consumer surplus would grow from the decline in equilibrium price from P_o to P_1, because consumers would be paying a lower price at P_1 (adding regions 3, 4, 5), and more consumers can enter the market at the lower price. The producer surplus would experience a mixed effect. It would grow from the decrease in marginal costs (region 6) and increased soybean production (region 7), but also shrink from the fall in price (loss of region 3). The amount of net change in total surplus depends on the proportionate increase in soybean production, variable input costs and the elasticities of supply and demand, which reveal how producers and consumers respond to changes in price.

We estimated the benefits of the fluopyram tactic through a three-step strategy. First, as a baseline we evaluated U.S. soybean production affected by SDS without the adoption of fluopyram treated seed. To discover potential damage to soybean yield by *F. virguliforme*, we predict soybean production under SDS pressure without fluopyram seed treatment. We next model the adoption of fluopyram seed treatments applied to soybean production at risk of SDS. We assume that growers adopt fluopyram treated seeds as they learn about this prophylactic management strategy and begin to plant treated seeds in areas at risk for economic loss to SDS. While the use of fluopyram treated seeds will incur additional production costs, the resulting reduction of SDS associated yield loss shift the supply curve to the right. To estimate the value of potential gains to growers adopting fluopyram treated seed, we compared the quantities and prices of soybean produced with and without adoption of fluopyram treated seeds annually throughout the time horizon of the fluopyram adoption path.

Management Induced Yield Change Parameterization

The economic impact was determined by comparing costs and benefits from the fluopyram seed treatment. The current U.S. soybean production acted as a baseline estimate of soybean market that has incorporated losses due to SDS, allowing a comparison to evaluate the impacts of SDS to soybean yield by the application of fluopyram seed treatments (NASS, 2017). To develop the counterfactual, we applied the percent yield change reported in Kandel et al., (2018b) meta-analysis of over 200 field trails in 12 states during 2013-2015, between the soybean seed treated with a commercial base plus fluopyram and soybeans treated with a commercial base alone. To isolate benefits from fluopyram, the commercial base treatment included a nematistat and insecticide (*Bacillus firmus* with clothianidin) and three fungicides (metalaxyl, penflufen and prothioconazole) known not to target *F. virguliforme*. While *B. firmus* is intended to account for nematistatic activities of current commercial base seed treatments, in comparison to nematistatic activity against nematodes by fluopyram, growers may receive yield benefits beyond the conventional base, which were included in this analysis. These additional benefits from fluopyram could occur by preventing a potential synergistic activity of *Heterodera glycines* and *F. virguliforme* causing elevated SDS severity (Xing and Westphal, 2006). Additionally, all field site locations had a historical presence of SDS with a diversity of disease severity that enabled characterization of yield benefits under a range of disease pressure (Kandel et al., 2018b). Also, field site locations included multiple soybean cultivars with varying levels of SDS resistance. The yield difference between the fluopyram-enhanced seed treatments and the counterfactual of soybean production with only a commercial base seed treatment was a 7.6% yield increase

under *F. virguliforme* pressure (Kandel et al., 2018b). This yield gain only applies to fields affected by SDS, and assumes no future advancement of soybean genetic resistance to SDS during the 15-year time horizon of this study.

Determining Changes in Economic Surplus

The precise spatial extent of SDS in the U.S. remains unclear. Specific environmental predictors of this disease remain ambiguous to growers and researchers as SDS incidence is very heterogeneous, even within an infested field (Roy et al., 1997; Allen et al., 2017). SDS is spreading and has been reported in new soybean production states over the last two decades, but the incidence of this disease is not reported. Often the impact of SDS is estimated by bushels lost based on disease surveys, feedback from university, industry, extension and farmer personnel, and personal exposure to disease severity or incidence. From these reports, percent disease loss is estimated and formulated to total bushels lost for each soybean disease based upon predicted yield before estimated losses (Crop Protection Network, 2016). Total incidence or area of soybean production with SDS present and at economic risk to yield loss across the soybean production region can be estimated from annual reports of percent yield loss (Crop Protection Network, 2016; Allen et al., 2017; United Soybean Board, 2017) divided by an average disease severity (e.g., the intensity of disease when presence) across affected soybean acres of 10.0% (Roy et al., 1997). This calcuated incidence of SDS across U.S. soybean production was determined to be at economic risk of SDS associated yield loss and assumed for gradual adoption of fluopyram treated soybean seed to alleviate SDS associated yield losses within this analysis.

To place an economic value on potential reduction in SDS-related yield loss from the use of fluopyram as a seed treatment, we assumed an adoption path similar to that observed for neonicotinoid soybean seed treatments, which were introduced to prophylactically manage insect pests of soybean, starting in 2004. Neonicotinoid seed treatments were rapidly adopted by 6% of U.S. growers in 2006, leading to a conservative estimate of 34% of soybean production planting neonicotinoid treated seeds in 2011 (Douglas and Tooker, 2015). Applying the key values of percent soybean area planted with neonicotinoid seed treatments in 2006 and 2011, with an upper limit 90%, revealed that neonicotinoid seed treatments were primarily adopted over a 15-year time frame (Figure 4). We applied the adoption path estimated for neonicotinoid treatments on soybean seeds to model the adoption of fluopyram seed treatments as a logistic trend, with a maximum adoption of 90% (rather than 100%, as some growers are averse to adopting new technologies (Fernandez-Cornejo et al., 1994)).

Early evidence of the adoption of fluopyram amended seed treatment appears strikingly similar to that of neonicotinoid seed treatments. Fluopyram treated soybean seed were commercially available to the U.S. soybean production from 2014 to 2018. Fluopyram-treated soybean seed was planted across 3 million acres in 2016, and increased to 8.5 million acres in 2018 (personal communication, Jeremiah Mullock, BASF). To model the future adoption of fluopyram, we assumed 1) that only growers with fields at risk of SDS infestation might adopt it, and 2) that not all growers with fields infested with soybean SDS would adopt this specific seed treatment, as some are averse to new technologies (Fernandez-Cornejo et al., 1994), thus the ceiling for future adoption was selected at 90%. Fitting the observed

percentages of soybean area planted with fluopyram seed treatments in 2016 and 2018, with a logistical adoption function and an upper adoption limit of 90%, implied that fluopyram seed treatments would be primarily adopted over a 15-year time frame as well (Figure 4).

The technologies presented in Figure 4 have similar capital inputs and benefits to growers, and the adoption area is very similar of a pest specific seed treatment. The barriers for growers to adopt fluopyram treated seed are lower than other technologies as many growers already own the equipment needed to plant the seeds and only require capital for purchasing treated seeds, along with an awareness of seed treatments as a cost-effective management tactic. Therefore, when considering barriers to adoption, we also propose to evaluate economic impacts from fluopyram treated seed adoption timeline explored over 15 years.

Data to Evaluate Economic Surplus and Net Present Value

To assess surplus changes in a parallel supply shift of S_T to S_{1FT}, we determined the vertical supply shift from P_o to P_1, denoted as K, and Z, the percent change in the equilibrium soybean price between soybean production with no adoption of fluopyram and the gradual adoption of fluopyram within SDS affected areas (Figure 3) (Alston et al., 1998; Song and Swinton, 2009). Soybean quantity changes between the scenarios of with or without fluopyram adoption were determined through the yield loss reduction equation below:

$$Yield = (1 - s - e) \cdot Y' + s \cdot (1 - d[1 - f \cdot Adopt\%]) \cdot Y' + e \cdot (1 - d[1 - f \cdot 0]) \cdot Y'$$

Where *Yield* is the quantity soybean yield produced under each scenario. s is the low incidence of soybean area with economic damage from SDS and e is the epidemic jump in proportion during five-yearly epidemics. Y' represents the soybean yield that is SDS free, assumed to be the USDA projected soybean quantities. The damage proportion from SDS of 7.6% is represented by d. Parameter f represents the proportional damage reduction from fluopyram, assumed to be 100%. $Adopt\%$, is the proportion of growers adopting fluopyram in areas normally experiencing SDS economic damage. We assume 0% fluopyram adoption in epidemic areas that do not normally experience SDS damage, so damage from SDS epidemics in these areas is unmitigated.

Changes to soybean quantities produced were analyzed by categorizing soybean yield into disease free proportion $((1 - s - e) \cdot Y')$ and the proportion of soybean yield at-risk to SDS associated losses $(s \cdot (1 - d[1 - f \cdot Adopt\%]) \cdot Y') + e \cdot (1 - d[1 - f \cdot 0]) \cdot Y'$. If growers adopted fluopyram treated seed, then SDS associated yield losses would decrease by 7.6% per acre within the proportion of soybean yield at-risk to SDS associated losses. The proportionate difference of soybean quantities produced by adoption of fluopyram treated seeds when compared to non-adoption of fluopyram in areas affected by SDS, represents total yield loss averted. To quantify the vertical supply shift, we adjusted four parameters that underpin changes in economic surplus: soybean and demand supply elasticities, costs of fluopyram adoption, incidence of SDS, and the projected rate at which farmers adopt fluopyram. The value of changes to surplus between the scenarios of fluopyram adoption and non-adoption was summed from 2018 to 2032 and discounted at an annual rate of 5% to determine the net present value (NPV) (Alston et al., 1998).

Supply and demand elasticities. Elasticities were reviewed from the literature and presented in Table 1. Since similar values for supply elasticities were recorded from several different literature sources, we chose 0.30 to represent the supply elasticity.

Cost change. The change in variable input costs were accounted from variable cost differences in annual production budgets between the two management options of the commercial base seed treatment or using commercial base with a fluopyram amended seed treatment. The commercial base seed treatment costs $12 per seed unit (140,000 seeds per seed unit), versus $25 per seed unit for the commercial base seed treatment with fluopyram (Gaspar et al., 2017). The increased cost of $13/acre for fluopyram amended seed treatments was assumed to entail an additional $0.32 per acre in borrowing costs at a 5% interest rate, resulting in a total increased cost for fluopyram seed treatment of $13.32 per acre, a 2.8% increase in total production costs (Ward et al., 2018) (Table 2).

Incidence of SDS in United States soybean production. The incidence of SDS in U.S. soybean production was estimated from annual yield losses from 1996 to 2015 (Allen et al., 2017), and 2011 (United Soybean Board, 2017), and soybean production data (USDA, 2019) from 1996 to 2015. Annual percent yield loss was estimated as follows and used as incidence of SDS in the U.S soybean production:

$$Yield\ Loss\ Share = \frac{Y_{Loss}}{Y_{Harvest} + Y_{Loss}}$$

Where Y_{Loss} share is the estimated proportional loss in soybean production due to SDS. Which is divided by total potential yield, measured as the total bushels harvested in the U.S. ($Y_{Harvest}$) plus the additional soybean bushels lost to SDS (Y_{loss}). Proportional yield loss was utilized to estimate incidence from the following equation:

$$\frac{Y_{Loss}}{Y_{Harvest} + Y_{Loss}} = Prob(SDS) \cdot Y_{Loss}|SDS$$

The percent yield loss occurring from SDS is a function of the incidence of SDS (*Prob(SDS)*) and the average percent yield loss occurring when severe SDS is present ($Y_{Loss}|SDS$). We used this equation to estimate incidence by dividing proportional yield loss by average disease severity of 10% across affected soybean acres (Roy et al., 1997). Holding disease severity constant, assumes incidence will reflect the variability of years with greater SDS yield loss. The incidence of SDS with an economic impact across the soybean production region was estimated from yield loss data collected annually from 1996 to 2015 (Figure 5). Over the last two decades of U.S. soybean reports, SDS incidence appeared to group at two distinct levels (Figure 5A). The first level we deemed SDS low incidence, or incidence without epidemics (below 11.90%) ranging from 1.5% in 1996 to 11.0% in 2015, increasing at a linear trend of 0.168% annually (Figure 5A). While we can estimate an annual rate of increase to a very precise rate, the accuracy of this annual increase of incidence may be much lower than calculated. Interestingly, a second group of SDS incidence was observed at levels of incidence above 11.9% (Figure 5A), which corresponded to years with epidemic levels of SDS associated yield loss (Leandro et al., 2013). SDS epidemics have been observed to cause

spikes in yield loss approximately every 4-5 years; the epidemics seem to correspond to decreases in annual mean temperature in the prior year (Figure 5B). The low incidence of SDS was modeled over the 15-year analysis using the low incidence values starting at 9.8% in 2018 and increasing annually at 0.168%, to a final incidence of 12.2% in 2032. Every 5 years the average incidence of the four previous epidemics was applied at 19.0%, with the first epidemic occurring in 2019, as five years had passed since the last epidemic.

Adoption of fluopyram amended seeds. The adoption path of fluopyram across SDS affected soybean production was based upon the estimated logistical adoption path of fluopyram treated seed (Figure 4). We applied the logistical adoption pattern of fluopyram, seed treatments from 2014 to 2032 to model the adoption path of fluopyram seed treatments. Fluopyram has been commercially available on the market since 2014, thus the adoption rate starts in 2018 at 8.0%. Following a logistical trend, the adoption rate swiftly increases to 12.5% in 2019, and 19.2% in 2020 (Figure 4). This increasing adoption rate of fluopyram corresponds in part to public outreach activities after the research was completed in 2018.

Price of soybeans. Projections of prices were taken from USDA through 2029 values (USDA, 2019). Projections were held constant at 2029 prices through 2032, mimicking trends from 2026-2029.

Quantity of soybeans. The quantity of soybeans produced was taken from historical accounts of soybeans produced in the U.S. (USDA, 2019) as well as projections to 2028 from the USDA (2019) and held stable at 2029 quantities through 2032.

Costs from research and outreach. Previous research costs associated with fluopyram were gathered from National Soybean Checkoff Base, which occurred from 2014 to 2019 totaling $844,000 in across seven U.S. states (United Soybean Board, 2019) (Appendix 1). Future research costs were estimated from National Soybean Checkoff Base funds allocated to SDS and fluopyram research and communication in 2019 at $93,500, and which was presumed to be allocated again in 2020 (Table 3). Additionally, we assumed there was one principal investigator and one technician for each field trial in Delaware, Indiana, Iowa, Kentucky, Michigan, South Dakota, and Wisconsin that would dedicate 5% of their annual time to conducting individual trials (Table 3). These associated research costs were estimated at $17,600 per trial site after incorporating 30% fringe benefits and 50% indirect costs (Table 2).

Outreach costs were estimated from 20 extension educators in each state allocating 2% of time annually from 2018 to 2032, repeated in each of the 33 soybean producing states in a similar method to Song and Swinton (Song and Swinton, 2009), at a total of $1,783,000 annually. An average salary was estimated from the 2019 reported values of Michigan extension educators' salaries on a continuing track, after incorporating 30% fringe benefits and 50% indirect costs and applied as salary for all extension agents.

Results

The net present value of adopting fluopyram for SDS control was estimated based upon comparison of two scenarios across soybean acreage at risk of SDS with and without

fluopyram adoption. Without the prophylactic control from this fungicidal seed treatment, soybean production would have suffered an estimated loss of 645 million bushels from 2018 to 2032 stemming from SDS, representing 0.96% of projected U.S. soybean production. Adopting fluopyram treated seeds reduces SDS-related losses to U.S. soybean production by an estimated 46.4%, decreasing production losses from 645 million bushels to $299 million bushels across 2018 to 2032. The increase of the estimated 346 million bushels of soybean represents the benefit of adopting fluopyram treated seeds on SDS at-risk acreage by averting associated yield loss. Net present value analysis of this increase over 15 years comes to $5,829 million in net benefits.

We applied an economic surplus approach to determine the value of fluopyram adoption, as not only do costs of production rise, but also the change in soybean output may alter market prices. Specifically, the increased soybean production entering the market from fluopyram adoption in SDS at-risk areas will cause a predicted drop in soybean prices. While the price reduction will slightly shrink producer surplus, the increase in soybean quantity produced due to fluopyram adoption will expand consumer surplus. The mechanism for this is that the decrease in soybean prices allows more consumers to enter the market and purchase soybeans at the lower price. Therefore, a shift of the supply curve to the right will expand consumer surplus from adoption of fluopyram in at-risk SDS areas, increasing the estimated benefits.

Sensitivity Analysis

Key parameters that may affect the economic impact of fluopyram treated seeds on soybean acreage at risk of SDS includes supply elasticity, disease incidence, price change, and adoption rate. To understand the impacts of multiple variables, the sensitivity of this analysis was explored through combining all variables in either a worst case or best-case scenario (Table 4). Since similar values for supply elasticities were recorded from several different literature sources and were similar to the value we used for this analysis, we did not model changes to values of supply elasticities. As additional fungicidal seed treatment chemistries targeting SDS will be on the market starting in 2019 (Syngenta, 2019), we adjusted the adoption rate of fluopyram based upon observed adoption of a neonicotinoid seed treatment that became available to growers five years after initial neonicotinoid soybean seed treatments came on the market. For the other two key variables of SDS incidence and soybean prices, we adjusted outcomes by one trend-adjusted standard deviation up or down as appropriate for "worst" and "best" case scenarios.

The level of incidence of soybean acres at economic risk to SDS in the U.S. is a primary factor to the economic benefits of fluopyram treated seeds on alleviating yield losses attributable to SDS. Currently no aggregate level of SDS incidence has been estimated across the U.S. soybean production. Therefore, we estimated this parameter based on percent annual yield loss estimates of total soybean production attributed to SDS, and an average severity of 10%. This method overlooks many local scale environmental factors, in addition to assuming a strong linear relationship between severity and incidence to generate yield loss. Also, SDS is

being discovered in new regions of the U.S. each growing season, thus, the rate at which incidence increase may be lower herein than actually realized. To account for uncertainties of the incidence of soybean acres at risk to SDS we calculated the trend-adjusted standard deviation at low SDS incidence (i.e. incidence below 11.9%) during 1996-2015 to be 5.8%. This standard deviation represented 77.1% change of incidence from the mean low incidence of 7.6% from 1996-2015. To represent the recorded variation of SDS low incidence we then reduced SDS low incidence 77.1% in 2018 to 2.2% for the worse-case scenario. In the best-case scenario, we increased SDS incidence by one standard deviation by 77.1% to 17.4%. While low incidence was altered in the sensitivity analysis, both scenarios still had epidemics in 2019, 2024 and 2029 with an incidence of 19%, and SDS low incidence still increased at a rate of 0.168% annually.

Soybean prices are a key factor to valuation of benefits in this analysis. Prices of soybeans over thirty years from 1989-2018 have varied from a high of $15.54 per bushel in 2012 to a low of $6.29 per bushel in 2002 after converting all prices to 2018 U.S. dollars (NASS, 2019; USDA, 2019). We wanted account for price fluctuations in the soybean market, to explore impacts upon benefits generated from fluopyram seed treatment in SDS at risk areas. Therefore, we adjusted soybean prices from 1989 to 2018 for inflation by converting to 2018 U.S. dollars. The standard deviation of inflation-adjusted soybean prices was $2.43, for a coefficient of variation of 23.2% around the mean soybean price of $10.45. To account for this observed variation in soybean prices in the sensitivity analysis, we decreased soybean prices by 23.2% annually in the worst-case scenario and added 23.2% to soybean prices annually in the best-case scenario.

As an *ex-ante* analysis, we projected future adoption of fluopyram based on adoption rates from 2016 and 2018. However, additional seed treatments registered for SDS management are coming on the market in 2019 (Kandel et al., 2019b, Syngenta, 2019). To take these additional products entering the SDS seed treatment market into consideration, we reviewed the adoption path of different neonicotinoid soybean seed treatments, as neonicotinoids had a similar adoption path as fluopyram. Imidacloprid (Bayer Crop Science) and thiamethoxam (Syngenta) are both neonicotinoid seed treatments that were registered in 2004 for use on soybean and were quickly adopted (Schulz et al., 2007; Douglas and Tooker, 2015). Clothianidin (Bayer Crop Science) was registered five years later. By 2012, after just three years, this product was estimated to be planted on 1 million soybean acres, or 1.2 % of U.S. soybean area (Myers and Hill, 2014). As a parallel, five years post registration of fluopyram for SDS management, new chemistries are currently proposed to be registered as seed treatments for SDS of soybean (Syngenta, 2019). With similar timelines for registration of products, as well as similar adoption paths of the seed treatments, we applied the observed values of clothianidin to model future adoption of new SDS seed treatments that could affect fluopyram adoption. Therefore, we reduced the adoption of fluopyram by 1.2 % in 2022 in the worst-case scenario, and increased it by 1.2% in 2022 in the best-case scenario.

The sensitivity analysis indicated a 77.5% decrease in worse-case and 93.9% increase in best-case scenario of net benefits, relative to the baseline analysis of $5,829 million in net benefits (Table 4). Changing variables critical to this analysis revealed that this analysis is highly sensitive to soybean prices, adoption path and incidence of SDS at risk soybean acres.

Discussion

Soybean sudden death syndrome is a leading cause of soybean yield losses, and was ranked among the top 5 yield-reducing diseases in U.S. soybeans during 2010 to 2014 (Allen et al., 2017). Industry reports SDS incidence up to 80% of U.S. soybean acreage (Bayer Crop Science, 2017). However, only part of this area reflects "economic incidence" where soybean yield loss occurred. Based on severity reports and 20 years of yield loss data we found an economic incidence near 10% where SDS is causing yield loss. At this economic incidence rate, we find moderate economic benefits of fluopyram amended seed treatments of 5,829 million for alleviation of SDS associated yield losses. Overall, this net present value represents an estimated 1.4% of the projected discounted national gross value of soybean production over the 15 year estimation. While the estimated benefit of fluopyram is a small percentage of the gross value of this crop, this value reflects the proportion of the national soybean production with SDS incidence that would receive an economic benefit from fluopyram adoption. As our parameter assumptions here are conservative and yield losses from soil borne diseases are often underreported (Crop Protective Network, 2017), the actual economic benefits may be greater than projected here. The moderate economic benefits estimated from this frame suggests that public investments in validation research and outreach of privately developed technology are beneficial to society.

Previous studies have compared adoption of management practices to alleviate yield loss from pests or diseases at an aggregate level and provide a framework to explore our findings. The concern of Asian soybean rust (*Phakopsora pachyrhizi*), sparked the investigation of

economic impacts through fungicide management applications. Johansson et al., (2006) estimated within the 2010 growing season a total of $623 million of soybean production would be lost if no treatment was applied. Additionally, exploration of economic losses stemming from soybean aphid (*Aphis glycines),* with and without IPM scouting management or fungicide management within 2010 as well, ranged from $274 to $698 million across soybean affected production (Song and Swinton, 2009). We found that if fluopyram were not adopted annual losses to SDS ranged from $297 to 407 million in non-epidemic years to $583 to 636 million during epidemic years. The non-epidemic annual loss estimates from SDS fall within range of soybean aphid and below Asian soybean rust. The higher impact of epidemics, greater than Asian soybean rust, originates from the nearly doubling of acres at risk to economic loss from SDS when these outbreaks occur. Previously estimated annual soybean yield losses stemming from SDS have been valued at annual soybean prices to determine economic losses. During non-epidemic years economic valuation of estimated annual yield losses stemming from SDS have varied from $29 million in 1996, to $474 million in 2016, with each non-epidemic year from 2009-2016 causing an excess of $300 million in losses (Bandara et al., 2019; Navi and Yang, 2016). Epidemic years caused greater losses, ranging from $275 to $445 million during 2004, and 2000 growing seasons, respectively, to $673 to $863 million during the 2014 and 2010 growing seasons (Bandara et al., 2019). Our estimates of annual losses to SDS fall within the range of estimations economic losses stemming from SDS during more recent growing seasons, as incidence of SDS increased from 1996-2016 to a level similar within our framework.

The profitability of fluopyram amended seed treatments and probability of a positive return on investment have previously been investigated at the farm level (Gaspar et al., 2017; Kandel et al., 2018b). These localized studies found that fluopyram was beneficial in sites with a history of SDS pressure, but the probability of returns to growers decreased with increasing seeds costs or decreasing soybean prices (Gaspar et al., 2017; Kandel et al., 2018b). Our sensitivity analysis reaches similar findings. In the worst case we model, if soybean prices fell by one standard deviation (23.2 %) while disease incidence decreased by one standard deviation (77.1% in 2018), and the adoption rate of fluopyram dropped by 1.2% in 2022, then the net benefits would decrease by 77.5%. By contrast, in the best case, if the rate of disease incidence rose by 77.1%, soybean prices increased by 23.2%, and the adoption rate rose by 1.2% in 2022, then this seed treatment net benefits rise by 93.990%.

The adoption of fluopyram across the soybean acres at risk to SDS associated yield losses could pose environmental costs that are difficult to value. While fluopyram is active against *F. virguliforme*, the SDHI fungicide also has activity against other fungi (Santísima-Trinidad et al., 2018), which could cause environmental microbial communities to change in response to this seed treatment or aid in fungal communities losing sensitivity to this mode of action (Nettles et al., 2016). The costs associated with these environmental changes are difficult to parameterize and evaluate but should be evaluated when considering SDS management and the potential benefits derived from fungicidal seed treatments.

Conclusions

The economic impacts of public investment through research and outreach of a privately developed technology estimated from adoption of fluopyram to alleviate SDS associated yield losses in at risk acres revealed an overall benefit with a net present value of $5,829 million over 15 years, indicating fluopyram can reduce the economic impact of SDS. This analysis also illustrates the investment of validation research and outreach to discover and implement privately developed management tactics of diseases do have an overall economic benefit. Sensitivity analysis of this framework indicates that the market price of soybeans, the incidence of SDS, and the adoption path of this seed treatment can alter overall net benefits from fluopyram. Nonetheless, even in the worst case scenario where all three of these factors were less favorable to fluopyram impacts, the net present value of fluopyram amended seed treatment targeting SDS management still reached $1.3 billion. In sum, if growers adopt this fluopyram seed treatment to reduce economic yield losses caused by SDS as predicted, the overall economic benefits to soybean producers and consumers should be significant.

Acknowledgements

We would like to recognize Michigan State University (MSU) project GREEEN, Plant Resilience Institute and the C.S. Mott Foundation for funding of ABY and research. Research is supported by the MSU AgBioResearch and the U.S.D.A. National Institute of Food and Agriculture for S.M.S.

Author Contributions

Designed framework: A.B.Y., S.M.S. M.I.C.; Analyzed data: A.B.Y., S.M.S.; Wrote the manuscript: A.B.Y., S.M.S. M.I.C.

Table 1. United States and rest of world supply and demand elasticities for soybean.

Elasticity	Kim and Moschini, 2018	Haile et al., 2016	Reimer et al., 2012	Masuda and Goldsmith, 2009	Zilberman et al., 2010	Lybbert et al., 2014
U.S. Supply	0.38	0.30			0.22	0.30
U.S. Demand				-0.61		
U.S. Export Demand			-0.90			
Rest of World Supply		0.34-0.55				

Table 2. Variable costs associated with fluopyram amended seed treatments. Total cost of growing soybeans in the U.S with a commercial base treated seed containing nematistat and insecticide (*Bacillus firmus* with clothianidin) and three fungicides (metalaxyl, penflufen and prothioconazole) or with the commercial base and fluopyram. Farm budget taken from (Ward et al., 2018).

ITEM	Cost (U.S.D./Acre)	
VARIABLE COSTS		
Commercial Base Treated Seed	62.00	
Commercial Base with Fluopyram Treated Seed		75.00
Interest on Operating Capital	4.70	5.02
TOTAL OF VARIABLE COSTS	66.70	80.02

Table 3. Cost associated with fluopyram seed treatments and communication of research. Cost were gathered from locations in Delaware (DE), Indiana (IN), Iowa (IA), Kentucky (KY), Michigan (MI), South Dakota (SD) and Wisconsin (WI) and associated research costs from 2014 to 2020 in U.S. $.

	Costs Per Trial Across States			
Year	IA	MI	Multilocation and Region Trials	Associated Research Costs
2014	-	-	121,196	125,844.00
2015	129,159	-	164,811	59,711.00
2016	121,196	21,500	50,000	82,248.00
2017	-	-	72,369	93,998.00
2018	-	-	65,328	82,248.00
2019	-	15,200	78,354	82,248.00
2020	-	15,200	78,354	82,248.00

Table 4. Sensitivity analysis of economic impacts to U.S. soybean production for fluopyram SDS management, from 2018-2032 (in millions U.S. $).

	Fluopyram		
Parameter	Worse Case	Baseline	Best Case
Parameters Changed:			
Incidence:			
Starting Rate in 2018	2.2%	9.8%	17.4%
Adoption Rate:			
2018 Percentage	8.0%	8.0%	8.0%
2022 Percentage	37.7%	38.9%	40.2%
Soybean Price:			
Price Per Bushel Average (2019-2032)	$7.34	$9.33	$11.40
Price change (%)	-23.2%		+23.2%
Gross Benefits (m)	2,204	9,531	18,548
Net Benefits (m)	1,311	5,829	11,303
Percent Change to Reference (%)	-77.5%		93.9%

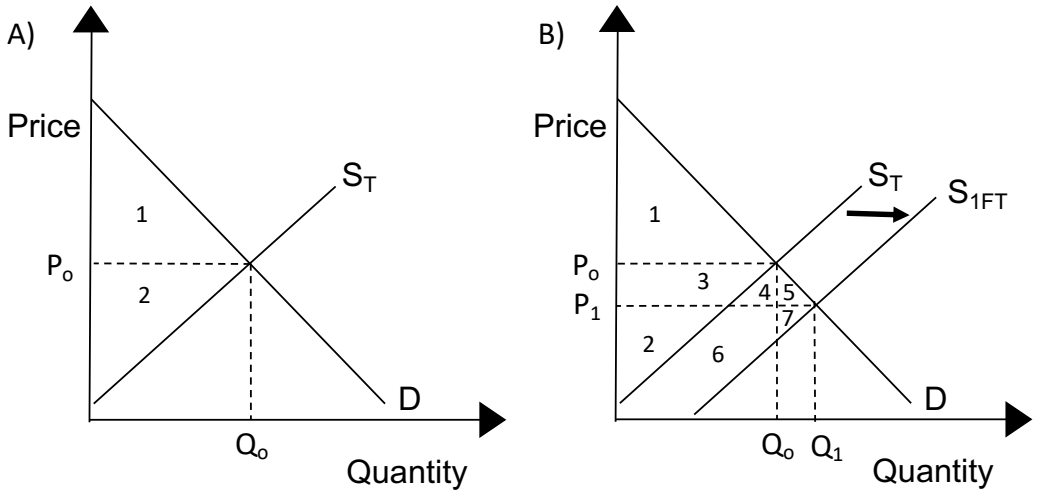

Figure 3. Proposed soybean supply shifts under fluopyram seed treatment. A) Current U.S. soybean production market. S_T: soybean supply curve with current adoption seed treatment for SDS (T). B) Proposed shift in U.S. soybean production market if fluopyram seed treatment was adopted. S_{1FT}: soybean supply curve under fluopyram seed treatment for SDS (FT).

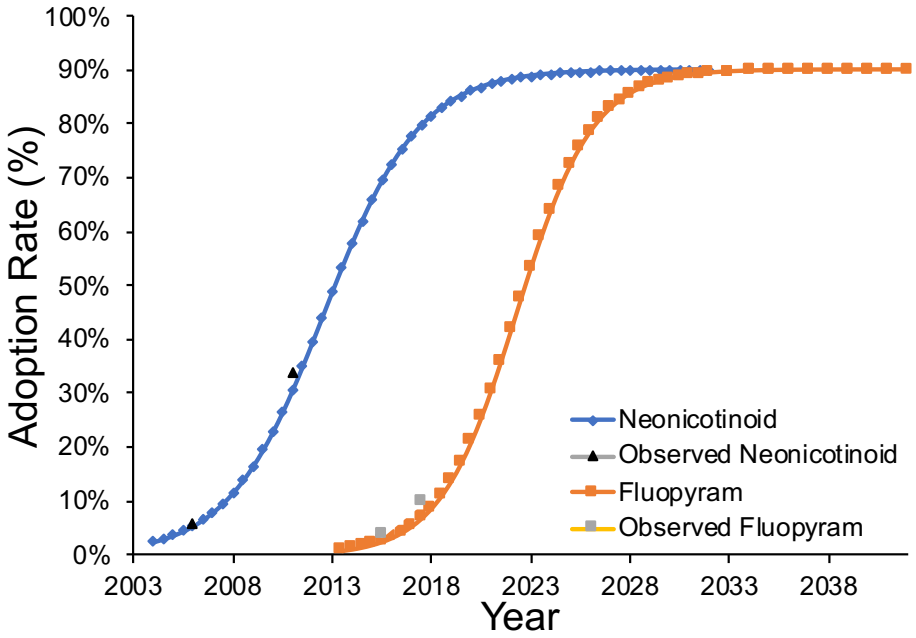

Figure 4. Adoption path of soybean seed treatments. Percent adoption area of soybean neonicotinoid seed treatments from 2004 to 2025. Predicted fluopyram adoption from 2018 to 2032 for SDS associated yield loss aversion.

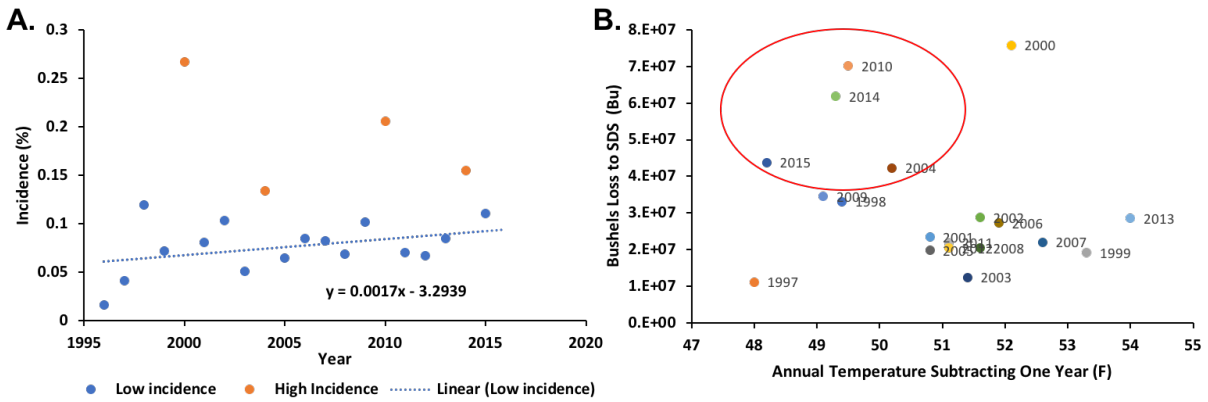

Figure 5. Soybean sudden death syndrome incidence. Scatter plot of incidence of soybean sudden death syndrome from 1996 to 2015 across U.S. soybean production region. Low incidence (blue) with trend line and high or epidemic incidence (orange) (A). Scatter plot of relationship of yield loss to soybean sudden death syndrome (SDS) to mean annual temperature one year before yield loss occurred. Red circle denotes epidemic years when low temperatures preceded the year of an epidemic loss (B).

REFERENCES

REFERENCES

Agrios, G.N. (2004). Plant Pathol. (San Diego: Elsevier Academic Press).

Allen, T.W., Bradley, C.A., Sisson, A.J., Byamukama, E., Chilvers, M.I., Coker, C.M., Collins, A.A., Damicone, J.P., Dorrance, A.E., Dufault, N.S., Esker, P.D., Faske, T.R., Giesler, L.J., Grybauskas, A.P., Hershman, D.E., Hollier, C.A., Isakeit, T., Jardine, D.J., Kelly, H.M., Kemerait, R.C., Kleczewski, N.M., Koenning, S.R., Kurle, J.E., Malvick, D.K., Markell, S.G., Mehl, H.L., Mueller, D.S., Mueller, J.D., Mulrooney, R.P., Nelson, B.D., Newman, M.A., Osborne, L., Overstreet, C., Padgett, G.B., Phipps, P.M., Price, P.P., Sikora, E.J., Smith, D.L., Spurlock, T.N., Tande, C.A., Tenuta, A.U., Wise, K.A., and Wrather, J.A. (2017). Soybean yield loss estimates due to diseases in the United States and Ontario, Canada, from 2010 to 2014. Plant Health Prog. **18,** 19-27.

Alston, J.M., Beddow, J.M., Pardey, P.G. (2008). Agricultural research, productivity, and food prices in the long run. Science. **325,** 1209-1210.

Alston, J.M., Norton, G.W., and Pardey, P.G. (1998). Science under scarcity: Principles and practice for agricultural research evaluation and priority setting. (New York: CAB International).

Alston, J.M., Pardey, P.G., Smith, V.S. (1998). Fianncing agricultural R&D in rich countries: what's happening and why. Aust. J. Agr. Resour. Ec. **42,** 51-82.

Bandara, A.Y., Weerasooriya, D.K., Bradley, C.A., Allen, T.W., Esker, P.D. (2019). Dissecting the economic impact of soybean diseases in the United States over two decades. bioRxiv. doi: http://dx.doi.org/10.1101/655837

Bayer Crop Science. (2017). Expanding sds threat in soybeans in a growing concern.

Brar, H.K.B., M.K. (2012). Expression of a single-chain variable-fragment antibody against a *Fusarium virguliforme* toxin peptide enhances tolerance to sudden death syndrome in transgenic soybean plants. Mol. Plant-Microbe Interact. **25,** 817-824.

Chong, S.K., Hildebrand, K.K., Luo, Y., Myers, O., Indorante, S.J., Kazakevicius, A., and Russin, J. (2005). Mapping soybean sudden death syndrome as related to yield and soil/site properties. Soil Till. Res. **84,** 101-107.

Crop Protection Network. (2016). Soybean disease loss estimates from the united states and ontario, canada – 2015. Crop Protection Network.

Douglas, M.R., and Tooker, J.F. (2015). Large-scale deployment of seed treatments has driven rapid increase in use of neonicotinoid insecticides and preemptive pest management in .S. Field crops. Environ. Sci. Tech. **49,** 5088-5097.

Fernandez-Cornejo, J., Beach, E.D., and Huang, W.-Y. (1994). The adoption of ipm techniques by vegetable growers in Florida, Michigan and Texas. J. Ag. Appl. Econ. o **26,** 158-172.

Gaspar, A.P., Mueller, D.S., Wise, K.A., Chilvers, M.I., Tenuta, A.U., and Conley, S.P. (2017). Response of broad-spectrum and target-specific seed treatments and seeding rate on soybean seed yield, profitability, and economic risk. Crop Sci. **57,** 2251-2263.

Greene, C.R., Kramer, R.A., Norton, G.W., Rajotte, E.G., and Robert M., M. (1985). An economic analysis of soybean integrated pest management. Am. J. Agr. Econ. **67,** 567-572.

Hershman, D.E. (2003). Soybean diseases control series: Are we missing opportunities? Part 2: Soybean sudden death syndrome. In Kentucky Pest News (University of Kentucky.).

Jin, H., Hartman, G.L., Nickell, D., and Widholm, J.M. (1996). Phytotoxicity of culture filtrate from *Fusarium solani*, the causal agent of sudden death syndrome of soybean. Plant Dis. **80,** 922-927.

Johansson, R.C., Livingston, M.J., Westra, J., and Guidry, K. (2006). Simulating the u.S. Impacts of alternative asian soybean rust treatment regimes. Agricultural and Resource Economics Review **35,** 227-242.

Kandel, Y.R., Leandro, L.F., and Mueller, D.S. (2019a). Effect of tillage and cultivar on plant population, sudden death syndrome, and yield of soybean in Iowa. Plant Heal. Prog.**,** doi:10.1094/PHP-1010-1018-0063-RS.

Kandel, Y.R., Wise, K.A., Bradley, C.A., Chilvers, M.I., Tenuta, A.U., and Mueller, D.S. (2016). Fungicide and cultivar effects on sudden death syndrome and yield of soybean. Plant Dis. **100,** 1339-1350.

Kandel, Y.R., Mueller, D.S., Legleiter, T., Johnson, W.G., Young, B.G., and Wise, K.A. (2018a). Impact of fluopyram fungicide and preemergence herbicides on soybean injury, population, sudden death syndrome, and yield. Crop Prot. **106,** 103-109.

Kandel, Y.R., Bradley, C.A., Chilvers, M.I., Mathew, F.M., Tenuta, A.U., Smith, D.L., Wise, K.A., and Mueller, D.S. (2019b). Effect of seed treatment and foliar crop protection products on sudden death syndrome and yield of soybean. Plant Dis.**,** PDIS-12-18-2199-RE.

Kandel, Y.R., McCarville, M.T., Adee, E.A., Bond, J.P., Chilvers, M.I., Conley, S.P., Giesler, L.J., Kelly, H.M., Malvick, D.K., Mathew, F.M., Rupe, J.C., Sweets, L.E., Tenuta, A.U., Wise, K.A., and Mueller, D.S. (2018b). Benefits and profitability of fluopyram-amended seed treatments for suppressing sudden death syndrome and protecting soybean yield: A meta-analysis. Plant Dis. **102,** 1093-1100.

Koenning, S.R., and Wrather, J.A. (2010). Suppression of soybean yield potential in the continental united states by plant diseases from 2006 to 2009. Plant Health Prog. **11,** 10.1094/php-2010-1122-1001-rs.

Leandro, L.F.S., Eggenberger, S., Chen, C., Williams, J., Beattie, G.A., and Liebman, M. (2018). Cropping system diversification reduces severity and incidence of soybean sudden death syndrome caused by *Fusarium virguliforme*. Plant Dis. **102,** 1748-1758.

Leandro., L.F.S., Robertson, A., Mueller, D.S., Yang, X.B. (2013). Climatic and environmental trends observed during epidemic and non-epidemic years of soybean sudden death syndrome in Iowa. Plant Health Prog. On-line: PHP-2013-0529-01-RS.

Musser, W.N., Tew, B.V., and Epperson, J.E. (1981). An economic examination of an integrated pest management production system with a contrast between e-v and stochastic dominance analysis. J. Ag. Appl. Econ. **13,** 119-124.

Myers, C., and Hill, E. (2014). Benefits of neonicotinoid seed treatments to soybean production, E.P. Agency, ed.

Navi, S.S., Yang, X.B. (2016). Sudden death syndrome- a growing threat of losses in soybeans. CAB Revivews. doi: 10.1079/PAVSNNR201611039.

NASS. (2017). Acreage (Washington, D.C: U.S. Department of Agriculture, National Agricultural Statistics Service).

NASS. (2019). Agircultural statistics data base (U.S. Department of Agriculture, National Agricultural Statistics Service).

Nettles, R., Watkins, J., Ricks, K., Boyer, M., Licht, M., Atwood, L.W., Peoples, M., Smith, R.G., Mortensen, D.A., and Koide, R.T. (2016). Influence of pesticide seed treatments on rhizosphere fungal and bacterial communities and leaf fungal endophyte communities in maize and soybean. Appl. Soil Ecol. **102,** 61-69.

Njiti, V.N., Shenaut, M.A., Suttner, R.J., Schmidt, M.E., and Gibson, P.T. (1996). Soybean response to sudden death syndrome: Inheritance influenced by cyst nematode resistance in pyramid × douglas progenies. Crop Sci. **36,** 1165-1170.

Norton, G.W., and Mullen, J. (1994). Economic evaluation of the integrated pest management programs: A literature review. (Blacksburg, VA: Virginia Tech).

O'Donnell, K., Sink, S., Mercedes Scandiani, M., Luque, A., Colletto, A., Biasoli, M., Lenzi, L., Salas, L., González, V., Ploper, L.D., Formento, N., Pioli, R.N., Aoki, T., Yang, X.B., and Sarver, B.A.J. (2010). Soybean sudden death syndrome species diversity within North and South America revealed by multilocus genotyping. Phytopathol. **100,** 58-71.

Rossman, D.R., Byrne, A.M., and Chilvers, M.I. (2018). Profitability and efficacy of soybean seed treatment in Michigan. Crop Prot. **114,** 44-52.

Roy, K.W., Rupe, J.C., Hershman, D.E., and Abney, T.S. (1997). Sudden death syndrome of soybean. Plant Dis. **81,** 1100-1111.

Rupe, J.C. (1989). Frequency and pathogenicity of *Fusarium solani* recovered from soybeans with sudden death syndrome. Plant Dis. **73,** 581-584.

Santísima-Trinidad, A.B.L., del Mar Montiel-Rozas, M., Diéz-Rojo, M.Á., Pascual, J.A., and Ros, M. (2018). Impact of foliar fungicides on target and non-target soil microbial communities in cucumber crops. Ecotox. Environm. Safety **166,** 78-85.

Scherm, H., and Yang, X.B. (1999). Risk assessment for sudden death syndrome of soybean in the north-central United States. Agricultural Systems **59,** 301-310.

Schulz, T., Thelen, K., Difonzo, C. (2007). Neonicotinoid seed treatments for soybeans. Michigan State Extension. Retrieved August 15, 2019 from https://www.canr.msu.edu/news/neonicotinoid_seed_treatments_for_soybeans.

Song, F., and Swinton, S.M. (2009). Returns to integrated pest management research and outreach for soybean aphid. J. Econ. Ent. **102,** 2116-2125.

Stern, V.M., Smith, R.F., van den Bosch, R., and Hagen, K.S. (1959). The integrated control concept. Hilgardia **29,** 81-101.

Syngenta. (2019) Be prepeared for soybean sudden death syndrome in 2019. Know More Grow More. Retrieved August 15, 2019 from https://knowmoregrowmore.com/be-prepared-for-soybean-sudden-death-syndrome-in-2019/

United Soybean Board. (2017). Soybean disease loss estimates report 2011.

United Soybean Board. (2019). National soybean checkoff database.

USDA. (2019). Department of agriculture agricultural projections to 2028. (Washington, D.C.: U.S. Department of Agriculture).

USDA. (2019). Commodity costs and returns. (Washington, D.C.: U.S. Department of Agriculture, Economic Research Service).

Vick, C.M., Bond, J.P., Chong, S.K., and Russin, J.S. (2003). Response of soybean sudden death syndrome to tillage and cultivar. Can. J. Plant Pathol. **28,** 77-83.

Von Qualen, R.H., Abney, T.S., Huber, D.M., and Schreiber, M.M. (1989). Effects of rotation, tillage, and fumigation on premature dying of soybeans. Plant Dis. **73,** 740-744.

Wang, S.L., Heisey, P.W., Huffman, W.E., Fuglie, K.O. (2013). Public R&D, and U.S. agricultural productivity growth: dynamic and long-run relationships. Amer. J. Agr. Econ. **95,** 1287-1293.

Ward, B., Lindsey, L., and Loux, M. (2018). Soybean production budget (RoundUp ready)-2019. In Farm Office (Ohio State University).

Xing, L., and Westphal, A. (2006). Interaction of *Fusarium solani* f. sp. *Glycines* and *Heterodera glycines* in sudden death syndrome of soybean. Phytopathol. **96,** 763-770.

Xing, L., and Westphal, A. (2009). Effects of crop rotation of soybean with corn on severity of sudden death syndrome and population densities of *Heterodera glycines* in naturally infested soil. Field Crops Res. **112,** 107-117.

CHAPTER 3

Implications of *Fusarium virguliforme* Temporal Colonization of Corn: Tillage and Residue Management of Soybean Sudden Death Syndrome

This chapter is unpublished, with intention to submit to Plant Disease.

Araldi Da Silva, G., Baetsen-Young, A. M., Jacobs, J. L., Byrne, A., Kandel Y., Leandro, L., Mueller, D. S., Smith, D. L., Teutna, A., Wise, K. A., Day, B., Chilvers, M. I. 20XX. Implications of *Fusarium virguliforme* Temporal Colonization of Corn: Tillage and Residue Management of Soybean Sudden Death Syndrome. Plant Dis. XXX:XX-XX.

Abstract

The asymptomatic host range of *Fusarium virguliforme* includes corn, a common crop rotation with soybean that we hypothesize may alter *F. virguliforme* population dynamics and disease management. A field-based approach explored the temporal dynamics of corn and soybean root colonization by *F. virguliforme* under tillage and residue management. Experiments were conducted in IA, IN, MI, Ontario and WI for two years. Corn and soybean roots were sampled at 1, 2, 4, 8, 12, and 16 weeks after planting (WAP) in MI, and corn roots 4 or 5, 8 and 16 WAP for IA, IN, and WI. DNA was extracted and analyzed by real-time qPCR for *F. virguliforme* quantification. Trials were rotated between corn and soybean, containing a two factorial of no tillage or tillage and no- corn residue or residue. In 2016, low (ca. 100 fg/10 mg root tissue) *F. virguliforme* was detected in the *F. virguliforme* inoculated MI, IA and IN, and non-inoculated WI corn fields, but in 2017 higher levels of *F. virguliforme* DNA was detected in MI, IA and IN across sampling time points. Overall, trials in MI, IA, IN and WI revealed consistent low-level detection of *F. virguliforme* in corn roots. Cultural tillage practices showed inconsistent effects on *F. virguliforme* root colonization between trials and locations. Yet, residue management did not alter root colonization of corn or soybean by *F. virguliforme*.

Introduction

Sudden death syndrome (SDS) is a devastating soybean (*Glycine max*) disease with an estimated annual yield loss impact around $330 million dollars in the United States, placing this disease in the top 5 most impactful on soybean production (Koenning and Wrather, 2010; Allen et al., 2017). Since the first report in 1971 in Arkansas, soybean SDS has quickly spread to nearly all soybean producing states (Hartman et al., 2015). In North America, soybean SDS is caused by the soilborne fungus *F. virguliforme* and *F. brasiliense*, while in South America, an additional two closely related species (e.g., *F. tucumaniae* and *F. cuneirostrum)* have also been identified as casual agents within the *Fusarium solani* species complex clade 2 (FSSC2) (O'Donnell et al., 2010; Wang et al., 2019b). *Fusarium virguliforme* is an asexual fungus that survives in soil and crop residues (Roy et al., 1997; O'Donnell et al., 2010). This fungus infects soybean roots during early plant growth stages causing root rot (Jin et al., 1996). As the pathogen colonizes the xylem tissues, it secretes phytotoxins, initiating programmed cell death of the soybean leaf (Brar, 2012). This host response creates a symptom of interveinal leaf scorch, characteristic of SDS. Root rot and leaf scorch lead to a reduction of overall plant biomass, flowers, pods, and yield (Roy et al., 1997). Yield losses of up to 80% have been reported in highly infested fields, but typically yield losses of 5 to 15% are observed (Hershman et al., 1990).

Integrated pest management is the strongest approach to control SDS, because no single strategy can fully manage the disease. One of the tactics to control SDS is the use of soybean cultivars with partial genetic resistance (Chang et al., 2018). However, if disease intensity is high in soybean fields, the partial resistance can be broken (Njiti et al., 1996). Environmental

conditions inducing high disease intensity are cool temperatures and wet compacted soil during planting, and increased soil moisture during early reproductive growth stages (Rupe, 1989; Roy et al., 1997; Scherm and Yang, 1999; Chong et al., 2005). Thus, planting into warmer soils by delaying planting date can been considered to reduce severity of SDS (Hershman et al., 1990), but, recently, multi-location research demonstrated that earlier planting is not strictly correlated with higher SDS severity, indicating that yield maximization in SDS infested fields can be achieved without altering planting date (Kandel et al., 2016a). Furthermore, the interaction of soybean cyst nematode (*Heterodera glycines*) with *F. virguliforme* (Gao et al., 2006; Westphal et al., 2014), and the disease pressure specific profitability of seed treatments for SDS (Kandel et al., 2016b; Gaspar et al., 2017) have further confounded disease management recommendations.

Cultural practices of tillage and residue management have independently been explored to reduce SDS symptoms development. Tillage can reduce root infection from *F. virguliforme*, by decreasing soil moisture and increasing soil temperature through increased porosity of the soil (Roy et al., 1997; Vick et al., 2003). However, a new study in a field with a long-term till and no-till treatments revealed that tillage does not impact soybean root and foliar SDS disease severity or yield (Kandel et al., 2019). Implementation of tillage has reduced SDS severity and root colony forming units (CFUs) of *F. virguliforme*, but has not decrease soil CFUs (Vick et al., 2003). Subsequently, infected soybean roots from no-till fields maintained summer level CFUs of *F. virguliforme* through the fallow season, whereas soil did not harbor detectable CFUs of *F. virguliforme* to spring (Luo et al., 2001).This indicates that plant residue, especially in no-till fields may lead to increased *F. virguliforme* populations and SDS

severity. Navi and Yang (2016) explored this hypothesis that plant residue contributes to *F. virguliforme* populations and found that corn (*Zea mays*) kernel residue increases soil CFUs of *F. virguliforme* in inoculated greenhouse and field experiments three and 12 months post treatment establishment. Freed et al. (2017) also demonstrated that corn kernels exudates can increase *F. virguliforme* population in vitro, and infested corn kernels can cause high soybean foliar and root rot disease severity. These studies suggest that tillage and residue management provide an opportunity to control *F. virguliforme* populations and SDS disease severity.

Another strategy for field crop disease management is crop rotation, which reduces pathogen population within soils by planting non-hosts for multiple years (Agrios, 2004). Previous research regarding corn, soybean, and wheat (*Triticum aestivum*) rotation found reduced SDS yield losses, when compared to continuous soybean (Von Qualen et al., 1989; Roy et al., 1997). However, more recent studies have shown that corn-soybean rotation has not reduced SDS incidence and severity (Hershman, 2003; Xing and Westphal, 2009; Leandro et al., 2018). A greenhouse study in 2012 indicated that corn can be an asymptomatic host for *F. virguliforme*. Kolander et al., (2012) found that *F. virguliforme* is able to colonize corn roots, as well as wheat, ryegrass, pigweed and lambsquarters roots without developing root or foliar symptoms, or reducing biomass, opposed to infected soybean, alfalfa, Canadian milk vetch, pinto and navy bean, white and red clover, pea, sugar beets and canola. Whereas, more recently Kobayashi-Leonel et al., (2017) explored the susceptibly cover and rotation crops to *F. virguliforme* and detected similar levels of *F. virguliforme* DNA as Kolander et al. (2012) in corn roots, but suggested that corn is a non-host because the *F. virguliforme* DNA from

corn roots was lower than soybean roots. Therefore, inconsistencies persist within the research community regarding whether crop rotation of corn and soybean enhances or reduces the severity of SDS, but have instead revealed a potential broad host range for *F. virguliforme*.

Although tillage and residue management practices have been explored for SDS management, no research has explored the impact of cultural tactics upon *F. virguliforme* colonization of corn, and the ability of this colonization to alter subsequent SDS symptoms when rotated to soybean. The dissection of tillage and residue management in combination with corn-soybean rotation tactics should provide clarity to variable reports, revealing if the interaction of these two cultural practices promotes or suppresses SDS. To examine the potential of cultural practices to alter disease development, trials were established in four states (IN, IA, MI, WI) and Ontario, Canada during the 2015 to 2017 field seasons. The objectives of this study were to: (i) identify if *F. virguliforme* can colonize corn, a predominate rotation crop, (ii) determine the temporal dynamics of corn and soybean root colonization by *F. virguliforme* under field conditions, and (iii) decipher if tillage and plant residue management affect *F. virguliforme* root colonization, SDS foliar symptom development and soybean yield.

Materials and Methods

Inoculum Preparation of *Fusarium virguliforme*

Inoculum was created for field experiments in Indiana, Iowa and Michigan by transferring a single-spore-derived isolate of *F. virguliforme* (Table 5) onto Nash Snyder agar (NSA) (Leslie and Summerell, 2006) in 100 mm x 15 mm petri dishes, and allowed to colonize the medium at 21°C ± 1°C in ambient light for three weeks. A sorghum grain inoculum was created by soaking sorghum grains in deionized water overnight. After draining, sorghum grains were placed in bags and sterilized by autoclaving. Media colonized with *F. virguliforme* was added to the cooled sorghum grains and the bags were sealed. The bags were incubated at 21°C ± 1°C with ambient light for 30 days and mixed every other day. Upon uniform grain colonization, the inoculum was spread on trays covered with paper and dried at room temperature. Colony forming units were utilized to determine strain concentration and contamination by counting colonies of 10^4 and 10^5 diluted spore suspensions on nutrient agar.

Corn Residue Establishment

In 2015, a three-year study was established in Indiana, Iowa, Michigan, Ontario and Wisconsin within a site location with a history of SDS. Each site was tilled and planted with corn at 84,014 seeds/ha on a 76.2 cm row spacing (Table 5). In Iowa, *F. virguliforme* inoculum was broadcasted after planting at 1.4 kg per 46 m^2. In Indiana, the trial was

inoculated with 4.9 g per row meter of inoculum at planting, and 414 mL per plot was broadcasted after planting at growth stage V5 on June 24. The Wisconsin site was not inoculated, and in Michigan, the site was inoculated at 11.5 ml/row meter and then broadcasted at 31.7 g per row meter on June 18th. Fertility and weed control followed local agronomic recommendations, and no foliar fungicides were applied throughout the growing season.

Field Site Design

Treatments of tillage and residue arrangement varied by location, but all treatments were applied in the fall of 2015. Iowa, Indiana and Ontario, Canada arranged treatments in a split-split plot design, with chisel plow tillage or no-till as the whole plot, soybean or corn as the sub-plot, and residue or no-residue as the sub-sub plot. Each sub-sub plot treatment consisted of four rows 6 m long, replicated four times and randomized within the sub-plot. Michigan designed the treatments in a strip-split plot design with corn or soybean as the whole plot. Then a strip of chisel plow tillage and no-till, 13 feet wide were randomly assigned within a block, and repeated four times within each whole plot. Opposing to strips of tillage, strips of residue or no-residue were applied to distinguish individual plots as four rows wide and was repeated four times, creating four replicates of each treatment within a single block. Wisconsin treatments were designed in a split plot design, with corn or soybean as the whole plot, but assigned the factors of chisel plow tillage or no-till and residue or no-residue to four blocks, in a completely randomized design. For all locations crop rotation included, in 2016 soybean followed where corn was planted in 2015 in half of the treatments,

and corn followed corn in the remaining treatments. In 2017, corn followed soybean 2016 planting, and soybean followed corn 2016 planting (Table 6).

In 2016 and 2017, planting date and cultivar varied by site (Table 5). Corn was planted at 98,840 and 308,875 seeds/ha for soybean in Iowa and Indiana, and 84,014 corn seeds/ha and 345,940 soybean seeds/ha in Michigan and Wisconsin into either no-tilled soil or tilled soil, that was chisel plowed in spring. Wisconsin did not inoculate either corn or soybean at planting. Michigan inoculated corn at planting with 4 ml per row meter. Indiana inoculated corn in 2016 at 4.1 mL per row meter but corn or soybean were not inoculated in 2017. Iowa did not inoculate corn in 2016, but soybean was inoculated at 8.2 mL per row meter in 2017 only. Soybean was irrigated in Michigan with a drip tape at V3 growth stage (Fehr et al., 1971) in 2016 and 2017. Both corn and soybean were irrigated in Indiana throughout the trial. In 2016, sandhill cranes (*Grus canadensis*) did extensive feeding damage to the corn stand in the Michigan trial, and thus had to be replanted on June 24 using different corn variety (DK5261), which was not inoculated. Fertility and weed control followed local agronomic recommendations, and no foliar fungicides were applied throughout the growing season. Following soybean harvest, corn residue was removed and/or soil was tilled for respective treatments.

Root Sampling and Processing

Michigan. In 2016 and 2017, roots were sampled at one, two, four, eight, 12 and 16 weeks after planting for both corn and soybean. Three roots were taken from the outer two rows of

one plot of each treatment from each block (n=4). The aboveground biomass was removed at the soil line, and loose soil was removed from the roots. The remaining soil was then washed off the roots, and roots were dried at ambient temperature. In 2016, due to crane feeding damage, remaining corn plants from the first planting were sampled throughout the growing season, but plants from the no-till treatments were sampled at a whole block level rather individual plot for blocks three and four, until no plants remained.

Iowa, Indiana and Wisconsin. In 2016, three corn plants were sampled from the two outer rows of each plot and sent to Michigan State University. Roots were sampled at 4, 8 and 16 weeks after planting for Iowa, Indiana and Wisconsin in 2016. In 2017, roots were received from Iowa and Indiana at 5, 8, and 16 weeks after planting. The aboveground biomass was removed at the soil line, and loose soil was removed from the roots before shipping. Upon arrival the roots were washed, then air dried at ambient temperature and stored at room temperature.

The primary root from the dried corn roots were sampled at each time point and ground into a fine powder by a TissueLyser (Qiagen) with a steel bead. Lower portions of soybean lateral and tap roots were sampled at each time point and were also ground into a fine powder by a TissueLyser with a steel bead. The homogenized roots were stored at room temperature until further processing.

DNA Extraction

DNA was extracted with an automated protocol with KingFisher Flex (Thermo Fisher Scientific) and Mag-BIND Plant DNA Plus 96 kit (Omega) from 10 mg of dried root power for both soybean and corn samples. The powder was loaded into 96 well 2 mL plate (Denville), and mixed with 700 μL of lysis buffer with 20 μL of proteinase K. Plates were incubated for one hour at 65°C with mixing every 20 minutes, after which plates were spun at 5,000 g for 20 minutes to clear the supernatant. Four hundred and fifty microliters were transferred to a KingFisher 96-deep well plate, and the DNA was extracted following manufacturers recommendations. DNA concentration was determined using a Nanodrop (ThermoFisher Scientific).

Fusarium virguliforme DNA Quantification

Fusarium virguliforme DNA detection was performed using a real time quantitative PCR (qPCR) *F. virguliforme* specific assay (Wang et al., 2015). The real time reactions were performed in duplicate on the ABI StepOnePlus thermocycler (Applied Biosystem), with a total reaction volume of 20 μL containing 2 μL of sample DNA. A three-point standard curve ranging from 1 ng to 100 fg of genomic *F. virguliforme* DNA was utilized in each 96-well experimental run to ensure PCR efficiency and to calculate sample DNA concentration.

Data Analysis

Data were analyzed in R v3.4.1 (R Development Core Team, 2010). Analysis of variance (ANOVA) was calculated using the "lme4" (Bates, 2015) "nlme" (Pinheiro, 2019) and "Car" (Fox and Weisberg, 2011) package. The average was taken of plants sampled within a plot to represent a single observation. Tillage and residue treatments were defined as fixed effects. For repeated measures sampling time was considered a fixed effect. Year by location interactions were tested and if significant ($P < 0.05$) each location was analyzed within year separately for the effects of tillage and residue. Means were separated within treatments or time by Tukey HSD "multicomp" (Hothorn, 2008) by $\alpha < 0.05$. Graphs were visualized using "ggplot2" (Wickham, 2016).

Results

Tillage and time significantly affected *F. virguliforme* DNA detected within soybean and corn roots. Thus, the main effects of tillage and residue are presented, as each site year was analyzed independently from significant location by year interaction.

Temporal Dynamics of *Fusarium virguliforme* Colonization of Corn Roots

2016. To understand the temporal pattern of corn primary root colonization, DNA levels were determined across three timepoints in Iowa, Indiana and Wisconsin sites and six timepoints in Michigan. *Fusarium virguliforme* DNA was detected within all treatments at

four weeks after planting (WAP) at low levels (less than 250 fg/10 mg dried root tissues, Figure. 6A and 7A). Additionally, *F. virguliforme* was detected at one and two WAP sampling time points in Michigan (Figure 8A and B). However, no root or foliar chlorosis and necrosis could be assigned to as symptoms derived from *F. virguliforme* colonization. DNA quantities changed throughout the growing season and varied by location. Across residue treatments, *F. virguliforme* DNA quantities were significantly higher at 4 WAP than 16 WAP in Indiana ($P = 0.0209$ and $P = 0.0087$, Table 7). Michigan and Iowa had similar levels of DNA quantities at four and 16 WAP in both tillage treatments (Iowa $P < 0.0389$, Michigan $P < 0.0258$) and Michigan no-residue treatment ($P = 0.0486$). The highest *F. virguliforme* DNA quantities were detected at 16 WAP across all tillage and residue treatments in Wisconsin ($P < 0.0001$, Table 5). Within earlier timepoints in the Michigan site, the treatment of tillage or residue had the highest DNA quantities at 1 WAP ($P < 0.0001$). Yet, in the no-till or no-residue treatment *F. virguliforme* DNA quantities were highest at 2 WAP ($P < 0.0001$, Table 8).

Comparison of *F. virguliforme* DNA quantities across tillage or residue treatments at each timepoint did not reveal any significant difference within each location after four WAP ($P > 0.0651$, Figure 6A and 7A). Two weeks after planting, *F. virguliforme* DNA quantities of this fungus in Michigan were significantly higher in the no-till treatment, when compared to the tillage treatment ($P = 0.0027$, Figure 8A).

To explore the effect of tillage or residue management over time, the area under the DNA progress curve (AUDPC) of *F. virguliforme* was calculated for each treatment. Comparing AUDPCs across tillage or residue treatments did not reveal any significant differences within

Iowa, Indiana and Wisconsin ($P > 0.2349$, Fig 4B and 5B). However, when considering the AUDPCs across the six sampling timepoints in Michigan, significantly higher *F. virguliforme* AUDPC was observed from samples from no-till treatments when compared to the tillage treatment ($P = 0.0038$, Figure 8C).

2017. The impacts of tillage and residue cultural practices on corn primary root colonization by *F. virguliforme* were evaluated in Iowa and Indiana across three timepoints, as well as Michigan across six timepoints. The first sampling timepoint from Iowa and Indiana in 2017 was at five WAP rather than four WAP, as in 2016. Similarly, to 2016, *F. virguliforme* DNA was detected at five WAP in all treatments, across all locations (Figure 6A, 7A and Table 7), ranging from 389.1 fg/10 mg of dried root tissue within the tillage treatment at the Indiana site, to 13,607.5 fg/10 mg of dried root tissue within the no-residue treatment at the Iowa site. Detected DNA quantities within the first sampling timepoint varied greatly by location, ranging from 389.1 to 655.0 fg/10 mg of dried root tissues in Indiana, Michigan fluctuated from 3,574.5 to 7,904.4 fg/10 mg dried root tissues, and Iowa varied from 5,924.6 to 13,607.5 fg/10 mg dried root tissues. The first sampling time point after planting contained the highest DNA quantities across all treatments within Iowa and Michigan no-till or residue treatments at four WAP ($P < 0.04$). At the Indiana site, tillage, residue and no-residue treatments all exhibited higher *F. virguliforme* DNA quantities detected at five WAP when compared to 16 WAP, but similar eight WAP ($P < 0.02$, Table 7). Sampling of corn roots at one or two WAP in Michigan revealed statistically similar levels of *F. virguliforme* DNA quantities to four WAP in all treatments ($P < 0.0001$), Table 8). Interestingly, tillage and no-

residue treatments at 16 WAP had similar DNA levels to one, two and four WAP ($P < 0.0001$, Table 7).

Treatment differences comparing tillage to no-till treatments were apparent within sampling timepoints at the Iowa location, with higher *F. virguliforme* DNA quantities in no-till at five WAP ($P = 0.001$) and eight WAP ($P = 0.0334$) (Figure. 6A). No differences of *F. virguliforme* DNA quantities were detected at Indiana or Michigan locations for tillage or residue treatments ($P > 0.2649$, Figure 6A, 5A, 6A).

When analyzing treatments over time, a comparable pattern appeared of *F. virguliforme* colonization of corn primary roots in Iowa within time points (Figure 6B). The AUDPC was significantly higher in the no-till treatment than the tillage treatment ($P = 0.0004$). While similar trends of elevated *F. virguliforme* AUDPCs were detected Indiana and Michigan in no-till treatments, no significant differences were found between till and no-till treatments ($P > 0.3115$, Figure 6B). Treatments of residue or no-residue did not have a significant effect on AUDPCs in any location ($P > 0.0783$, Figure 7B).

Temporal Dynamics of *Fusarium virguliforme* Colonization of Soybean Roots Under Cultural Management

2016. *Fusarium virguliforme* DNA was discovered in soybean tap root tissues as early as one WAP, across all treatments in Michigan (Figure 9 A and B, Table 9). During 2016, the DNA quantities varied from 102.1 to 476.7 fg/10 mg of dried root tissues) at one WAP across

treatments and did not significantly increase until eight WAP for all treatments ($P < 0.0001$). DNA quantities of *F. virguliforme* were significantly higher at 12 WAP than eight WAP ($P < 0.0001$). The highest *F. virguliforme* DNA quantities were observed at 16 WAP ($P < 0.0001$), ranging from 1,004,828.8 to 1,607,338.6 fg/10 mg dried root tissues (Table 9). Comparing *F. virguliforme* DNA quantities across residue or tillage treatments did not reveal any significant effects ($P > 0.9633$, Figure 9A and B). Analyzing the AUDPC of each cultural treatment over time sampling time course found similar DNA quantities between tillage or residue treatments ($P > 0.3139$, Figure 9C and D).

2017. As observed in 2016, *F. virguliforme* DNA was detected in soybean roots at one WAP. However, the overall quantities of DNA detected at one WAP tended to be lower in 2017 (Table 9). *Fusarium virguliforme* DNA quantities detected increased at two WAP in no-till and no-residue treatments ($P < 0.0001$), whereas DNA detected in tilled and residue treatments did not significantly increase until four WAP ($P < 0.0001$). *Fusarium virguliforme* DNA quantities were significantly higher at 12 WAP than two WAP, but not at four or eight WAP, across all treatments ($P < 0.0001$, Table 9). Quantities from *F. virguliforme* were the highest at 16 WAP for all treatments ($P < 0.0001$), ranging from 126,716.9 to 2,488,780.1 fg/10 mg dried root tissues (Table 9).

Across tillage or residue treatments at each timepoint, no significant effect was found upon *F. virguliforme* DNA quantities from one to 12 WAP ($P > 0.0875$, Figure 9A and B). Yet, at 16 WAP *F. virguliforme* DNA quantities were significantly higher in the no-till treatment ($P < 0.0169$, Figure 9A) when compared to the tillage treatment. Exploring the effects of

treatments upon *F. virguliforme* colonization of soybean lower tap and lateral roots over time revealed comparable trends to the temporal results (Figure 9C and D). Specifically, no significant differences of AUPDCs between residue treatments ($P = 0.2845$). However, tillage management, particularly the implementation of no-till increased detected *F. virguliforme* DNA AUPDC when compared to tilled ($P = 0.0069$, Figure 9C).

Discussion

The detection of *F. virguliforme* in corn roots across four states demonstrates the ability of this soybean pathogen to colonize living corn tissue. Additionally, this fungus was quantified inside both soybean and corn roots at one WAP, highlighting the early interactions of *F. virguliforme* and hosts. Cultural treatment of no-till may enhance *F. virguliforme* root colonization in corn and soybean roots, but this elevated colonization was not consistently observed in all field sites, indicating potential need for site specific management. Corn residue did not alter *F. virguliforme* root colonization of corn or soybean. This gained knowledge suggests that corn in addition to soybean should be considered as a host for SDS disease management.

Infield Detection of *Fusarium virguliforme* in Corn Roots.

Soybean are often rotated with corn to reduce soilborne pathogen populations. Yet, corn rotations with soybeans have not reduced SDS severity and incidence (Xing and Westphal, 2009; Leandro et al., 2018). In field experiments during 2016 and 2017 across four North

Central soybean production states, *F. virguliforme* was detected in the primary root tissues of corn. *Fusarium virguliforme* was detected in living corn roots within experimental sites with variable management, including without pathogen inoculation, irrigation, and differing corn cultivars (Table 1), highlighting the relevance of this detection across soybean production. Previously colonization of corn roots by *F. virguliforme* was discovered in greenhouse settings (Kolander et al., 2012; Kobayashi-Leonel et al., 2017), but our findings are the first report of living corn root colonization in field settings.

The colonization of corn roots among other crops by *F. virguliforme*, demonstrates the broad host range of this soybean pathogen (Kolander et al., 2012). The increasing reports of *F. virguliforme* colonization of corn roots, communicates the need to consider corn as an asymptomatic host. Therefore, crop rotations to manage SDS should contain crops outside of corn or soybean to reduce SDS severity (Leandro et al., 2018) and potentially alter the soil microbiome of with rotation of diverse crop species (Gdanetz and Trail, 2017) .

Temporal Dynamics of *Fusarium virguliforme* Root Colonization

Development of root diseases are distinct from foliar counterparts, as within soil environments the fungal propagules are majorly immobilized, and the plant roots move throughout the soil. Thus, the probability of infection or fungal root colonization highly depends on the growth stage of the host root during initial contact with the fungus (Huisman, 1982). The elevated levels of *F. virguliforme* DNA across early (one to four WAP), corresponding to active growth and development of the primary root system within corn

(Fusseder, 1987). These developing corn roots secrete exudates, which are documented to stimulate *F. virguliforme* growth (Freed et al., 2017). However, as post embryonic roots (i.e. crown and nodal roots) develop, nutrient acquisition and water uptake from the primary root decreases (Hochholdinger et al., 2004; Ahmed et al., 2018). Corn samples in this study at four or five WAP had minimal crown root development and at eight WAP, corn roots had matured. Decreases in *F. virguliforme* DNA biomass at eight WAP may correspond with these changes in root development and metabolic activity. The decrease in this fungal DNA biomass at eight WAP and root activity could potentially be caused by senescence of cortical root cells by programed cell (Schneider and Lynch, 2017). Fusseder (1987) noted a decrease of viable nuclei in the cortex of the primary root after the nine-leaf stage, indicating cell death of primary root cortex, which corresponds to the aboveground growth stage and a reduction of *F. virguliforme* biomass during the eight WAP timepoint. Senescence of roots attenuates plant defenses, enabling saprophytic colonization by *F. virguliforme* at 12 and 16 WAP (Schneider and Lynch, 2017).

The quantities of *F. virguliforme* DNA within corn roots varied substantially between 2016 and 2017 field seasons. There were two major differences that could account for variation of *F. virguliforme* colonization of corn roots. The weather during months of May and June, when early root fungal interactions occurred, differed between 2016 and 2017. The temperature was 0.82 °C in May, and 0.48 °C in June cooler in 2017 when compared to 2016 when averaged across all locations. Precipitation in 2017 had additional 1.42 cm in May, and 1.37 cm in June, when compared to 2016 (NOAA, 2019). Both temperatures and soil moisture play a key role in colonization of plant roots by *F. virguliforme* (Rupe, 1989; Roy et al., 1997;

Scherm and Yang, 1999; Chong et al., 2005) and these annual differences may have altered temporal dynamics of root colonization. Secondly, crop rotation from soybean to corn may have added additional *F. virguliforme* inoculum to the soil than a corn-corn rotation. Infected tap roots with sporulating *F. virguliforme* may have increased fungal inoculum, more than colonized corn roots. Infested soybean residue provides an overwintering structure for *F. virguliforme* (Luo et al., 2001). Recently, two-year corn-soybean rotations were found to contain five-fold greater *F. virguliforme* density in soil than a four-year corn-soybean-oat+alfalfa-alfalfa rotations, indicating short crop rotations could promote greater *F. virguliforme* soil persistence (Leandro et al., 2018). Thus, the rotation to soybean, between corn plantings could have increased the opportunity for infection of corn roots in 2017.

Fusarium virguliforme Temporal Dynamics in Soybean Roots

Similar to *F. virguliforme* corn root colonization, *F. virguliforme* DNA was detected within soybean roots at one WAP across 2016 and 2017 experiments. This detection at one WAP illustrates the early interactions between soybean roots and *F. virguliforme*, as observed by (Gongora-Canul et al., 2011). *Fusarium virguliforme* DNA quantities gradually increased at four and eight WAP, but rapidly increased at 12 and 16 WAP. This rapid rate of colonization by *F. virguliforme* in senescensing soybean roots was noted by Wang et al. (2019a) and indicates a potential change to saprotrophy from necrotrophy. The temporal dynamics of *F. virguliforme* in soybean roots initializes at a similar level to corn root colonization at one-four WAP (Table 6 and 7), but then diverges as *F. virguliforme* proliferates in soybean roots. Detecting *F. virguliforme* in soybean roots at one WAP, highlights the need to protect soybean

seedlings through the use of resistant germplasm or seed treatments such as fluopyram to prevent colonization (Kandel et al., 2018).

Impacts of Cultural Practices on *F. virguliforme* Root Colonization

The cultural practice of tillage has previously yielded variable management of SDS root or foliar severity. Herein, we discovered similar findings of inconsistent effects of *F. virguliforme* root colonization by use of tillage. Only two of the eight corn field experiments found an increase in *F. virguliforme* root colonization under no-till management, and one of the two soybean field experiments. The remaining experiments did not differ in temporal dynamics of *F. virguliforme* root colonization under tillage or no-tillage management. These experiments support recent findings by Kandel et al. (2019), that tillage does not impact symptom development on root components. However, the increase in *F. virguliforme* colonization under no-tillage implementation in three experiments may indicate site specific factors that enhanced root colonization such as soil chemical and chemical properties (Roy et al., 1997; Vick et al., 2003).

In combination with no-tillage, residue left on the soil surface could potentially act as an inoculum source for *F. virguliforme*. Previous studies have indicated that corn residue could harbor viable *F. virguliforme*, when inoculated (Kolander et al., 2012), and that corn kernels could increase *F. virguliforme* soil populations (Navi and Yang, 2016). Interestingly, we did not observe any effects of corn residue management on *F. virguliforme* colonization of corn or soybean roots. These findings contrast with the common conviction that residue of a host

left on the soil surface can further promote a soilborne disease (Agrios, 2004; Katan, 2017). While *F. virguliforme* can saprophytically colonizes aboveground corn tissues when inoculated (Kolander et al., 2012) the potential occurrence in field settings does not promote subsequent root colonization of corn or soybean across the North Central production region.

Conclusions

In total, these field experiments revealed that corn is an asymptomatic host for *F. virguliforme* across the North Central soybean production region. We were able to establish that corn and soybean interactions with *F. virguliforme* occur within one week of planting, highlighting the need to prevent root colonization through use of prophylactic management strategies. Surprisingly, corn residue management did not alter root colonization of soybean or corn. Tillage management for root colonization did not provide clear conclusions, indicating additional variables relating to soil ediphatic factors may be critical to understanding the complex nature of this soilborne pathogen.

Acknowledgements

We would like to thank the North Central Soybean Research Program, Michigan Soybean Promotion Committee, Michigan State University Project GREEEN, Michigan State University Plant Resilience Institute, and the Charles Stewart Mott Foundation for funding. We would also like to thank the Michigan State University College of Agriculture and Natural Resources Statistical Consulting Center for data analysis suggestions.

Author Contributions

Designed framework: K.Y., L.L., D.S.M., A.T., K.A.W., G.A.D.S., A.B.Y., M.I.C.; Conducted Experiments: K.Y., L.L., D.S.M., A.T., K.A.W., G.A.D.S., A.B.Y., M.I.C., J.L.J., A.B.; Analyzed data: A.B.Y., G.A.D.S., K.Y.; Wrote the manuscript: K.Y., L.L., D.S.M., A.T., K.A.W., G.A.D.S., A.B.Y., M.I.C.; J.L.J., A.B.

Table 5. Field trial location and management in Iowa, Indiana, Michigan, and Wisconsin during 2015 to 2017.

Year	State	Planting Date	Cultivar	Inoculation [z]	Irrigation
2015	MI	June 11	Corn:P9807AM	+ Corn	+
	IA	May 22	Corn: DKX57-75 RIB	+ Corn	-
	IN	May 28	Corn: P9917AMX	+ Corn	+
	WI			-	-
2016	MI	June 6	Corn:P9807AM	+ Corn	-
			Soybean:DF5242R2Y	-	+
	WI	May 19	Corn:197-31V2PRIB	-	-
			Soybean:DSR-2110/R2Y	-	-
	IA	May 6	Corn: N41Y	-	-
			Soybean: AG2431	-	-
	IN	May 24	Corn:197-31V2PRIB	+ Corn	+
			Soybean:5N293R2	-	+
2017	MI	May 11	Corn 5556VT2RIB	+ Corn	-
			Soybean:DF5242R2Y	-	+
	IA	April 26	Corn: N41Y	-	-
			Soybean: AG2431	+ Soybean	-
	IN	May 17	Corn: P9917AMX	-	+
			Soybean:5N293R2	-	+

[z]Corn or Soybean plants were inoculated at planting with sorghum seeds infested with isolate NE305 in Iowa, INS12-10 in Indiana, and Mont-1 in Michigan.

Table 6. Experimental treatments and crop rotation schedule from 2016 to 2017.

		Crop rotation schedule	
Treatment	Description	2016	2017
1	Chisel plow, no residue	Corn following corn	Soybean following 2 years of corn
2	Chisel plow, residue	Corn following corn	Soybean following 2 years of corn
3	Chisel plow, no residue	Soybean following corn	Corn following soybean
4	Chisel plow, residue	Soybean following corn	Corn following soybean
5	No-till, no residue	Corn following corn	Soybean following 2 years of corn
6	No-till, residue	Corn following corn	Soybean following 2 years of corn
7	No-till, no residue	Soybean following corn	Corn following soybean
8	No-till, residue	Soybean following corn	Corn following soybean

Table 7. Temporal dynamics of *Fusarium virguliforme* colonization of corn roots in Michigan, Wisconsin, Indiana and Iowa during the 2016 and 2017 field season under tillage and residue management.

			Weeks After Planting			
			WEEK 4/5[z]	WEEK 8	WEEK 16	P-value
Location	Year	Treatment	*F. virguliforme* DNA (Fg/10 mg Dried Root Tissue)			
Michigan	2016	TILL	227.6 ab[y]	9.69 b	72.5 a	0.0258
		NO TILL	160.2 a	32.8 a	215.7 a	0.1082
	2017	TILL	6,266.7 a	3,86.9 b	5,001.4 ab	0.0005
		NO TILL	5,212.1 a	1,48.3 b	656.0 b	0.0021
	2016	RESIDUE	221.5 a	17.5 a	61.4 a	0.0617
		NO RESIDUE	166.3 a	25.0 a	226.8 a	0.0486
	2017	RESIDUE	7,904.4 a	4,26.6 b	486.3 b	0.0001
		NO RESIDUE	3,574.5 a	4,17.5 b	200.3 ab	0.0046
Wisconsin	2016	TILL	7.0 b	49.7 ab	44.4 a	<0.0001
		NO TILL	4.6 b	15.2 ab	20.7 a	<0.0001
	2016	RESIDUE	5.9 b	33.8 ab	28.9 a	<0.0001
		NO RESIDUE	5.3 b	21.9 ab	32.1 a	<0.0001
Indiana	2016	TILL	67.9 a	46.8 a	11.6 a	0.2366
		NO TILL	164.2 a	167.4 ab	55.2 b	0.0003
	2017	TILL	627.9 a	184.8 b	244.1 b	0.0030
		NO TILL	369.1 a	184.1 a	252.4 a	0.1665
	2016	RESIDUE	181.2 a	226.0 ab	53.6 b	0.0209
		NO RESIDUE	133.0 a	71.9 ab	40.7 b	0.0087
	2017	RESIDUE	526.6 a	249.9 a	326.1 a	0.1441
		NO RESIDUE	655.1 a	211.2 b	296.5 b	0.0043
Iowa	2016	TILL	88.7 a	43.4 a	114.9 a	0.0389
		NO TILL	48.0 a	45.2 a	55.6 a	0.1380
	2017	TILL	5,924.6 a	903.5 b	1,212.4 b	<0.0001
		NO TILL	12,408.9 a	1,157.9 b	1,627.5 b	<0.0001
	2016	RESIDUE	82.5 a	47.3 a	69.2 a	0.1907
		NO RESIDUE	78.1 a	63.9 a	54.4 a	0.4210
	2017	RESIDUE	10,930.5 a	1,205.6 b	1,350.2 b	<0.0001
		NO RESIDUE	13,607.5 a	1,434.7 b	2,303.4 b	<0.0001

[z]In 2017 at Iowa and Indiana sites the first sampling occurred at 5 weeks after planning, and in 2016 the first sampling occurred at 4 weeks after planting

[y] Asterisks or letters denote significance as determined by $\alpha \leq 0.05$ by ANOVA and HSD means separation.

Table 8. Temporal dynamics of *Fusarium virguliforme* colonization of corn radical roots in Michigan during the 2016 and 2017 field season under tillage and residue management.

		Weeks After Planting						
		WEEK 1	WEEK 2	WEEK 4	WEEK 8	WEEK 12	WEEK 16	P-value
Year	Treatment	*F. virguliforme* DNA (Fg/10 mg Dried Root Tissue)						
2016	TILL	1,164.1 a[y]	1,118.4 a	227.6 b	9.7 d	55.2 c	72.5 bc	0.0001
	NO TILL	1,082.3 b	5,434.5 a	160.2 c	32.8 d	45.9 cd	215.7 cd	0.0001
2017	TILL	1,784.3 ab	2,531.2 ab	6,266.7 a	386.9 c	464.2 c	5,001.4 bc	0.0001
	NO TILL	4,137.2 a	5,665.6 a	5,212.1 a	148.2 b	222.4 b	656.0 ab	0.0001
2016	RESIDUE	1,442.2 a	3,079.6 a	166.2 b	25 c	57.4 c	226.8 b	0.0001
	NO RESIDUE	804.1 b	3,473.4 a	221.5 b	17.5 c	43.7 c	61.4 b	0.0001
2017	RESIDUE	2,282.1 a	4,547.1 a	3,574.5 a	417.45 b	200.3 b	5,230.45 ab	0.0001
	NO RESIDUE	3,639.4 a	3,649.8 a	7,904.4 a	117.7 b	486.3 b	426.9 b	0.0001

[y] Asterisks or letters denote significance as determined by $\alpha \leq 0.05$ by ANOVA and HSD means separation

Table 9. Temporal dynamics of *Fusarium virguliforme* colonization of soybean tap roots in Michigan during the 2016 and 2017 field season under tillage and residue.

		Weeks After Planting						
		WEEK 1	WEEK 2	WEEK 4	WEEK 8	WEEK 12	WEEK 16	P-value
Year	Treatment	*F. virguliforme* DNA (Fg/10 mg Dried Root Tissue)						
2016	TILL	464.6 d[y]	217.7 cd	128.7 d	12,163.8 c	88,539.5 b	1,367,292.6 a	0.0001
	NO TILL	114.2 d	512.4 cd	415.8 cd	11,056.7 c	380,959.6 b	1,244,924.9 a	0.0001
2017	TILL	31.0 d	243.3 cd	739.5 c	283.5 c	4,812.5 b	126,716.9 a	0.0001
	NO TILL	79.7 d	426.9 c	1,139.7 c	6,958.1 c	211,027.7 b	2,488,780.1 a	0.0001
2016	RESIDUE	102.1 d	194.5 cd	176.9 cd	5826.5 c	240,623.3 b	1,004,828.8 a	0.0001
	NO RESIDUE	476.7 d	535.6 cd	367.5 cd	17,394.1 c	228,875.8 b	1,607,388.6 a	0.0001
2017	RESIDUE	73.4 d	341.7 cd	806.7 c	583.9 cd	198,486.4 b	1,580,731.5 a	0.0001
	NO RESIDUE	37.2 e	328.4 d	1,072.5 cd	6657.7 d	17,353.8 bc	1,034,765.5 a	0.0001

[y] Asterisks or letters denote significance as determined by $\alpha \leq 0.05$ by ANOVA and HSD means separation

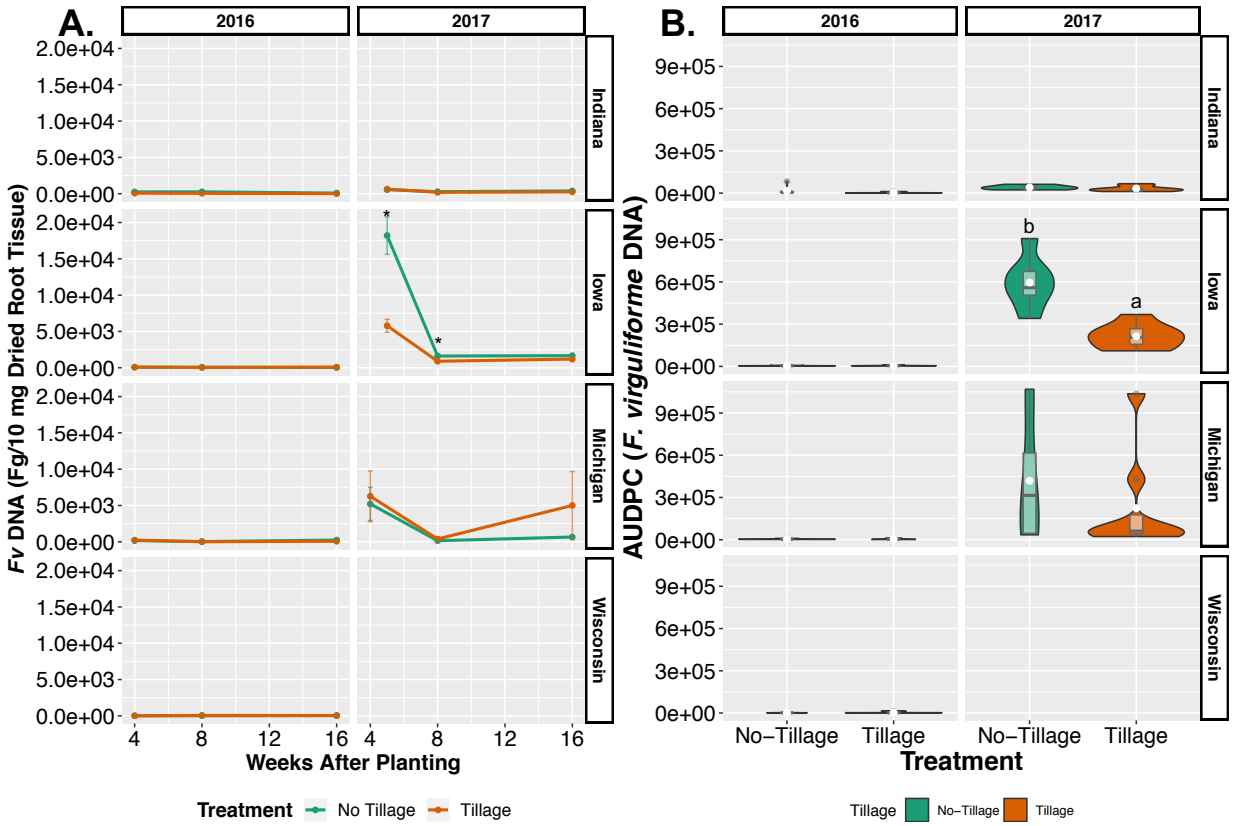

Figure 6. Corn radical root colonization by *Fusarium virguliforme* under two tillage treatments over three timepoints during the 2016 and 2017 field season. Treatment values of *F. virguliforme* DNA are the average of three samples replicated within four blocks. DNA temporal dynamics of *F. virguliforme* under tillage management in Indiana, Iowa, Michigan, or Wisconsin (A). Area under the DNA progress curve (AUDPC) violin plots, containing boxplots was calculated for tillage management in Indiana, Iowa, Michigan or Wisconsin (B). Asterisks or letters denote significance as determined by $\alpha \leq 0.05$ by ANOVA and HSD means separation.

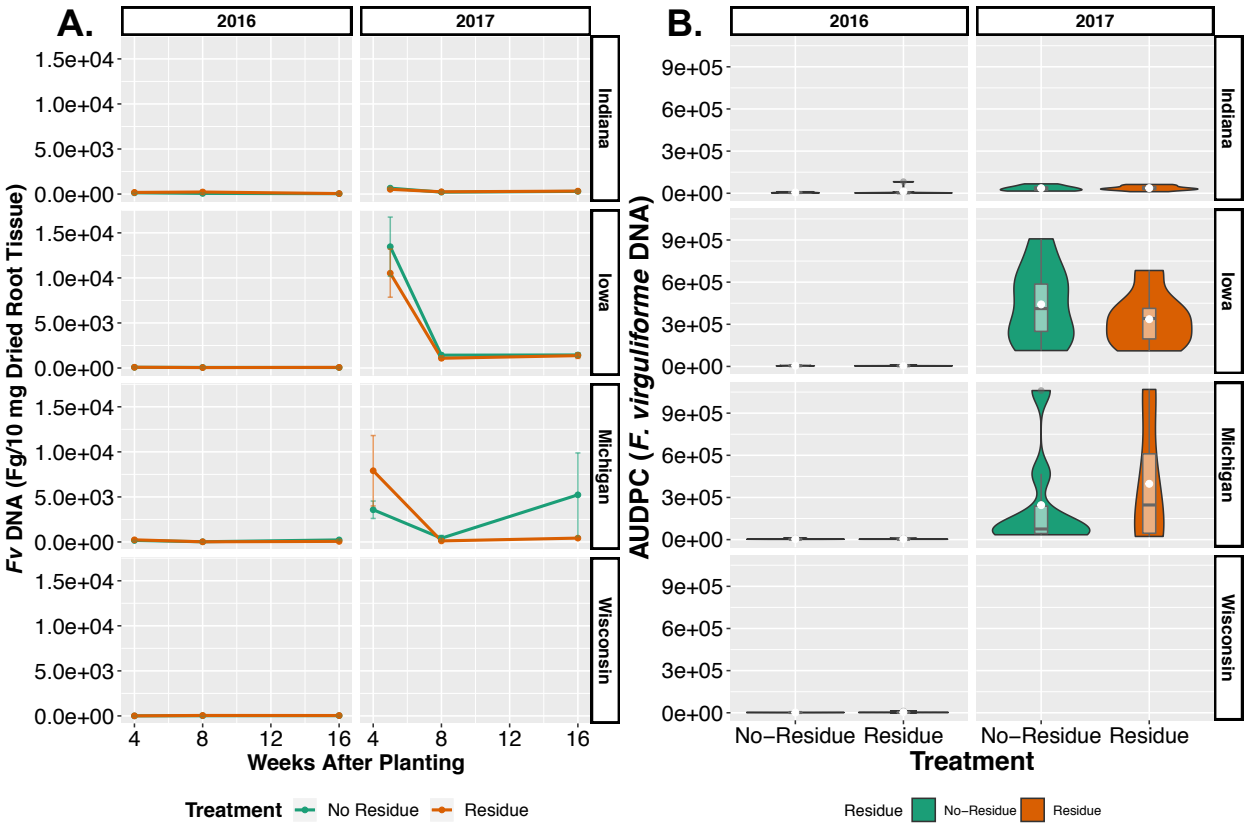

Figure 7. Corn radical root colonization by *Fusarium virguliforme* under two corn residue treatments over three timepoints during the 2016 and 2017 field season. Treatment values of *F. virguliforme* DNA are the average of three samples replicated within four blocks. DNA temporal dynamics of *F. virguliforme* under residue management in Indiana, Iowa, Michigan or Wisconsin (A). Area under the DNA progress curve (AUDPC) violin plots, containing boxplots was calculated for residue management in Indiana, Iowa, Michigan, or Wisconsin (B). Asterisks or letters denote significance as determined by $\alpha \leq 0.05$ by ANOVA and HSD means separation.

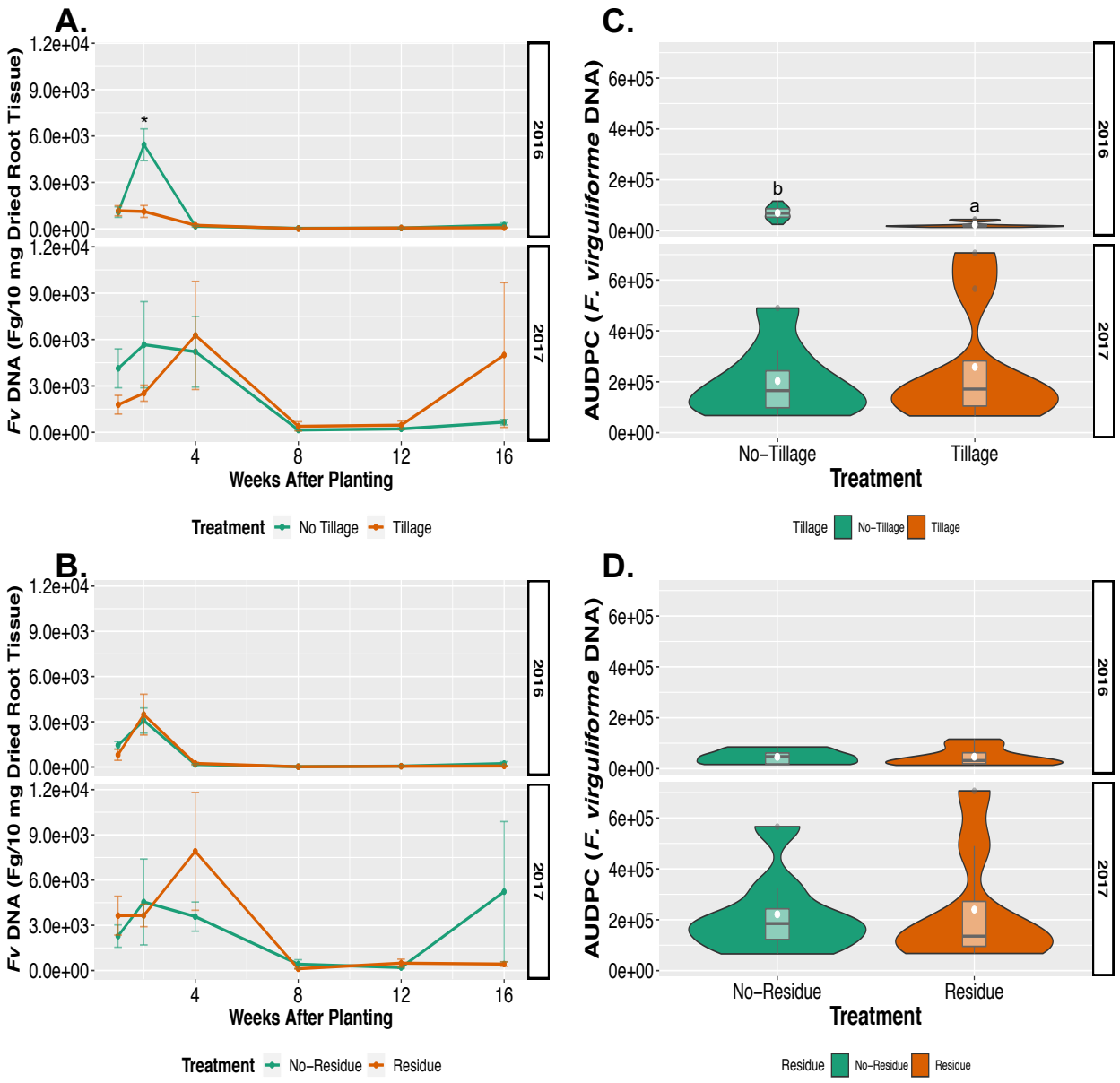

Figure 8. Corn radical root colonization temporal dynamics by *Fusarium virguliforme* under tillage and residue management in Michigan, during the 2016 and 2017 field season over six time points. Treatment values of *F. virguliforme* DNA are the average of three samples replicated within four blocks, for tillage (A) and residue (B) management. Area under the DNA progress curve (AUDPC) violin plots, containing boxplots was calculated for tillage (C) and residue (D) management. Letters denote significance as determined by $\alpha \leq 0.05$ by ANOVA and HSD means separation.

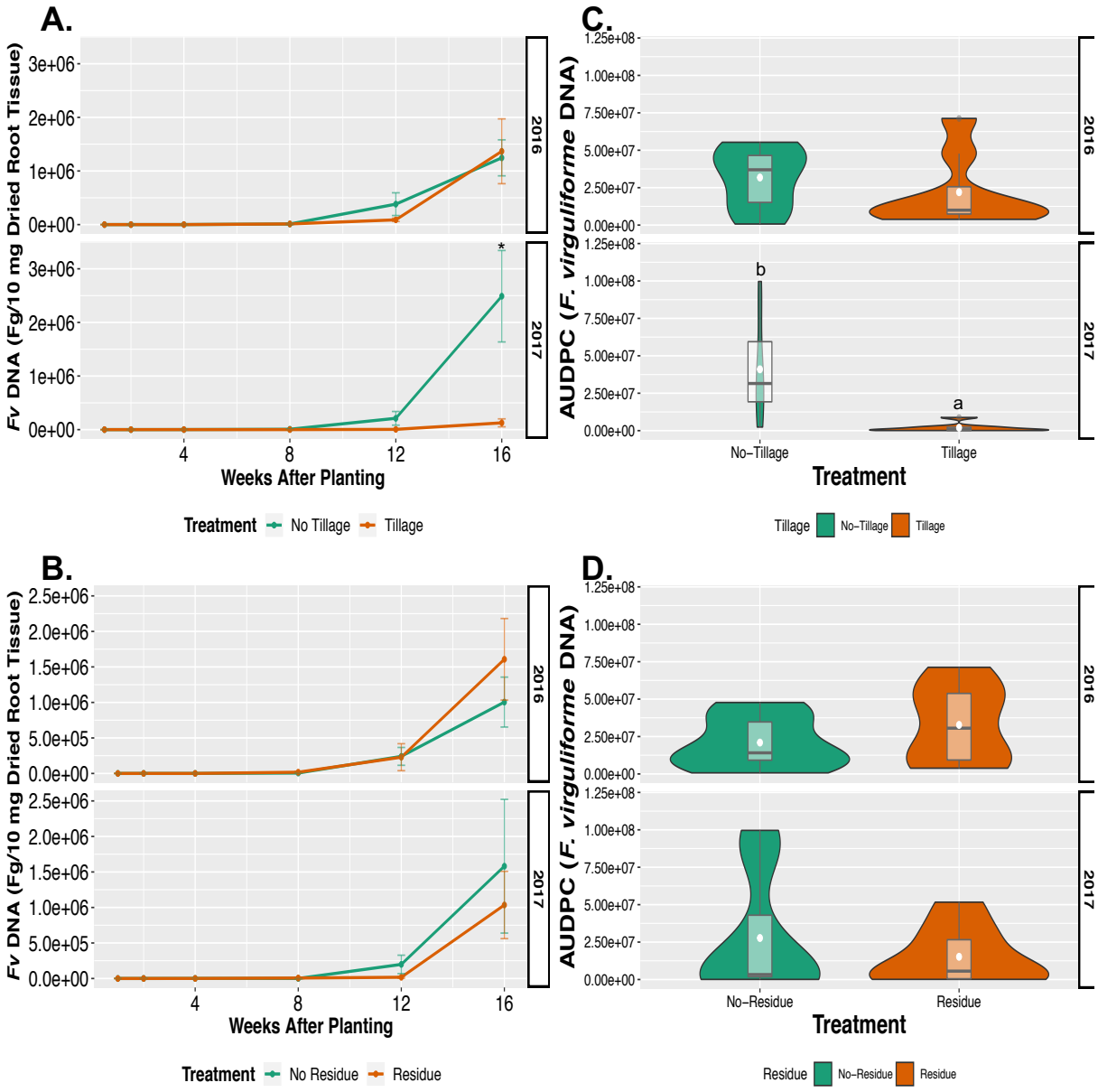

Figure 9. Soybean lower tap and lateral root colonization temporal dynamics by *Fusarium virguliforme* under tillage and residue management in Michigan, during the 2016 and 2017 field season over six time points. Treatment values of *F. virguliforme* DNA are the average of three samples replicated within four blocks, for tillage (A) and residue (B) management. Area under the DNA progress curve (AUDPC) violin plots, containing boxplots was calculated for tillage (C) and residue (D) management. Letters denote significance as determined by $\alpha \leq 0.05$ by ANOVA and HSD means separation.

REFERENCES

REFERENCES

Agrios, G.N. (2004). Plant pathology. (San Diego: Elsevier Academic Press).

Ahmed, M.A., Zarebanadkouki, M., Meunier, F., Javaux, M., Kaestner, A., and Carminati, A. (2018). Root type matters: Measurement of water uptake by seminal, crown, and lateral roots in maize. J. Exp. Bot. **69,** 1199-1206.

Allen, T.W., Bradley, C.A., Sisson, A.J., Byamukama, E., Chilvers, M.I., Coker, C.M., Collins, A.A., Damicone, J.P., Dorrance, A.E., Dufault, N.S., Esker, P.D., Faske, T.R., Giesler, L.J., Grybauskas, A.P., Hershman, D.E., Hollier, C.A., Isakeit, T., Jardine, D.J., Kelly, H.M., Kemerait, R.C., Kleczewski, N.M., Koenning, S.R., Kurle, J.E., Malvick, D.K., Markell, S.G., Mehl, H.L., Mueller, D.S., Mueller, J.D., Mulrooney, R.P., Nelson, B.D., Newman, M.A., Osborne, L., Overstreet, C., Padgett, G.B., Phipps, P.M., Price, P.P., Sikora, E.J., Smith, D.L., Spurlock, T.N., Tande, C.A., Tenuta, A.U., Wise, K.A., and Wrather, J.A. (2017). Soybean yield loss estimates due to diseases in the united states and ontario, canada, from 2010 to 2014. Plant Health Prog. **18,** 19-27.

Bates, D., Machler, M., Bolker, B., Walker, S. (2015). Fitting linear mixed-effects models using {lme4}. J Stat. Soft. **67,** 1-48.

Brar, H.K.B., M.K. (2012). Expression of a single-chain variable-fragment antibody against a *Fusarium virguliforme* toxin peptide enhances tolerance to sudden death syndrome in transgenic soybean plants. Mol. Plant-Microbe Interact. **25,** 817-824.

Chang, H.-X., Roth, M.G., Wang, D., Cianzio, S.R., Lightfoot, D.A., Hartman, G.L., and Chilvers, M.I. (2018). Integration of sudden death syndrome resistance loci in the soybean genome. Theor Appl Gen. **131,** 757-773.

Chong, S.K., Hildebrand, K.K., Luo, Y., Myers, O., Indorante, S.J., Kazakevicius, A., and Russin, J. (2005). Mapping soybean sudden death syndrome as related to yield and soil/site properties. Soil Till Res. **84,** 101-107.

Freed, G.M., Floyd, C.M., and Malvick, D.K. (2017). Effects of pathogen population levels and crop-derived nutrients on development of soybean sudden death syndrome and growth of *Fusarium virguliforme*. Plant Dis. **101,** 434-441.

Fusseder, A. (1987). The logevity and acitivity of the primary root of maize. Plant Soil **101,** 257-265.

Gao, X., Jackson, T.A., Hartman, G.L., and Niblack, T.L. (2006). Interactions between the soybean cyst nematode and *Fusarium solani* f. Sp. *Glycines* based on greenhouse factorial experiments. Phytopathol. **96,** 1409-1415.

Gaspar, A.P., Mueller, D.S., Wise, K.A., Chilvers, M.I., Tenuta, A.U., and Conley, S.P. (2017). Response of broad-spectrum and target-specific seed treatments and seeding rate on soybean seed yield, profitability, and economic risk. Crop Sci. **57,** 2251-2263.

Gongora-Canul, C., Nutter, F.W., and Leandro, L.F.S. (2011). Temporal dynamics of root and foliar severity of soybean sudden death syndrome at different inoculum densities. Eur J. Plant Pathol. **132,** 71-79.

Gdanetz, K., and Trail, F. (2017). The wheat microbiome under four management strategies, and potential for endophytes in disease protection. Phytobiomes J. **1,** 158-168.

Hartman, G.L., Chang, H.X., and Leandro, L.F. (2015). Research advances and management of soybean sudden death syndrome. Crop Prot. **73,** 60-66.

Hershman, D.E. (2003). Soybean diseases control series: Are we missing opportunities? Part 2: Soybean sudden death syndrome. In Kentucky Pest News (University of Kentucky.).

Hershman, D.E., Hendrix, J.W., Stuckey, R.E., Bachi, P.R., and Hendson, G. (1990). Influence of planting date and cultivar on soybean sudden death syndrome in Kentucky. Plant Dis. **74,** 761-766.

Hochholdinger, F., Woll, K., Sauer, M., and Dembinsky, D. (2004). Genetic dissection of root formation in maize (*Zea mays*) reveals root-type specific developmental programmes. Ann. Bot. **93,** 359-368.

Hothorn, T.B., F.; Westfall, P. (2008). Simultaneous inference in general parametric models. Biomet J. **50,** 346-363.

Huisman, O.C. (1982). Interrelations of root growth dynamics to epidemiology of root-invaiding fungi. Ann Rev Phytopathol. **20,** 303-327.

Jin, H., Hartman, G.L., Nickell, D., and Widholm, J.M. (1996). Phytotoxicity of culture filtrate from *Fusarium solani*, the causal agent of sudden death syndrome of soybean. Plant Dis. **80,** 922-927.

Kandel, Y.R., Leandro, L.F., and Mueller, D.S. (2019). Effect of tillage and cultivar on plant population, sudden death syndrome, and yield of soybean in iowa. Plant Heal. Prog.**,** doi:10.1094/PHP-1010-1018-0063-RS.

Kandel, Y.R., Wise, K.A., Bradley, C.A., Tenuta, A.U., and Mueller, D.S. (2016a). Effect of planting date, seed treatment, and cultivar on plant population, sudden death syndrome, and yield of soybean. Plant Dis. **100,** 1735-1743.

Kandel, Y.R., Wise, K.A., Bradley, C.A., Chilvers, M.I., Tenuta, A.U., and Mueller, D.S. (2016b). Fungicide and cultivar effects on sudden death syndrome and yield of soybean. Plant Dis. **100,** 1339-1350.

Kandel, Y.R., McCarville, M.T., Adee, E.A., Bond, J.P., Chilvers, M.I., Conley, S.P., Giesler, L.J., Kelly, H.M., Malvick, D.K., Mathew, F.M., Rupe, J.C., Sweets, L.E., Tenuta, A.U., Wise, K.A., and Mueller, D.S. (2018). Benefits and profitability of fluopyram-amended seed treatments for suppressing sudden death syndrome and protecting soybean yield: A meta-analysis. Plant Dis. **102,** 1093-1100.

Katan, J. (2017). Diseases caused by soilborne pathogens: Biology, management and challenges. J. Plant Path. **99,** 305-315.

Kobayashi-Leonel, R., Mueller, D., Harbach, C., Tylka, G., and Leandro, L. (2017). Susceptibility of cover crop plants to *Fusarium virguliforme*, causal agent of soybean sudden death syndrome, and *Heterodera glycines*, the soybean cyst nematode. J Soil Water Conserv. **72,** 575-583.

Koenning, S.R., and Wrather, J.A. (2010). Suppression of soybean yield potential in the continental united states by plant diseases from 2006 to 2009. Plant Health Progress **11,** 10.1094/php-2010-1122-1001-rs.

Kolander, T.M., Bienapfl, J.E., Kurle, J.E., and Malvick, D.K. (2012). Symptomatic and asymptomatic host range of *Fusarium virguliforme*, the causal agent of soybean sudden death syndrome. Plant Dis. **96,** 1148-1153.

Leandro, L.F.S., Eggenberger, S., Chen, C., Williams, J., Beattie, G.A., and Liebman, M. (2018). Cropping system diversification reduces severity and incidence of soybean sudden death syndrome caused by *Fusarium virguliforme*. Plant Dis. **102,** 1748-1758.

Leslie, J.F., and Summerell, B.A. (2006). The Fusarium laboratory manual. (Blackwell Publishing Professional).

Luo, Y., Chong, S.K., and Myers, O. (2001). Spatio-temporal analysis of soybean root colonization by *Fusarium solani* f. sp. *Glycines* in fields. Plant Dis. **18,** 303-310.

Navi, S.S., and Yang, X.B. (2016). Impact of crop residue and corn-soybean rotation on survival of *Fusarium virguliforme* a causal agent of sudden death syndrome of soybean. J. Plant Path. Microbiol. **7,** 330.

Njiti, V.N., Shenaut, M.A., Suttner, R.J., Schmidt, M.E., and Gibson, P.T. (1996). Soybean response to sudden death syndrome: Inheritance influenced by cyst nematode resistance in pyramid × douglas progenies. Crop Sci. **36,** 1165-1170.

NOAA. (2019). National centers for environmental information, climate at a glance: Statewide time series.

O'Donnell, K., Sink, S., Mercedes Scandiani, M., Luque, A., Colletto, A., Biasoli, M., Lenzi, L., Salas, L., González, V., Ploper, L.D., Formento, N., Pioli, R.N., Aoki, T., Yang, X.B., and Sarver, B.A.J. (2010). Soybean sudden death syndrome species diversity within North and South America revealed by multilocus genotyping. Phytopathol. **100,** 58-71.

Pinheiro, J.B., D.; DebRoy, S.; Sarkar, D.; R Core Team. (2019). Nlme: Linear and nonlinear mixed effects models. Retrieved from https:// CRAN.R-project.org/package=nlme.

R Development Core Team. (2010). R: A language and environment for statistical computing. In Vienna, Austria: R Foundation for Statistical Computing.

Roy, K.W., Rupe, J.C., Hershman, D.E., and Abney, T.S. (1997). Sudden death syndrome of soybean. Plant Dis. **81,** 1100-1111.

Rupe, J.C. (1989). Frequency and pathogenicity of *Fusarium solani* recovered from soybeans with sudden death syndrome. Plant Dis. **73,** 581-584.

Scherm, H., and Yang, X.B. (1999). Risk assessment for sudden death syndrome of soybean in the north-central united states. Agri. Sys. **59,** 301-310.

Schneider, H.M., and Lynch, J.P. (2017). Functional implications of root cortical senescence for soil resource capture. Plant Soil **423,** 13-26.

Vick, C.M., Bond, J.P., Chong, S.K., and Russin, J.S. (2003). Response of soybean sudden death syndrome to tillage and cultivar. Can J. Plant Pathol. **28,** 77-83.

Von Qualen, R.H., Abney, T.S., Huber, D.M., and Schreiber, M.M. (1989). Effects of rotation, tillage, and fumigation on premature dying of soybeans. Plant Dis. **73,** 740-744.

Wang, J., Jacobs, J.L., Byrne, J.M., and Chilvers, M.I. (2015). Improved diagnoses and quantification of *Fusarium virguliforme*, causal agent of soybean sudden death syndrome. Phytopathol. **105,** 378-387.

Wang, J., Jacobs, J.L., Roth, M.G., and Chilvers, M.I. (2019a). Temporal dynamics of *Fusarium virguliforme* colonization of soybean roots. Plant Dis. **103,** 19-27.

Wang, J., Sang, H., Jacobs, J.L., Oudman, K., A., Hanson, L.E., and Chilvers, M.I. (2019b). Soybean sudden death syndrome causal agent *Fusarium brasiliense* present in michigan. Plant Dis. 10.1094/PDIS-1008-1018-1332-RE.

Ward, B., Lindsey, L., and Loux, M. (2018). Soybean production budget (roundup ready)-2019. In Farm Office (Ohio State University).

Westphal, A., Li, C., Xing, L., McKay, A., and Malvick, D. (2014). Contributions of *fusarium Virguliforme* and *Heterodera glycines* to the disease complex of sudden death syndrome of soybean. PLoS One **9,** e99529.

Wickham, H. (2016). Ggplot2: Elegant graphics for data analysis. (Springer-Verlag New York).

Xing, L., and Westphal, A. (2009). Effects of crop rotation of soybean with corn on severity of sudden death syndrome and population densities of *Heterodera glycines* in naturally infested soil. Field Crops Res. **112,** 107-117.

CHAPTER 4

Divergence in Transcriptomic Response of Symptomatic and Asymptotic Hosts Following *Fusarium virguliforme* Inoculation Highlights Senescence Triggered Susceptibility

This chapter is unpublished, with intention to submit to Plant Cell.

Baetsen-Young, A.M., Shiu, S.H., Day, B. 20XX. Divergence in transcriptomic response of symptomatic and asymptotic hosts following *Fusarium virguliforme* inoculation highlights senescence triggered susceptibility. Plant Cell. XX:XX-XX

Abstract

Broad host-range plant pathogens have evolved the ability to modulate defense and immune signaling in a broad array of hosts. However, recent transcriptome analyses have only explored pathogenic interactions within species; thus, a comparative transcriptomic approach across diverse plant species will reveal complex processes that regulate host immunity and defense. In the current study, we exploited the broad host range of *Fusarium virguliforme* as a comparative model to identify and define differentially induced root responses between an asymptomatic monocot, corn, and a symptomatic eudicot, soybean. We posit that this approach offers a unique perspective to uncover immune regulatory responses encoding tolerance and susceptibility. Following pathogen inoculation, enriched orthologous defense response transcripts within both hosts varied in duration of upregulation, indicating earlier temporal induction of immunity may play a role in tolerance of *F. virguliforme* by corn. Transcription factors upregulated within corn suggest tolerance is potentially aided by no apical meristem (NAM), ATAF1/2, cup-shaped cotyledon2 (CUC2) (NAC) and Ethylene Responsive Factor (ERF) stress reduction whereas, many senescence promoting NACs were differentially regulated within soybean as the infection time-course proceeded. Activation senescence processes occurred only within the susceptible host during colonization by *F. virguliforme* through NACs transcription factors, reinforcing the concept of necrotrophy activated senescence. In total, this supports our hypothesis that *F. virguliform*e induces an environment within symptomatic hosts which favor susceptibility through transcriptomic reprogramming to promote cell senescence.

Introduction

Contrasting phenes have answered large scale questions across biology and provided clues to the molecular underpinnings of host susceptibility and resistance following pathogen perception. Indeed, comparative approaches between phenotypically distinct responses of the same plant species to a single pathogen has been applied to numerous pathosystems, providing details of the intimate interactions from physiological- to genetic/genomic-scale resolution (O'Connell et al., 2012; Lorrain et al., 2018). In total, each of these has shed light on the varied responses plants induce to thwart pathogen infection and colonization. In brief, these typically include 1) the hypersensitive response (HR), a key hallmark of effector-triggered immunity (Chisholm et al., 2006; Dangl and Jones, 2006), 2) pattern triggered immunity (PTI; (Bagnaresi et al., 2012; Zhang et al., 2018), 3) the expression of secondary antimicrobial metabolites (Dupont et al., 2015), leading to the activation of resistance (*R*) genes (Etalo et al., 2013) and 4) the temporal infection dynamics between susceptible and resistant cultivars (Kong et al., 2015; Burkhardt and Day, 2016). While many critical processes underlying plant immunity have been clarified by pairwise genomics- and transcriptomics-based approaches, most studies have focused on comparison(s) of host response within cultivars of a single species or species within a genera. As a result, numerous knowledge gaps remain in understanding how pathogens with broad host ranges modulate immunity of diverged hosts.

Many fungal pathogens can colonize a broad suite of agronomically important crops, yet only a few are true pathogens (Gdanetz and Trail, 2017; Banerjee et al., 2019). One exception to

this is phytopathogenic Ascomycetes, found within the species complex of *Fusarium solani* and *F. oxysporum*, which can colonize over 220 diverse hosts, including both monocots and eudicots (Michielse and Rep, 2009; Šišić et al., 2018). Comparing host responses across such highly diverged species colonized by the same fungus could provide novel insights into immunity induced pathways relevant to resistance and tolerance. These comparisons would be highly relevant to agroecosystems containing monocultures of rotated crops, interacting with the same microbial community each growing season (Gdanetz and Trail, 2017; Katan, 2017; Leandro et al., 2018). Surprisingly, while growers often rotate to different crops to prevent pathogen associated yield loss, recent explorations have discovered many field crops asymptomatically support fungi pathogenic to other crops (Kolander et al., 2012; Malcolm et al., 2013; Lofgren et al., 2018). Interestingly, these asymptomatic hosts could provide a comparative system to explore regulatorily networks and pathways promoting tolerance to severe phytopathogens.

The fundamentals of plant immunity were built upon the framework of the eudicot *Arabidopsis thaliana*. Therefore, while a robust understanding of eudicot immune signaling and pathways exists, immune signaling in monocots remain enigmatic (Balmer et al., 2012; Balmer et al., 2013). Often similar genetic orthologs or paralogs are encoded within the genome of monocots, yet these well elucidated pathways in eudicots do not consistently express in the same manner in monocots (Lu et al., 2011; Balmer et al., 2013). Furthermore, attempting to translate host immune responses below ground to root-pathogen interactions remains an even larger challenge as the vast majority of phytopathology studies have focused on above ground infections and symptom development (De Coninck et al., 2015;

Chuberre et al., 2018). Exploring differential induced root responses to between a monocot and eudicot may unveil an immune genetic regulatorily response encoding tolerance upon an asymptomatic host that was previously unknown.

To explore such a hypothesis, soybean sudden death syndrome (SDS) provides an excellent model. Differing phenotypic host responses are prominent by crops colonized by *Fusarium virguliforme*, the causal agent SDS (Kolander et al., 2012). Disease management is limited in soybean to chemical, cultural practices and partial host resistance, enabling an estimated annual yield loss impact greater than $330 million dollars in the United States, placing this disease in the top 5 most impactful on soybean production (Koenning and Wrather, 2010; Allen et al., 2017). Soybean and corn are often rotated in the vast majority of soybean production for agronomic and disease management reasons (Katan, 2017), yet recent research has revealed corn is an asymptomatic host for *F. virguliforme* (Kolander et al., 2012). With the limited resolution of molecular cross talk between this root fungal pathogen and soybean to derive mechanisms of susceptibility (Hartman et al., 2015) and the large gaps within the scientific literature surrounding asymptomatic root responses to fungal colonization, the comparison *F. virguliforme* colonization of corn and soybean roots provides an unique system to explore pathway rewiring of transcriptional response underlying tolerance and susceptibility within roots. To uncover genetic signatures responsible for visible phenes in corn and soybean roots, we explored (1) early temporal interactions between *F. virguliforme* and soybean or corn through *in planta* assays, (2) what early transcriptional responses of corn or soybean to *F. virguliforme* colonization are induced, (3) if orthologous transcriptional responses are induced in a similar temporally dependent

manner between soybean and corn roots, (4) to what extent non-orthologous induced defense responses aid in tolerance of corn and susceptibility of soybean to *F. virguliforme*.

Materials and Methods

Plant and *Fusarium virguliforme* Assay

Soybean c.v. Sloan (provided by Martin Chilvers, Michigan State University), and corn hybrid E13022S (Epley Brothers Hybrids Inc, Shell Rock, IA, provided by Martin Chilvers) were surface sterilized in 70% ethanol for 30 sec, 10% bleach solution for 20 min, and then triple rinsed in sterile water for 1 min. Soybeans seeds were placed between two sheets of sterile 100 mm Whatman filter paper with 5 mL of sterile water inside a petri dish. Seeds were incubated for five days in total darkness at 21°C. Corn seeds were incubated in sterile water for 24 hours in darkness and placed between two sheets of sterile 100mm Whatman filter paper with 5 mL of sterile water inside a petri dish. Seeds were incubated for five days in total darkness at 21°C.

Fusarium virguliforme Mont-1 isolate (provided by Martin Chilvers) was propagated on potato dextrose agar (Difco, Fisher Scientific) for seven weeks. Asexual macroconidia spores were collected, diluted to 1×10^5 macroconidia mL^{-1} and sprayed onto five-day old corn or soybean seedlings with a 3 oz travel spray bottle. Twenty-five sprays were applied to the seedlings at angles of 0°, 90°, 180°, and 270° to ensure seeds were properly covered. For mock inoculated samples, water was sprayed onto the seedlings. Seedlings were incubated

for 30 min with the inoculum, then excess inoculum was removed, and seedlings were incubated for an additional hour. Following incubation, three corn or soybean seedlings were placed into seed germination pouches (Mega International), containing 25 mL of sterile distilled water. Pouches containing seedlings were placed in a BioChambers Bigfoot Series Model AC-60 growth chamber with 140 μE m^{-2} sec^{-1} and 14:10 h light/dark cycle at 12°C for seven days and then 25°C for seven days. Plants were watered as needed with sterile water. Tap root from soybean or radical from corn root samples were taken at the same time (16:00 h) of day from the original 4 cm inoculation site throughout the time course. The two-week time course was repeated three independent times in the same growth chamber, with sampling of six plants for RNA isolation and three plants for DNA isolation at 0, 2, 4, 7, 10, and 14 days post inoculation (DPI) in each biological repeat. Time point 0 was sampled after completion of fungal or mock inoculation. Plant growth and disease symptomology was recorded at each timepoint by photography with a D50 Nikon camera.

Fungal Colonization Analysis

To visualize fungal growth on samples, microscopic analyses of corn and soybean roots were conducted at each time point for all treatments. Roots were cleared in 100% ethanol, followed by staining in a 0.05% trypan blue solution containing equal parts of water, glycerol and lactic acid (Savory et al., 2012). Fungal structures were observed using a MZ16 dissecting scope (Lecia).

DNA Extraction and Real Time PCR for *Fusarium virguliforme*

DNA for real-time quantitative polymerase chain reaction (qPCR) was extracted from flash-frozen root tissue to determine the amount of fungal biomass present in samples throughout the time course. A total of 60 mg of ground root tissue from individual corn or soybean plants from each time point were extracted with a NucleoSpin Plant II Kit (Macherey-Nagel), with an additional incubation on 1 hour at 65°C during lysis. Samples were prepared for *F. virguliforme* DNA detection by qPCR following (Wang et al., 2015). Analysis of variance (ANOVA) was calculated for DNA quantities using the "lme4" (Bates, 2015) and "Car" (Fox, 2011) package in R v3.4.1(R Development Core Team, 2010). Means were separated at $P \leq 0.05$ using Tukey's least significant different test using the "multicomp" package (Hothorn, 2008).

RNA Extraction

Total RNA was isolated from 200 mg of ground flash frozen germinating macroconidia and plant root samples for messenger RNA (mRNA) sequencing with a miRNeasy Mini Kit (Qiagen). Contaminating DNA was removed with TURBO DNA Free DNase (Invitrogen). RNA quality was determined by gel electrophoresis and the 2100 Bioanalyzer (Agilent) with the Agilent RNA 6000 Pico kit.

Library Preparation and Sequencing

The same extraction for each sample was used for mRNA and sRNA library preparation. Libraries were prepared using the Illumina TruSeq mRNA Library Preparation Kit from three biological repeats of each time point of *F. virguliforme* or mock inoculated corn or soybean or germinating macroconidia samples by the Michigan State Research Technology and Support Facility. Samples were pooled and sequenced on the Illumina HiSeq 4000 under single end 50 bp mode. Base calling was done by Illumina Real Time Analysis (RTA) v2.7.7 and output of RTA was demultiplexed and converted to FastQ format with Illumina Bcl2fastq v2.19.1 Samples for sRNA were prepared using the NEB Next Small RNA Sample Prep Kit at University of Illinois at Urbana-Champaign W.M Keck Center. Samples were pooled and sequenced on the Illumina HiSeq 4000 under single end 50 bp mode. Fastq files were generated and demultiplexed with the bcl2fastq v2.20 Conversion Software (Illumina).

mRNA-Sequencing Processing and Differential Analysis

Reads were trimmed for adapter presence and quality score by Trimmomatic (v0.33) (Bolger et al., 2014). The trimmed reads were uniquely mapped to the corresponding reference genomes of soybean (Wm82.a2.v1), and corn (B73 RefGen_v4, AGPv4) HISAT2 (v 2.1.0) (Kim et al., 2015) with the following parameters --dta --rna-strandness F. Hits from HISAT2 were converted from SAM to BAM format by Picard (v 2.18.1) (http://broadinstitute.github.io/picard/). Alignments were then counted by HTSeq (v0.6.1) (Anders et al., 2014) with the following options: --minaqual 50 -m intersection-strict -s

reverse --idattr=gene_id. Gene counts were imported into DESeq2 (v1.22.2) (Love et al., 2014) conducted in R, normalized for library size and log2 transformed to determine correlation of biological replicates at each time point.

To determine differential gene expression DESeq2 (v1.22.2) executed in R (R Development Core Team, 2010) with raw HTSeq counts. Gene counts were filtered less than 10 across 90% of samples. DESeq2 was applied to determine significant genes with an adjusted $P \leq 0.05$ and greater than 1-fold difference between mock and inoculated. Pairwise comparison within each time point and within each host, of *F. virguliforme* and mock inoculated samples.

Differential Gene Co-expression Network Analysis

Genes were also filtered for differential gene correlation analysis (DGCA) (McKenzie et al., 2016) implemented in R (R Development Core Team, 2010) for 90% of genes with less than 10 across all samples. These 43,308 soybeans or 28,956 corn genes were variance stabilized transformed for importation and Pearson correlation of individual gene pairs within each treatment of were calculated and compared to across mock or inoculated treatments to assign differential correlation by significance of median difference in z-score in default settings, with an Bonferroni correction of p-values (McKenzie et al., 2016). Significant gene pairs from differentially induced classes (e.g. +/0, -/0, 0/-, +/0, +/- and -/+) were weighted by the z-score difference between treatments to convert into a planar filtered network (PFN). These gene pairs were imported into MEGENA and multiscale modules and hubs were identified, with a hub detection significance threshold of $P < 0.05$, module significance

threshold of $P < 0.005$, network permutations of 100 and module size greater than 10 (Song and Zhang, 2015). Overall differential gene expression correlation within corn discovered 129 significant gene pairs from 419,152,582 gene pairs between mock and inoculated. Soybean differential gene expression correlation identified 5,526,057 significant gene pairs from 904,379,186 gene pairs between treatments. While corn differential gene correlation PFN was limited, soybean differential gene pairs were clustered by MEGENA into 1,161 modules. Modules were visualized in ggplot2 (v3.1.1) package (Wickham, 2016) in R.

Identification of Orthologous Genes

The longest protein sequences for genes from soybean and corn were analyzed by OrthoFinder (v2.2.7) in default settings. Protein sequences were accessed from Ensembl Plants (http://plants.ensembl.org/index.html). A total of 25,362 soybean and 15,158 corn genes were discovered to be contained within 10,700 orthogroups. This dataset was then applied to filter $\log_2$ fold changes between mock and inoculated corn or soybean at the orthogroup level. As many orthogroups contain more than a one: one relationship, the median of gene log2 fold changes of all genes within one host orthogroup was completed, as the median transformation of genes within an orthogroup captured the most variation between soybean and corn (Figure 10)

Differential Analysis of Orthogroups

To determine differential orthogroup expression DESeq2 (v1.22.2) executed in R (R Development Core Team, 2010) with median transformed gene HTSeq counts within each orthogroup. Orthogroup counts were filtered less than 10 across 90% of samples. DESeq2 was applied to determine significant genes with an adjusted $P \leq 0.05$ and greater than 1-fold difference between mock treatments between soybean and corn, as well as, inoculated treatments between soybean and corn at each time point.

Gene Ontology Enrichment Analysis

The gene ontology was retrieved from the GFF file of the soybean genome annotation (Wm82.a2.v1) and the revised gene ontology annotation for corn (Wimalanathan et al., 2018). The gene ontology annotation varies in completeness between soybean and corn. For example, the defense response term (GO:0006952), has 374 genes annotated in corn, however, in soybean only 86 genes are annotated. To have an ontology that is similar for an ortholog comparison, we merged gene ontologies from corn and soybean within each orthogroups, keeping only unique ontology terms. In total, all 10,700 orthogroups had gene ontology assignment.

Orthogroup lists from either differential analysis were analyzed by TopGO (2.34.0) conducted (Alexa A and Rahnenfuhrer J, 2018) in R. Fishers Exact Test was conducted on each orthogroup set with an adjusted *P-value* ≤ 0.05 to determine significance of enrichment

across all orthogroups. Additionally, lists of genes from differential analysis or gene differential clustering modules were analyzed for GO term enrichment by the singular enrichment analysis within AgriGO (v2) website (Tian et al., 2017) with the Fisher statistical adjustment method at a significance level of 0.05.

Orthologous Transcription Factor Analysis

Transcription factors for corn were retrieved from http://planttfdb.cbi.pku.edu.cn/. Genome v3 gene ID were converted to v4 IDs for the 2,290 transcription factors and orthologous genes with soybean were discovered within the orthogroup dataset, entailing 508 orthogroups. These orthogroups were filtered for significant defense induction over the time course.

Results

Fusarium virguliforme Growth is Similar on Symptomatic and Symptomatic Hosts

To explore induced defense genes, time-series samples between water (mock) and *F. virguliforme*-inoculated soybean and corn was conducted over a 2-week period. This experimental design permits the discovery of stage-specific immune/susceptibility responses enabling a better understanding of the genetic processes required for immunity (Burkhardt and Day, 2016a). As shown in Figure 11 and Figure 12, plant growth and development were observed to be similar between mock and inoculated plants of soybean

and corn. As shown, in soybean, the radical elongated from 0-4 days post inoculation (DPI), with lateral roots developing at 7 DPI. Secondary laterals formed at 10 DPI, with unfolding of the cotyledons. By 14 DPI, prolific lateral and tap root growth had occurred in both treatments, and full expansion of cotyledons, representing a final VC plant developmental stage for soybean. Consistent with the hemibiotrophic lifestyle of *F. virguliforme*, no symptoms were apparent on soybean roots form 0-4 DPI, indicative of a biotrophic stage (Ngaki et al., 2016). At 7 DPI, a chlorotic discoloration of the lower tap root of the *F. virguliforme* treatment was observed, which developed into necrotrophic streaking of the tap root by 10 DPI. Total necrosis engulfed lower hypocotyl, upper tap root and spread to lower lateral roots adjoining the tap root (Figure 12A). No necrosis was noted in mock treatments. Inoculated and mock inoculated corn seedlings exhibited comparable growth and development patterns as well. The radical and seminal roots were slowly extending and by 4 DPI had expanded in length. At 7 DPI lateral roots were initializing along the primary root, and the crown roots had started emerging (Figure 12B). By 14 DPI, the seminal, crown, and primary roots had grown prolifically, and above ground, leaves had fully expanded to the V1 growth stage.

As no visual symptom development was observed on *F. virguliforme*-inoculated corn roots, we applied a more sensitive approach to evaluate fungal growth and penetration. To this end, we employed qPCR to identify and quantify fungal level from our time-course inoculation analysis (Figure 11B). *Fusarium virguliforme* DNA concentrations increased on both soybean and corn roots throughout the time-course, with 0 and 2 DPI displaying significantly lower levels of *F. virguliforme* DNA quantities than 14 DPI ($P < 0.0001$, Fig. 9B).

Both inoculated soybean and corn exhibited similar levels of *F. virguliforme*, as determined by qPCR at each time-point and were significantly different from mock treatments ($P < 0.001$). Background levels of *F. virguliforme* DNA were detected in mock inoculated roots, which corresponds to the non-specific nature of the qPCR assay below 10 fg of DNA (Wang et al., 2015).

Once we established that *F. virguliforme* had colonized both hosts over our time-course in both corn and soybean, we next conducted a comparative RNA-sequencing at six time-points across a 0-14-day interval, post-inoculation to explore induced defenses between soybean and corn. After trimming for adapters and low-quality reads, 76-83% of soybean and 77-81% of the corn reads could be uniquely mapped to the respective genomes (Fig. 9C, Supplemental Data Set 1-1). The percent of reads aligning varied throughout the time-course, indicating a host mRNA production varied across the time-course and between the hosts. However, in *F. virguliforme* inoculated samples, mRNA alignments decreased over time, particularly within soybean at 10 DPI. We hypothesize that this decrease in read alignment may correspond to necrosis development and cell death of tissues, thus resulting in a lack of mRNA production (Chen et al., 2008).

Temporal Expression of Defense Induced Genes in Corn or Soybean

To determine if defense-induced responses underpin phenotypic symptomatic and asymptomatic disease development, a comparative transcriptional approach was undertaken. We posit that this approach will reveal pathway rewiring of transcriptional

response underlying tolerance and susceptibility within roots (Chen et al., 2016; Chowdhury et al., 2017) We identified a high correlation (i.e., >96%) between biological replicates; this indicates the robustness of both the experiment and the sampling (Figure 13). To explore expression patterns between treatments of mock and *F. virguliforme*, we clustered samples by principle coordinate analysis. As shown in Figure 14A, gene expression from corn roots tended to be primarily affected by time, instead of fungal treatment. This indicates that plant (i.e., root) development had a larger impact on gene expression than fungal colonization, with distinct clustering at 0, 2-7, 10, or 14 DPI. While this highlights significant changes in gene expression throughout the time course may be driven by development, the comparison of mock and fungal-inoculated treatments at each time point provided us an opportunity to discover genes that are specific to defense and immunity. Conversely, samples from soybean clustered by treatment throughout the time-course (Figure 14B). Indeed, at 0 and 2 DPI, both gene expression profiles clustered together; however, by 4 DPI, mock and fungal inoculated treatments had separated into distinct groups. The remaining samples were noticeably separated by treatment over the time-course. We posit that the large separation between treatments suggests large global expression changes within soybean roots, a response that is coincident with *F. virguliforme*-induced disease symptom development.

Next, to explore genes that were induced by *F. virguliforme* treatment, we filtered the dataset for genes that were significantly up or down regulated (adjusted P-value < 0.05, $|\log_2(\text{fold change})| > 1$) in the fungal-inoculated samples compared to the mock inoculated. In total, 28,956 genes were expressed in at least one timepoint over the time course in corn roots. A threshold of 1-$\log_2$ fold change was selected, as only 600 unique in corn was were

differentially expressed at this threshold across all time points. Of the significantly induced genes in corn roots to *F. virguliforme*, 267 were up regulated across the entire time course, with the majority of expression occurring at 0 and 14 DPI (Figure 14C, Table 10). In soybean root tissue, a total of 43,308 genes were expressed at one or more time points. Of these, more were significantly induced by *F. virguliforme* than in corn roots, within the time course, for a total of 10,898 unique genes. There was an almost equal ratio of positively and negatively regulated genes (5,326 and 5,644, respectively). But majority of induced genes primarily occurred after 7 DPI (Figure 14D, Table 11). This contrasts with the temporal induction of defense related genes in corn, highlighting this differential expression may promote the divergence in phenotype between corn and soybean.

To understand the function of genes underlying temporal differences of expression, we next conducted a Gene Ontology (GO) gene set enrichment analysis of the defense-response associated induced genes. Previous studies have observed that fungal interactions within roots elicit an array of immune responses, including the production of both reactive oxygen species (ROS) and secondary metabolites associated with immunity (Pusztahelyi et al., 2016; Zhang et al., 2017). Interestingly, we identified an enriched defense related response specifically from corn roots upregulated genes throughout the time course (Table 12). These genes were enriched for defense response, oxidation reduction, and terpenoid biosynthetic processes (Figure 14E), suggesting that corn, while phenotypically asymptomatic, recognized *F. virguliforme* as a pathogen. As expected, a broader response was enriched in samples from soybean roots, with 47 significant biological processes identified (Table 13). Among these processes were also defense responses and oxidation reduction pathways, but

additionally, phosphate metabolism, protein ubiquitination and cell to cell processes are indicative of a larger disruption and alteration of soybean root processes by *F. virguliforme*. Interestingly, the response of defense related processes were upregulated at earlier (0-4 DPI) time points in corn than soybean roots (Figure 14F). Specifically, defense responses and oxidation processes appeared to be up regulated in soybean 7-14 DPI. The divergence of temporal reactions related to defense may support tolerance in corn and susceptibility in soybean.

To define the broader implications of defense response induction in corn and soybean, we next explored the global co-expression of each host's transcriptome. As such, we hypothesized that changes in gene interactions stem from specific fungal interactions with each host. To address this, a differential gene correlation analysis (DGCA, see methods) was undertaken to discover significant changes within gene pairs resulting from treatment by employing the median z-score difference of the gene pair correlations in the first condition compared to the second condition, and then compared to all gene pairs. Investigating individual gene pair interactions enables one to discover gene co-expression on a much finer scale (McKenzie et al., 2016). Through this approach, in samples from corn, we found that 0.00003% of gene pairs were significantly differentially correlated, representing 129 gene pairs (Supplemental Dataset 1-2). Surprisingly, within this analysis, two *R*-genes were identified as having significant differential correlations. Resistance to *Pseudomonas syringae* pv. *maculicola* (*RPM1*) (Zm00001d014099) was positively correlated with xyloglucan galactosyl-transferase (Zm00001d029862) in the fungal treatment, which was negatively correlated in the mock treatments. Expression of *RPM1* was non-significantly down

regulated by 4.29 $\log_2$ fold change at 0 DPI, but gradually increased over the time course to 1 $\log_2$ fold change. Interestingly, this correlation analysis also highlighted the negative correlation of disease resistance protein *RPP13*-like 4 (Zm00001d018786) with Rho-N domain containing protein (Zm0001d051967); this correlation was positive under mock-inoculation conditions. Interestingly, this *R*-gene was identified as a candidate in SDS resistance through a genome-wide association study (GWAS) of soybean populations (Zhang et al., 2015). Herein, this *R*-gene was significantly down regulated at 4 DPI between treatments, indicating while this trait is associated with resistance in soybean, it is not significantly upregulated in corn and is likely not associated with pathogen tolerance.

Similar to the differential gene expression analysis within soybean, significantly more gene pairs were observed as significantly differentially correlated when compared to corn, totaling 5,526,057, or 0.61% gene pairs. To understand how these differentially correlated gene pairs were co-expressed, we built a planar filtered network to resolve a multi-scale co-expression network of these genes (see Methods). The fine scale of the DGCA enabled 1,161 modules to be formed. Of these modules, 198 contained hub genes related to defense and disease development and were hierarchically organized into four clusters (Figure 15). However, these small modules were not enriched by GO. The lack of enrichment could stem from the small scale (< 100 genes) of these clusters.

Orthologous Host Pathways Reveal Different Patterns of Induced Defense Responses

Previous studies comparing susceptible and resistant cultivars have identified temporal changes in gene expression, a process hypothesized to be associated with both compatible and incompatible pathogen interactions (Dupont et al., 2015; Kong et al., 2015). As noted above, we observed temporal changes in induction of defense related gene expression in both soybean and corn (Figure 14F). To understand if defense induced responses between soybean and corn response in a temporally similar or diverged manner, we compared expression of orthologous genes between hosts. As we observed temporal patterns of earlier upregulation of corn defense processes, we focused upon these genes within orthogroups that were significantly regulated within both hosts. To explore if defense response induction was dependent upon respective host, we clustered orthogroup response by significant upregulation unique to each host or across both hosts (Figure 16A). The vast majority of orthogroups that were significantly upregulated, were uniquely induced in soybean, accounting for 94% of up regulated orthogroups. Only 1.2% of orthogroups were uniquely upregulated in corn, and 4.7% were conserved in upregulation across both hosts in response to *F. virguliforme*.

Orthogroups that were uniquely upregulated in soybean were enriched for ROS processes, responses to defense and external stimuli, terpenoid metabolism, and abscisic acid metabolism (Table 14). Similarly, orthogroups that were upregulated in both hosts in response to *F. virguliforme* were enriched for multi-organismal processes, defense (Table 15). No orthogroups that were upregulated only in corn were enriched by GO. This lack of

enrichment stems from the few orthogroups (19) within this classification. While both clusters of orthogroup regulation unique to soybean and shared between soybean and corn were related to defense, we were interested in exploring how temporal patterns of orthogroup induction differed between soybean and corn. Therefore, we applied upregulated defense relevant GO groups that were enriched within corn at earlier (0-4 DPI) (Figure 14E) to capture the temporal response of orthologous genes that were enriched within soybean. Filtering upregulated orthogroup for GO processes of defense response, defense response to fungus, negative regulator protein metabolism processes, ROS and terpenoid biosynthesis (Figure 16B) revealed a shift in temporal expression between hosts. This change in upregulation of orthologous genes occurred at 2 and 4 DPI, in corn, whereas this regulation did not initialize until 4 to 7 DPI in soybean. Genes within these upregulated orthogroups encoded antifungal genes, including pathogenesis related protein 10 (*PR10*), stress induced protein 1, terpene synthase and Browman-Birk type trypsin inhibitor, suggesting corn activates specific responses to thwart *F. virguliforme* growth earlier than soybean. Interestingly, ROS production was similar during interactions between soybean and corn, indicating ROS bursts from fungal interaction upon roots were consistent in both hosts at early time points.

Non-orthologous Defense Processes within Soybean and Corn

While orthologous defense-related processes between soybean and corn identified temporal divergence in host response to this pathogen, we were also curious if these induction patterns were host-specific, as well as potentially relevant to the observed disease

phenotype. To address this, we interrogated the same defense related GO categories that were classified as enriched in corn (Figure 14E) and asked if non-orthologous genes were also significantly upregulated following fungal infection. Using this approach, we found that non-conserved temporal gene expression patterns related to defense were similar between soybean and corn; this includes processes associated with terpenoid biosynthesis, defense response to fungus, and ROS (Figure 17A). Similar to orthologous defense genes comparisons, broad defense processes related to antifungal activity were upregulated earlier in corn. Genes associated with this response include pathogenesis related maize seed (*PRSM*), *TIFY10B* (containing *JASMONATE ZIM DOMAINE* repressors), and hevein-like. Interestingly, both PRSM and hevein were previously identified as induced by fungal colonization (Majumdar et al., 2017; Wong et al., 2017). Similarly, TIFY10B was up-regulated in corn roots, and further analysis exploring the jasmonate biosynthesis pathway revealed minimal changes in expression between mock and treated, demonstrating jasmonic acid pathways in corn roots were repressed (Figure 17B, Figure 18).

As jasmonate precursor expression was not altered by *F. virguliforme* colonization in corn, we were curious as to what role, and through what mechanism(s) corn roots might perceive this fungal pathogen. To explore this question, we next interrogated several defense makers specific to corn root fungal interactions, as previously described (Balmer et al., 2013; Chuberre et al., 2018). As show in Figure 16B and Figure 17, pathogenesis related (*PR*) genes were induced over the selected time-course. However, while the array of *PR* genes that were expressed indicates that defense pathways were induced, *NONEXPRESSER OF PR GENES 1* (*NPR1*) was not up regulated in corn roots (Figure 18), suggesting upregulation of *PR* genes

is salicylic acid independent (Balmer et al., 2012). Early responses of callose deposition in response to chitin perception did not seem to be activated either, and instead CYP7A12 was downregulated at 4 DPI. Auxin and gibberellic acid expression did not appear to be modified in transcriptional expression throughout the time course. Ethylene biosynthesis was upregulated in corn roots (Figure 18), additionally *ETHYLENE RESPONSIVE FACTOR 105-LIKE* (*ERF-105-like*) was significantly upregulated in corn (Figure 17B) at 0 DPI. This is significant, as ethylene biosynthesis has been recently reported to be induced in SDS resistant soybean cultivars (Abdelsamad et al., 2019), a mechanism proposed to enhance host resistance to necrotrophs (Laluk and Mengiste, 2010). ERF-105-like transcription factor is associated with ethylene-responsive ROS regulation, limiting cellular damage (Bolt et al., 2017). In total surveying the phytohormonal landscape through transcriptomic expression has suggested that ethylene regulation may play key role in activating corn root defenses to *F. virguliforme.*

Constitutive Expression of Corn Genes within Orthologous Defense

While our primary goal herein was to characterize induced defense responses following fungal inoculation, as well to define the orthologous defense networks between during infection of a symptomatic (i.e., soybean) and asymptomatic (i.e., corn) host, the role of constitutive defense-associated responses remains. Previous studies suggest divergence in the temporal induction of defense responses between plants (Liu et al., 2018). To determine if the duration of constitutive orthologous gene expression in corn might underpin these responses, we next compared expression of soybean and corn orthogroups following mock

inoculation. Using this approach, we identified 182 orthogroups that were significantly upregulated in corn, in comparison to soybean, over the duration of the inoculation time-course (Figure 19). Based on this, we hypothesized that these orthogroups provide tolerance to *F. virguliforme* within corn through elevated expression during early interactions and moreover their expression would decrease in contrast to an induction in defenses in *F. virguliforme* inoculated soybeans. Surprisingly, a similar pattern of temporal expression of the constitutively up-regulated orthogroups was observed from 2-14 DPI in both hosts inoculated with *F. virguliforme* (Figure 19). Additionally, constitutively induced corn responses were 2 $\log_2$ higher in the *F. virguliforme* treatment when compared to the constitutive expression of the same genes under mock conditions. Orthologs in soybean do not appear to be upregulated to a similar extent upon colonization by *F. virguliforme* colonization, suggesting these responses within corn may assist in tolerance to *F. virguliforme.*

Divergence of Defense Expression Patterns Across Orthologous Transcription Factors

The temporal expression patterns of defensed induced orthologous genes by *F. virguliforme* colonization varied by host, indicating potential differences in pathway activation or repression by transcription factor expression. Within our orthologous dataset between soybean and corn, we extracted the transcription factors, and compared the changes in differential expression induced within each host by *F. virguliforme*, across the infection time course. Similar to orthologs that were upregulated by *F. virguliforme*, the vast majority of the differentially expressed transcription factors were uniquely to soybean. Only four

transcription factor orthogroups were uniquely induced in corn, while 11 were induced in both soybean and corn in response to *F. virguliforme.* Being we were interested in transcription factors altering temporal expression across both hosts, we focused our attention on transcription factors induced within both hosts.

Within the selected cluster of transcription factors orthogroups, three were expressed at 2 $\log_2$ fold change greater in corn when compared to soybean at 0 DPI (Black box, Figure 20A). A *NAC042* transcription factor (*No Apical Meristem (NAM), Arabidopsis Transcription Activation Factor (ATAF), and Cup-Shaped Cotyledon (CUC)*) exhibited the largest expression difference when comparing soybean changes between mock and inoculated treatments to the expression differences in corn induced by treatment. This transcription factor is responsive to hydrogen peroxide (Wu et al., 2012). Hydrogen peroxide production was elevated by transcription factor *ZAT12* (C_2H_2-zinc finger proteins) (Mittler et al., 2006) in corn at 0 DPI, indicating ROS production stimulated *NAC042* mRNA accumulation in corn more so than soybean, which may account for the >2 $\log_2$ fold change difference. The third transcription factor that was induced greater in corn was *DREB1A* (*DEHYDRATION-RESPONSIVE ELEMENT-BINDING PROTEIN 1A*). *NAC042* can bind and activate *DREB1A* to lower oxidative stress homologs in tomato (Thirumalaikumar et al., 2018). This process suggests that corn is able to quickly attenuate ROS production after defense responses are activated and lowers plant cell stress. However, *NAC042* is also a negative regulator of senescence (Wu et al., 2012). If *F. virguliforme* activates ethylene defense responses in corn, we hypothesize that it may be as a result of host recognition of *F. virguliforme* as a necrotroph, and that prolonged expression of *NAC042* is promoting cell longevity, thereby

inhibiting the induction of cell death. Interestingly, *NAC042* expression in soybean did not exceed levels of > 2 $\log_2$ fold change till 7 DPI, after symptom development. This made us wonder if host senescence plays a key role in sudden death syndrome development.

To explore this, we filtered the soybean transcriptome for significantly expressed *NACs*. Using this approach, we identified an additional seven *NACs* that were differentially expressed in soybean; interestingly, previous work demonstrated that these *NACs* play a role in both the negative and positive regulation of senescence, as well as in root development (Majid and Abbas, 2019) (Figure 20B, Supplemental Data Set 1-3). Three of these *NACs* have roles in senescence development, and include *NAC047*, *NAC055* and *NAC087*, of which *NAC055* and *NAC087* are abscisic acid responsive (Huysmans et al., 2018). In addition to ROS production, an increase of *9-CIS-EXPOSYCAROTENOID DIOXYGENASE* (*NCED*), the first step in ABA production (Xiong and Zhu, 2003) increased at 2 DPI to 4 $\log_2$ fold change and NACs upregulation was initialized at 4 and 7 DPI. However, these genes were not up regulated in corn roots. Several senescence associated genes (*SAG*s) were identified as up-regulated in soybean as early as 4-7 DPI. This is interesting, as previous work showed that *SENESCENCE ASSOCIATED GENE 13* (*SAG13*) is associated with the cell death response (Pell et al., 2004), *SAG21* and *SAG24* are both upregulated during early senescence (Salleh et al., 2012). Intriguingly, *SAG20* is activated by Necrosis and Ethylene Inducing Peptides (NEPs) from *Fusarium* spp, including similar phytotoxins produced in *F. virguliforme* (Chang et al., 2016). Also, *SENESCENCE REGULATORY GENE 1* (*SAG 1*) mRNA was elevated at 7 DPI. Again, none of these senescence-inducing processes, or associated genes, were significantly induced in corn across the time course of infection.

Plant development is also regulated by *NACs* transcription factors, which were induced in soybean roots when exposed to *F. virguliforme*. Lateral root growth is induced by *NAC022* (Xie et al., 2000), which was down regulated in soybean when colonized by *F. virguliforme*. In similar fashion, *NAC074* positively regulates xylem development (Xia et al., 2018), which was down regulated in soybean starting at 7 DPI. Vascular development, negatively regulated by *NAC083* by repressing *VASCULAR-RELATED NAC-DOMAIN7* (*VND7*) (Yamaguchi et al., 2010) was upregulated across the time course. However, root hydraulic conductivity was upregulated by decreasing the expression of *NAC104*, which negatively regulates water conductivity in association with differentiating tracheary elements (Zhao et al., 2008; Tang et al., 2018). In total, these processes demonstrate root development was altered when colonized by *F. virguliforme*, reducing development of vascular system and altering differentiation.

Discussion

Transcriptomic dissection of resistant and susceptible host responses to phytopathogens is common, and numerous studies have illuminated our understanding as to how host-specific pathogens modulate immunity. This approach provides a foundation to comparatively explore how immune pathways respond across diverged hosts to a single pathogen with a broad host range. Here, we applied the broad host range of *F. virguliforme* as a comparative system to probe differentially induced root responses between a monocot and a eudicot to uncover immune regulatory responses encoding tolerance and susceptibility. To do this, we

generated 72 transcriptomes across mock and inoculated hosts to pinpoint host responses specific to fungal root colonization throughout a two-week infection time course.

Soybean and corn have distinct phenotypic responses to *F. virguliforme* colonization. Soybean becomes symptomatic with root chlorosis at 7 DPI, and tap root necrosis at 14 DPI, and corn roots do not develop symptoms. Yet, underlying phenotypic differences are similar levels of fungal colonization, supporting corn as an asymptomatic host for *F. virguliforme* (Kolander et al., 2012). Corn root growth and development did not appear to shift in response to *F. virguliforme* colonization and were reflected by changes in gene expression when colonized, enriched for immune responses. Inversely, soybean roots exhibited a massive reprogramming of transcriptomic responses induced by symptom development. The divergence in magnitude of host responses has been observed within studies of a single host being colonized by pathogenic and non-pathogenic isolates (Lanubile et al., 2015).

While the number of genes induced by *F. virguliforme* root colonization varied substantially, both hosts exhibited gene expression that were enriched for defense, indicating temporal induction of immunity may play a role in tolerance of *F. virguliforme* by corn. Comparing orthologous expression of defense related processes highlighted the differential host responses between soybean and corn. Very few orthologous genes were differentially express in both hosts, suggesting a large transcriptomic shift in soybean. Orthologs encoding defense responses that were induced by *F. virguliforme* exhibited disparate temporal patterns of induction. Gene expression of corn and soybean changed the most between 2 and 7 DPI, representing recognition of the fungal interactor, and initiating defense responses, as

well as the fungus shifting form a biotrophic phase to a necrotrophic phase on soybean. Shifts in host gene expression derived from fungal life style changes during colonization have been recorded in hemibiotrophic interactions (Njiti et al., 1996; Chowdhury et al., 2017). Defense related process are upregulated both hosts encoding hydrogen peroxide bursts, and anti-microbial proteins to limit fungal growth. However, as the infection time course proceeds many orthologous defense genes within corn are lower in expression, indicating a return to normalization, similar to pathogen resistant cultivars (Chen et al., 2016). Inverse to corn, soybean defense responses were increasing to highest levels at 14 DPI, highlighting a delayed response to *F. virguliforme* colonization. Non-orthologous defense induced responses exhibited similar trends between hosts for majority of defense processes, suggesting the temporal dynamics of orthologous response maybe key to enabling tolerance in corn. Expression of orthologous anti-fungal metabolites by 2 DPI may restrict further spread of this fungus to other root structures (Allardyce et al., 2013; Kuhar et al., 2013).

Overall, this suggests early recognition and activation of defense s in critical for tolerance. Early activation of defense responses in corn may stem from induction of ethylene production and ROS production. Induction of ethylene in soybean roots lowered disease severity and activated *PR* gene and ROS (Abdelsamad et al., 2019), as observed herein. Reactive oxygen species also induce transcription factors regulating cell stress, such as *ERF-105* (Bolt et al., 2017) and *NAC042* (Thirumalaikumar et al., 2018). The reduction. The reduction of ROS may limit further colonization as the fungus switches from a biotrophic to necrotrophic lifestyle (Chowdhury et al., 2017).

As *F. virguliforme* transitions from a biotrophic to necrotrophic lifestyle on soybean, a large transcriptomic rewiring occurs. Plant pathogens acting as necrotrophs will promote plant cell death, which results in a drastic shift in host gene expression. Indeed, over the time-course of analysis, we observed several critical senescence related transcription factors from soybean as being distinctly activated, or repressed, following pathogen infection. This in turn activated several senescence related genes within soybean root, promoting inhibition of protein synthesis, hydrolysis of macromolecules and degeneration of cells (Podzimska-Sroka et al., 2015). The up-regulation of cell senescence would promote further colonization of by a necrotrophic fungus, such as *F. virguliforme*. Colonization of soybean roots by *F. virguliforme* triggers further ROS production, which will in turn actives the induction of NAC senescence-associated transcription factors (Haffner et al., 2015). Additionally, senescence processes through NAC transcription factors are also induced by abscisic acid; this is interesting, as we observed induced expression in soybean roots at 2 DPI, concomitant with *NAC055* and *NAC087* were upregulation at 4 and 7 DPI, respectively. We posit that *F. virguliforme* susceptibility in soybean is mediated in part by pathogen-induced senescence responses during infection.

This activation of senescence by necrotrophs has been noted for other fungi. When *Sclerotinia sclerotium* colonized a compatible host, the pathogen will secrete oxalic acid, triggering ROS production and program cell death to the advantage of the necrotrophy (Williams et al., 2011). Similarly, *F. virguliforme* can secrete toxins to initiate cell death; however, this has only been documented in foliar tissues (Chang et al., 2016). Hemibiotrophic vascular pathogen *F. oxysporum* activates senescence by targeting the COI1

of the JA-binding JAZ-COI1 co-receptor (Thatcher et al., 2009) We demonstrated the activation senescence processes occurred only within the susceptible host during colonization by *F. virguliforme* through NACs transcription factors, reinforcing the concept of necrotrophy activated senescence.

The lack of information surrounding the molecular signature(s) responsible for senescence in roots lessens our ability to precisely define the factors critical for triggered senescence. Further studies regarding root senescence within or without pathogen colonization would provide clarity to mechanisms of senescence with plant's organs below ground. Plant senescence and defense have many critical pathways that overlap (Yuan et al., 2019). Several NAC transcription factors discovered to be altered in expression herein, have played roles in immunity and susceptibility. Knock out of *NAC055* increases resistance of Arabidopsis to *Botrytis* spp. infection (Bu et al., 2008). Also, *NAC042* activates an anti-microbial camalexin biosynthesis in Arabidopsis to *Alternaria brassicicola* (Saga et al., 2012). Additionally, hypersensitive responses within plant defenses utilizes similar pathways as host natural senescence by induce program cell death (Yuan et al., 2019). The resolution to decipher if gene expression is indicative of pathogen triggered senescence or host induced susceptibility remains currently enigmatic. However, the mounting evidence presented herein, and previously seems to suggest that necrotrophic pathogen manipulation of genetic pathways leading to a favorable host environment are evident (Häffner et al., 2010; Williams et al., 2011; Haffner et al., 2015; Podzimska-Sroka et al., 2015; Chowdhury et al., 2017). The culmination of pathogen lifestyle, host genetics and plant development should be further

explored to decipher the interaction of defense responses and pathogen accelerated senescence.

Acknowledgments

We would like to recognize Michigan State University (MSU) project GREEEN and the C.S. Mott Foundation for funding of ABY and research. Marty Chilvers for providing the *Fusarium virguliforme* mont-1 isolate. We would also like to recognize the support staff at the MSU Institute for Cyber enabled Research High Performance Computing Cluster for assistance in software optimization. This research was supported by funding from the MSU Plant Resilience Institute.

Author Contributions

Designed framework: B.D., S.H.S., A.B.Y.; Conducted Experiments: A.B.Y; Analyzed data: A.B.Y., S.H.S., B.D. Wrote the manuscript: A.B.Y., S.H.S., B.D.

Table 10. **Significantly induced defense genes in corn.** To be considered significantly induced genes needed to be 1-fold change or greater in *F. virguliforme* treated compared to mock inoculated with an adjusted $P > 0.05$.

		Corn Inoculated					
	DPI	0	2	4	7	10	14
Corn Mock	0	92					
	2		13				
	4			11			
	7				24		
	10					57	
	14						457

		Corn Inoculated Up Regulated					
	DPI	0	2	4	7	10	14
Corn Mock	0	86					
	2		7				
	4			7			
	7				21		
	10					35	
	14						151

		Corn Inoculated Down Regulated					
	DPI	0	2	4	7	10	14
Corn Mock	0	6					
	2		5				
	4			4			
	7				3		
	10					17	
	14						306

Table 11. **Significantly induced defense genes in soybean.** To be considered significantly induced genes needed to be 1-fold change or greater in *F. virguliforme* treated compared to mock inoculated with an adjusted $P > 0.05$.

		Soybean Inoculated					
	DPI	0	2	4	7	10	14
Soybean Mock	0	771					
	2		151				
	4			266			
	7				1,737		
	10					4,564	
	14						9,542

		Soybean Inoculated Up Regulated					
	DPI	0	2	4	7	10	14
Soybean Mock	0	724					
	2		121				
	4			232			
	7				1,538		
	10					3,256	
	14						4,957

		Soybean Inoculated Down Regulated					
	DPI	0	2	4	7	10	14
Soybean Mock	0	47					
	2		35				
	4			34			
	7				199		
	10					1,308	
	14						4,585

Table 12. Gene ontology enrichment of biological processes within corn genes significantly up regulated between *Fusarium virguliforme* inoculated and mock treatments across the time-course of two weeks.

GO term	Ontology	Description	Adjusted P-value
GO:0055114	P	oxidation-reduction process	0.0012
GO:0016114	P	terpenoid biosynthetic process	0.0012
GO:0006721	P	terpenoid metabolic process	0.002
GO:0006952	P	defense response	0.0026
GO:0051346	P	negative regulation of hydrolase activity	0.0098
GO:0044710	P	single-organism metabolic process	0.0098
GO:0008299	P	isoprenoid biosynthetic process	0.0098
GO:0051248	P	negative regulation of protein metabolic process	0.016
GO:0032269	P	negative regulation of cellular protein metabolic process	0.016
GO:0050832	P	defense response to fungus	0.021
GO:0006720	P	isoprenoid metabolic process	0.022
GO:0009620	P	response to fungus	0.032

Table 13. Gene ontology enrichment of biological processes within soybean genes significantly up regulated between *Fusarium virguliforme* inoculated and mock treatments across time course of two weeks.

GO term	Ontology	Description	Adjusted P-value
GO:0055114	P	oxidation reduction	2.40E-25
GO:0008152	P	metabolic process	1.40E-21
GO:0043687	P	post-translational protein modification	4.20E-19
GO:0006464	P	protein modification process	1.50E-18
GO:0006468	P	protein amino acid phosphorylation	1.10E-17
GO:0043412	P	macromolecule modification	7.80E-17
GO:0016310	P	phosphorylation	2.60E-16
GO:0006796	P	phosphate metabolic process	2.60E-16
GO:0006793	P	phosphorus metabolic process	2.60E-16
GO:0051704	P	multi-organism process	3.70E-11
GO:0009875	P	pollen-pistil interaction	4.40E-11
GO:0008037	P	cell recognition	4.40E-11
GO:0048544	P	recognition of pollen	4.40E-11
GO:0009856	P	pollination	4.40E-11
GO:0000003	P	reproduction	8.00E-11
GO:0022414	P	reproductive process	8.00E-11
GO:0032501	P	multicellular organismal process	4.90E-10
GO:0006979	P	response to oxidative stress	1.80E-05
GO:0016567	P	protein ubiquitination	9.60E-05
GO:0070647	P	protein modification by small protein conjugation or removal	0.00012
GO:0032446	P	protein modification by small protein conjugation	0.00012
GO:0006952	P	defense response	0.00031
GO:0007154	P	cell communication	0.00048
GO:0009607	P	response to biotic stimulus	0.0014
GO:0016052	P	carbohydrate catabolic process	0.0015
GO:0044283	P	small molecule biosynthetic process	0.0028
GO:0042221	P	response to chemical stimulus	0.0028
GO:0043436	P	oxoacid metabolic process	0.0031
GO:0044282	P	small molecule catabolic process	0.0031
GO:0006082	P	organic acid metabolic process	0.0031
GO:0019752	P	carboxylic acid metabolic process	0.0031

Table 13. (cont'd)

GO term	Ontology	Description	Adjusted P-value
GO:0044267	P	cellular protein metabolic process	0.005
GO:0016053	P	organic acid biosynthetic process	0.0072
GO:0046394	P	carboxylic acid biosynthetic process	0.0072
GO:0008610	P	lipid biosynthetic process	0.0096
GO:0044281	P	small molecule metabolic process	0.011
GO:0046164	P	alcohol catabolic process	0.012
GO:0044275	P	cellular carbohydrate catabolic process	0.017
GO:0006066	P	alcohol metabolic process	0.019
GO:0032787	P	monocarboxylic acid metabolic process	0.029
GO:0006006	P	glucose metabolic process	0.029
GO:0006631	P	fatty acid metabolic process	0.031
GO:0006720	P	isoprenoid metabolic process	0.038
GO:0008299	P	isoprenoid biosynthetic process	0.038
GO:0005996	P	monosaccharide metabolic process	0.041
GO:0019318	P	hexose metabolic process	0.045

Table 14. Gene ontology enrichment of biological processes within soybean orthogroups of uniquely upregulated significantly between *Fusarium virguliforme* inoculated and mock treatments across time course of two weeks.

GO term	Ontology	Description	Adjusted P-value
GO:0050896	P	response to stimulus	5.33E-14
GO:0002679	P	respiratory burst involved in defense re...	1.78E-05
GO:0042221	P	response to chemical	1.78E-05
GO:0045730	P	respiratory burst	1.78E-05
GO:0009628	P	response to abiotic stimulus	1.78E-05
GO:0006952	P	defense response	3.82E-05
GO:0051704	P	multi-organism process	3.91E-05
GO:0006811	P	ion transport	0.00023134
GO:0015849	P	organic acid transport	0.00032902
GO:0006082	P	organic acid metabolic process	0.00061075
GO:0006950	P	response to stress	0.00061075
GO:0043436	P	oxoacid metabolic process	0.00061075
GO:0046942	P	carboxylic acid transport	0.00062641
GO:0019752	P	carboxylic acid metabolic process	0.00079318
GO:0015711	P	organic anion transport	0.00103642
GO:0032787	P	monocarboxylic acid metabolic process	0.00115672
GO:0017144	P	drug metabolic process	0.00155853
GO:1901700	P	response to oxygen-containing compound	0.00155853
GO:0002252	P	immune effector process	0.00155853
GO:0010033	P	response to organic substance	0.00203583
GO:0044283	P	small molecule biosynthetic process	0.00253817
GO:0080167	P	response to karrikin	0.0025574
GO:0006820	P	anion transport	0.00257496
GO:0001101	P	response to acid chemical	0.00431842
GO:0009607	P	response to biotic stimulus	0.00540989
GO:0044281	P	small molecule metabolic process	0.00540989
GO:0046394	P	carboxylic acid biosynthetic process	0.00603207
GO:0016053	P	organic acid biosynthetic process	0.00663717
GO:0071702	P	organic substance transport	0.00663717
GO:0055085	P	transmembrane transport	0.00764977
GO:0009698	P	phenylpropanoid metabolic process	0.00883584
GO:0007154	P	cell communication	0.01226122
GO:0051716	P	cellular response to stimulus	0.01226783

Table 14. (cont'd)

GO term	Ontology	Description	Adjusted P-value
GO:1903825	P	organic acid transmembrane transport	0.01226783
GO:0051707	P	response to other organism	0.01439472
GO:0009605	P	response to external stimulus	0.01460592
GO:0043207	P	response to external biotic stimulus	0.0185075
GO:0010038	P	response to metal ion	0.0185075
GO:0002376	P	immune system process	0.0185075
GO:1905039	P	carboxylic acid transmembrane transport	0.02166732
GO:0010035	P	response to inorganic substance	0.02291405
GO:0000165	P	MAPK cascade	0.030285
GO:0019748	P	secondary metabolic process	0.030285
GO:0023014	P	signal transduction by protein phosphory...	0.03454733
GO:0098656	P	anion transmembrane transport	0.03540565
GO:0006810	P	transport	0.037015
GO:0006721	P	terpenoid metabolic process	0.037015
GO:0034220	P	ion transmembrane transport	0.04079204
GO:0009687	P	abscisic acid metabolic process	0.0424987
GO:0043288	P	apocarotenoid metabolic process	0.0424987
GO:1902644	P	tertiary alcohol metabolic process	0.0424987
GO:0006865	P	amino acid transport	0.0424987
GO:1900424	P	regulation of defense response to bacter...	0.0424987

Table 15. Gene ontology enrichment of biological processes within soybean and corn orthogroups of shared in upregulated between *Fusarium virguliforme* inoculated and mock treatments across the time-course of two weeks.

GO term	Ontology	Description	Adjusted P-value
GO:0051704	P	multi-organism process	3.70E-05
GO:0009719	P	response to endogenous stimulus	3.70E-05
GO:0009725	P	response to hormone	8.39E-05
GO:0042221	P	response to chemical	0.000192478
GO:0098542	P	defense response to other organism	0.000192478
GO:0010033	P	response to organic substance	0.000285544
GO:0071495	P	cellular response to endogenous stimulus	0.000285544
GO:0009605	P	response to external stimulus	0.000481195
GO:0042493	P	response to drug	0.000501759
GO:0032870	P	cellular response to hormone stimulus	0.000636658
GO:1901700	P	response to oxygen-containing compound	0.0007403
GO:0050896	P	response to stimulus	0.000925375
GO:0071310	P	cellular response to organic substance	0.001216207
GO:0001101	P	response to acid chemical	0.001216207
GO:0014070	P	response to organic cyclic compound	0.001233833
GO:0051707	P	response to other organism	0.002844311
GO:0050776	P	regulation of immune response	0.002844311
GO:0070887	P	cellular response to chemical stimulus	0.002844311
GO:0043207	P	response to external biotic stimulus	0.002844311
GO:0009607	P	response to biotic stimulus	0.0037015
GO:0007154	P	cell communication	0.0037015
GO:0071229	P	cellular response to acid chemical	0.0037015
GO:0006952	P	defense response	0.0037015
GO:0007165	P	signal transduction	0.0037015
GO:0009751	P	response to salicylic acid	0.00384956
GO:0044550	P	secondary metabolite biosynthetic proces...	0.003986231
GO:0023052	P	signaling	0.005483704
GO:0009755	P	hormone-mediated signaling pathway	0.007931786
GO:0009966	P	regulation of signal transduction	0.008636833
GO:0019748	P	secondary metabolic process	0.008636833
GO:0071407	P	cellular response to organic cyclic comp...	0.01146271

Table 15. (cont'd)

GO term	Ontology	Description	Adjusted P-value
GO:0023051	P	regulation of signaling	0.012193176
GO:0035556	P	intracellular signal transduction	0.012193176
GO:0006955	P	immune response	0.0133254
GO:0010646	P	regulation of cell communication	0.014806
GO:0002682	P	regulation of immune system process	0.014806
GO:0032501	P	multicellular organismal process	0.016948974
GO:0010374	P	stomatal complex development	0.018982051
GO:1901701	P	cellular response to oxygen-containing c...	0.022209
GO:1901615	P	organic hydroxy compound metabolic proce...	0.024173061
GO:0010941	P	regulation of cell death	0.024173061
GO:0032101	P	regulation of response to external stimu...	0.024173061
GO:0009595	P	detection of biotic stimulus	0.024173061
GO:0009697	P	salicylic acid biosynthetic process	0.024173061
GO:0031640	P	killing of cells of other organism	0.024173061
GO:0044364	P	disruption of cells of other organism	0.024173061
GO:0048583	P	regulation of response to stimulus	0.024173061
GO:0000165	P	MAPK cascade	0.024173061
GO:0023014	P	signal transduction by protein phosphory...	0.0251702
GO:0009617	P	response to bacterium	0.029031373
GO:0046677	P	response to antibiotic	0.031320385
GO:0006468	P	protein phosphorylation	0.036316604
GO:0043900	P	regulation of multi-organism process	0.037015
GO:0032502	P	developmental process	0.037688
GO:0042742	P	defense response to bacterium	0.038336964
GO:0001906	P	cell killing	0.041560702
GO:0007584	P	response to nutrient	0.043396897
GO:0031347	P	regulation of defense response	0.046885667
GO:0042445	P	hormone metabolic process	0.046885667

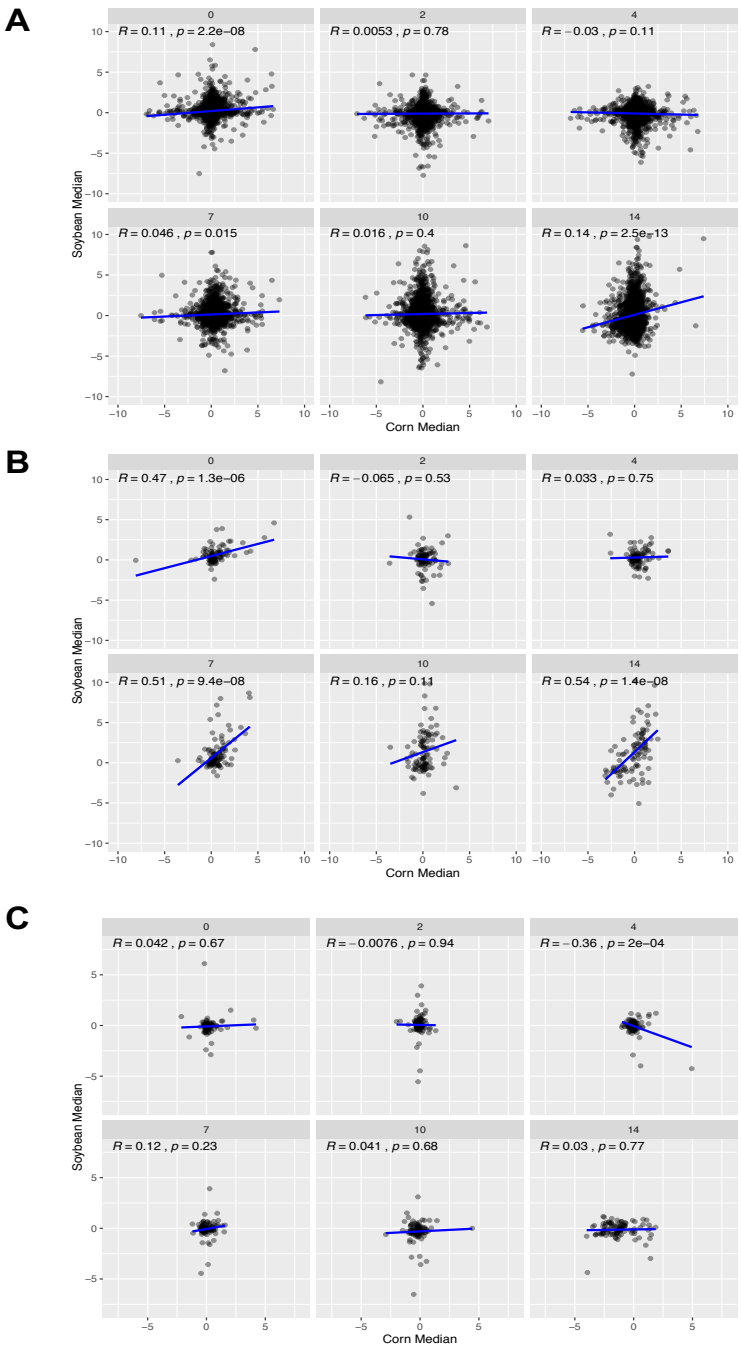

Figure 10. Correlation plots of differentially induced orthogroups between soybean and corn. Correlation of median transformed $\log_2$ fold changes between *F. virguliforme* inoculated and mock inoculated orthogroups within soybean against corn at each timepoint within the infection time course for (A) orthogroups uniquely differentially regulated in soybean, (B) orthogroups differentially regulated in corn and soybean, (C) orthogroups uniquely differentially regulated only in corn.

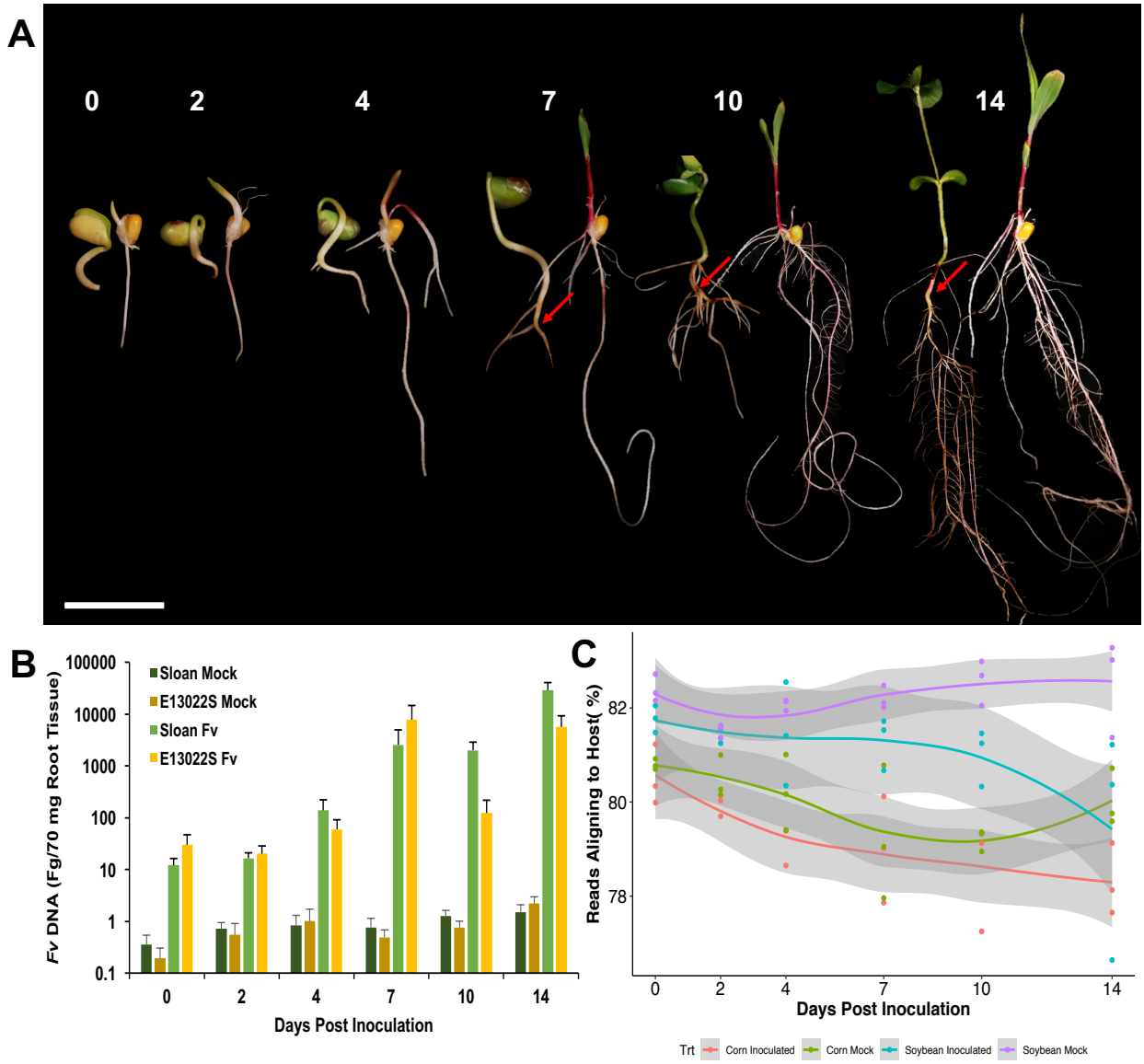

Figure 11. ***Fusarium virguliforme*** **root inoculation time course phenotypes of soybean and corn.** (A) Representative images plant growth and development over 14 days post inoculation with *F. virguliforme*. White scale bar is equivalent to 4 cm. (B) *F. virguliforme* DNA on inoculated and mock soybean and corn roots as detected by quantitative PCR. Values are average of two plants from three biological replicates ± SEM (n=6). (C) The percent of unique trimmed reads aligning to each respective genome within corresponding treatments of corn or soybean inoculated with *F. virguliforme* or mock (water), across 0-14 days post inoculation. Each sample is indicated by a colored dot and lines are the average of three biological repeats. Grey shade indicates SEM.

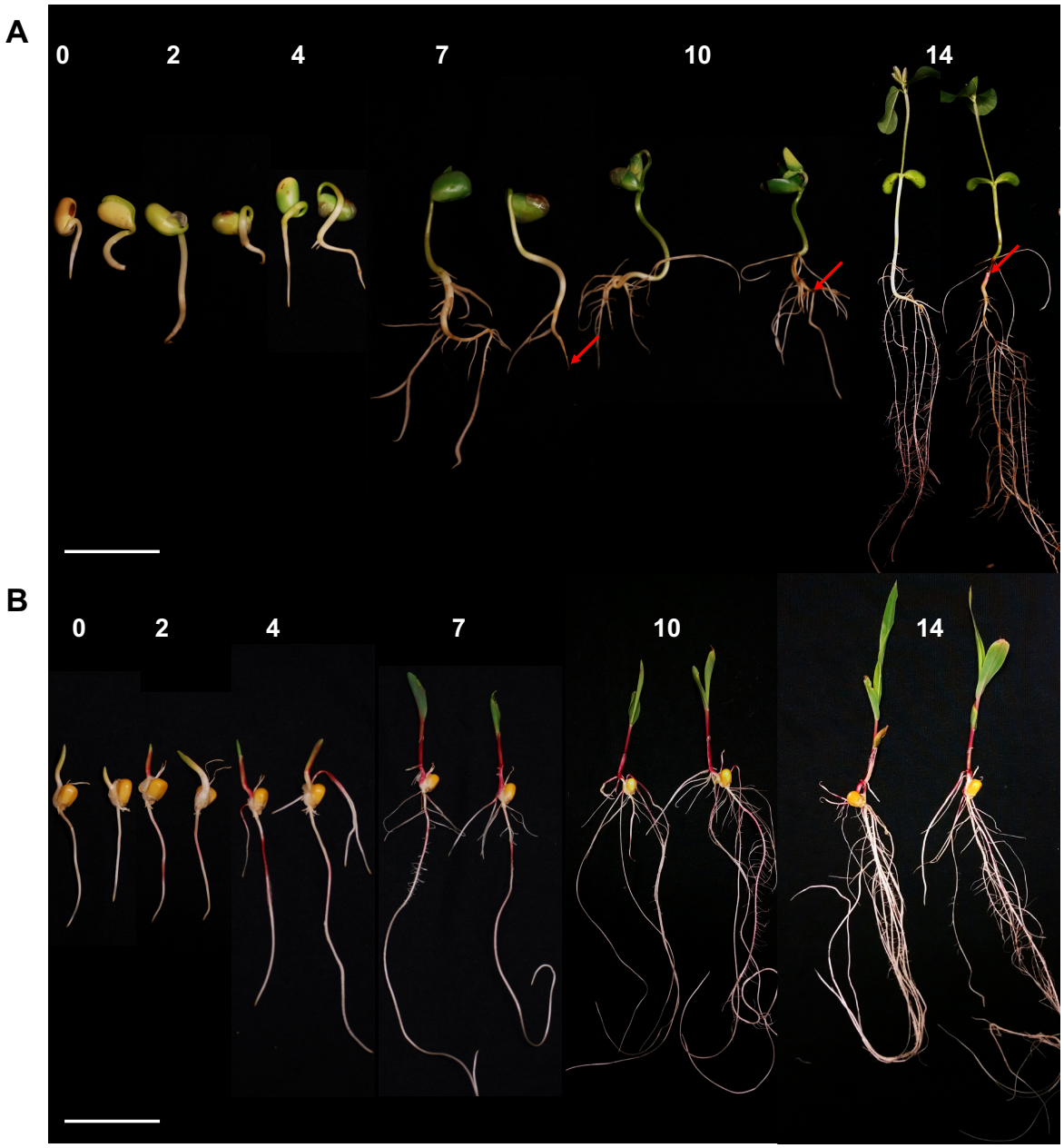

Figure 12. Plant growth and development over infection time course. Representative images plant growth and development over 14 days post inoculation with *Fusarium virguliforme* for soybean (A) and corn (B). White scale bar is equivalent to 4 cm. Mock inoculated host is of the left of each pair, *F. virguliforme* is on the right side of each timepoint. Representative images are also duplicated in Figure 10.

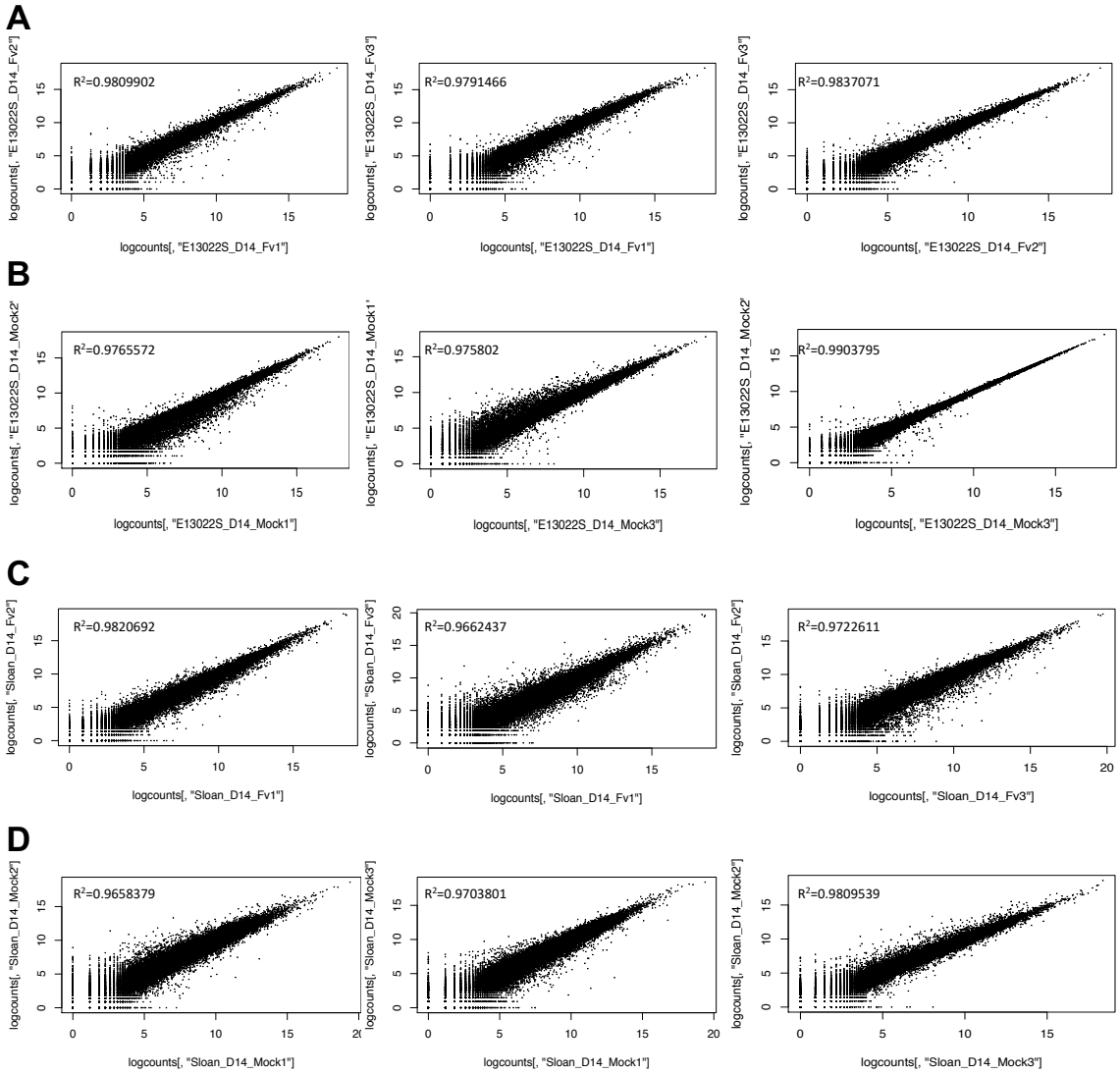

Figure 13. Biological reproducibility of samples from different time courses. Correlation of gene expression values in three biological replicates from 14 DPI samples of corn inoculated with *Fusarium virguliforme* (A) or mock (B) inoculated with water, and soybean inoculated with *F. virguliforme* (C) or mock (D) inoculated with water.

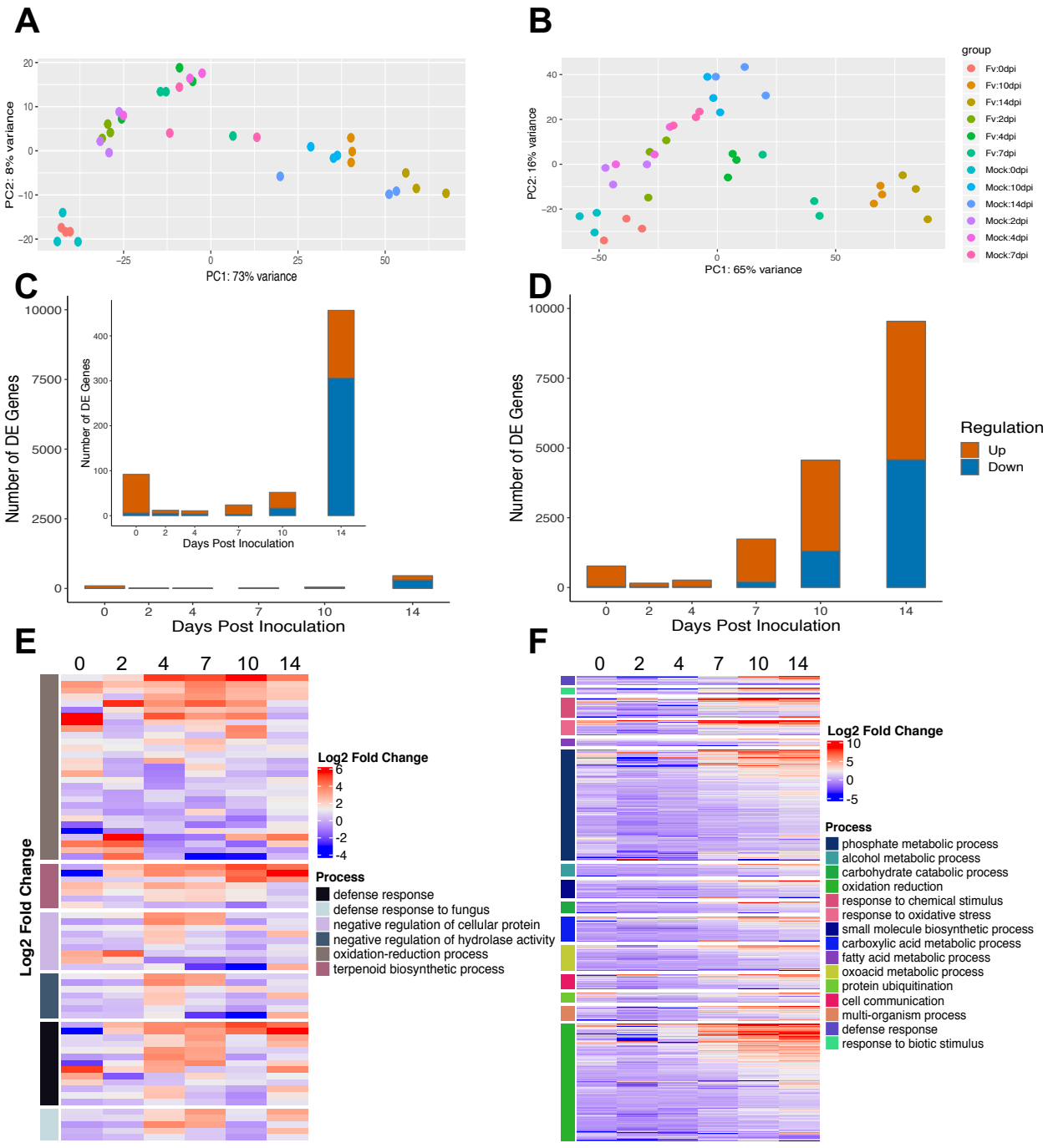

Figure 14. Temporal expression patterns of defense response genes in corn and soybean. (A) and (B) Principle component analysis (PCA) of gene expression values of either corn or soybean inoculated with *Fusarium virguliforme* or mock inoculated with water. (C) and (D) Number of significant differentially regulated genes with $\log_2(FC) > 1$ between mock and inoculated of corn with inset of early differentially regulated genes in corn or soybean over six timepoints. (E) and (F) Heatmap of significant gene ontology enrichment of up-regulated genes across pooled time points for corn (n=70) and soybean (n=1,792).

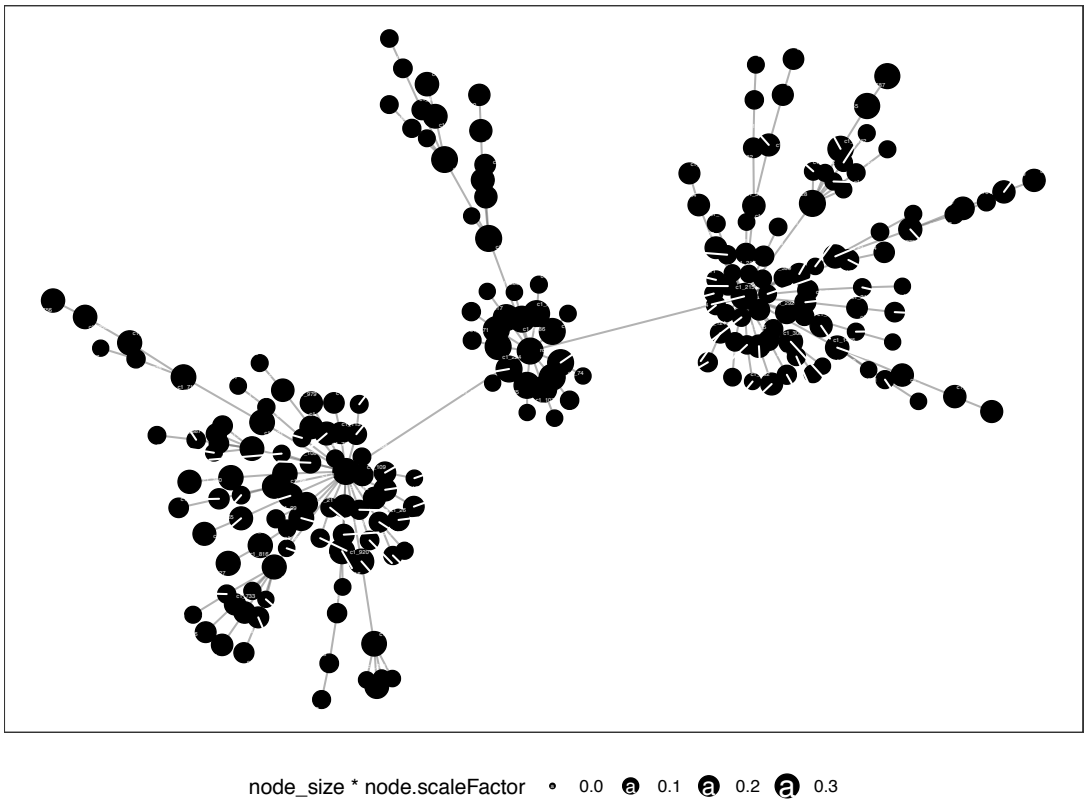

Figure 15. **Module hierarchy of modules hubs containing defense related genes within soybean.** These modules were identified using MEGENA. Node size are proportional to the number of connections for each gene.

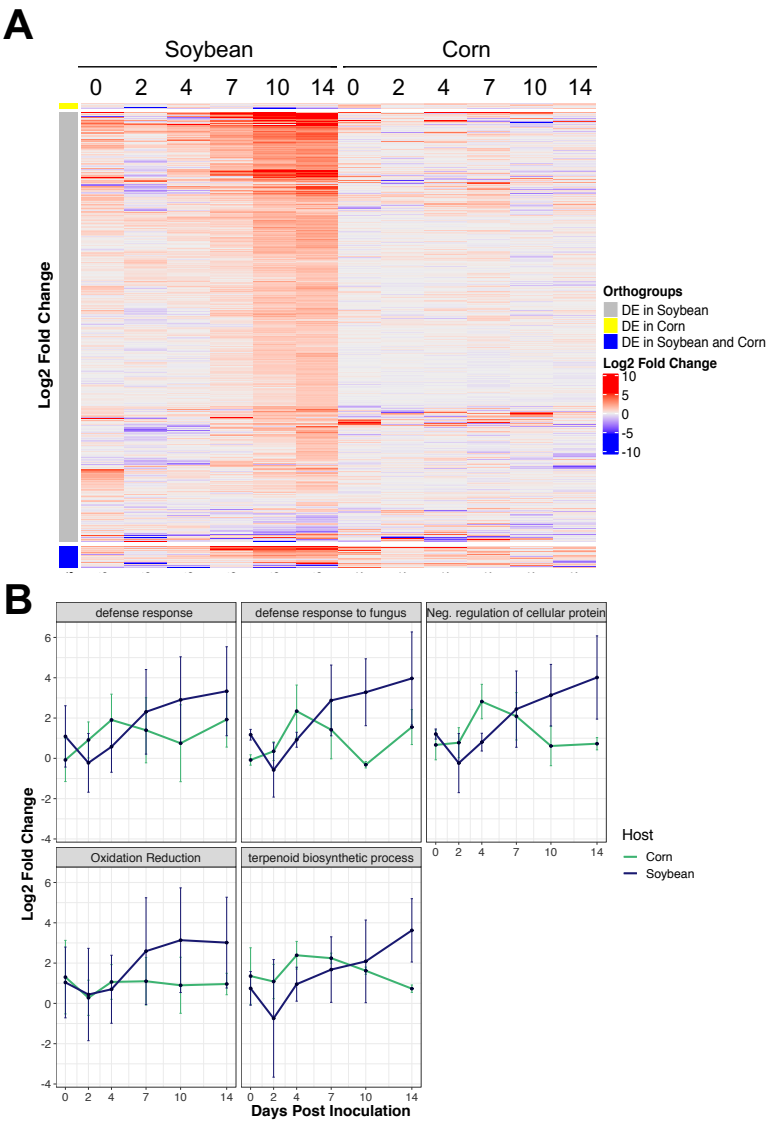

Figure 16. Orthologous host processes reveal different patterns of induced defense response. (A) Heatmap of $\log_2$(FC) > 1 of significantly upregulated genes at a single timepoint in at least one host between mock and inoculated (n=1,453). Blue indicates orthologous genes from soybean and corn were significant, grey indicates orthologous genes from soybean were significant, blue, that corn orthologous genes were significantly differential expressed (DE). (B) Mean expression patterns of $\log_2$(FC) > 1 of significantly upregulated orthologous genes at a single timepoint in both hosts, over the infection time course of orthologous gene ontology pathways enriched in corn. Error bars indicated 1 standard deviation of the mean.

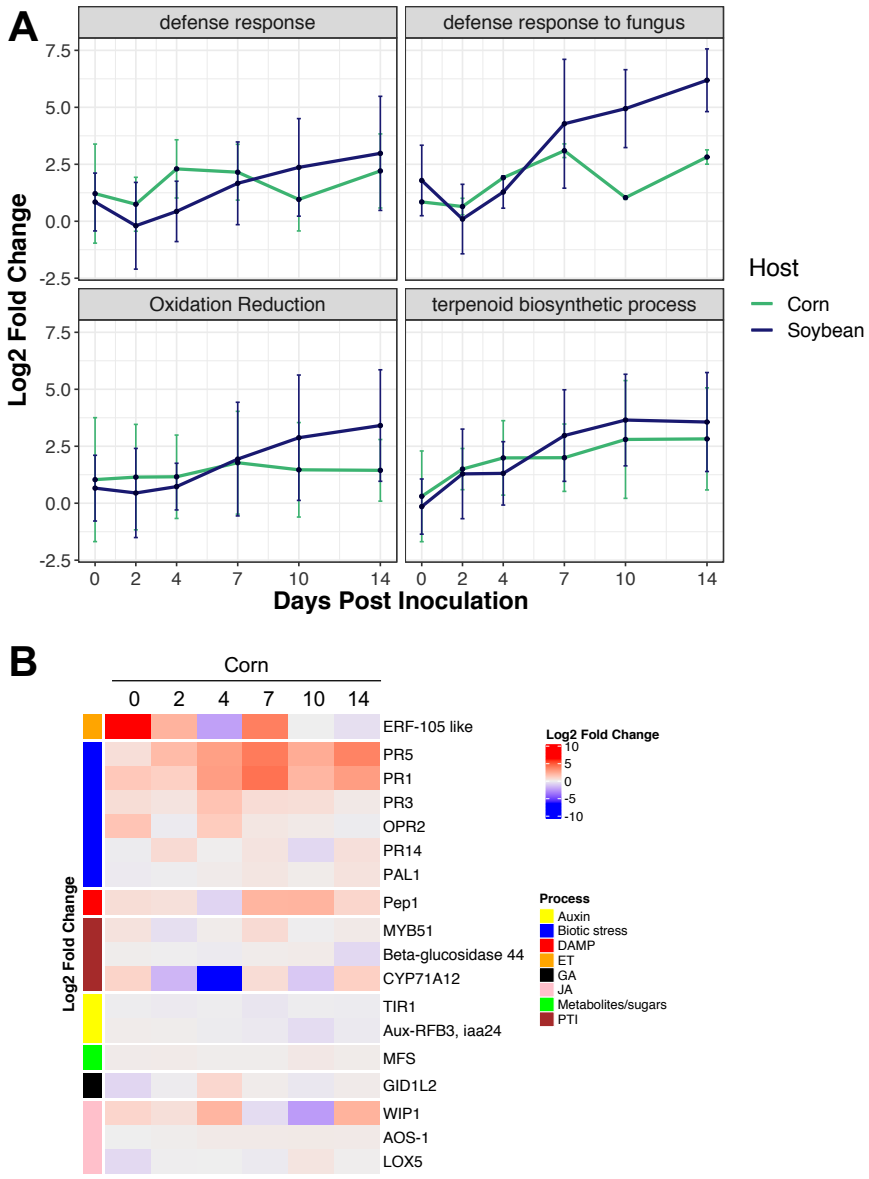

Figure 17. Processes unique to corn aid in immune responses to *Fusarium virguliforme*. (A) Mean expression patterns of $\log_2(FC) > 1$ of significantly upregulated non-orthologous genes in at least a single timepoint in both hosts over the infection time course of genes identified within the same gene ontology categories but not orthologous. Error bars indicated 1 standard deviation of the mean. (B) Gene expression of corn root defense markers across infection time course, without a soybean orthologous group.

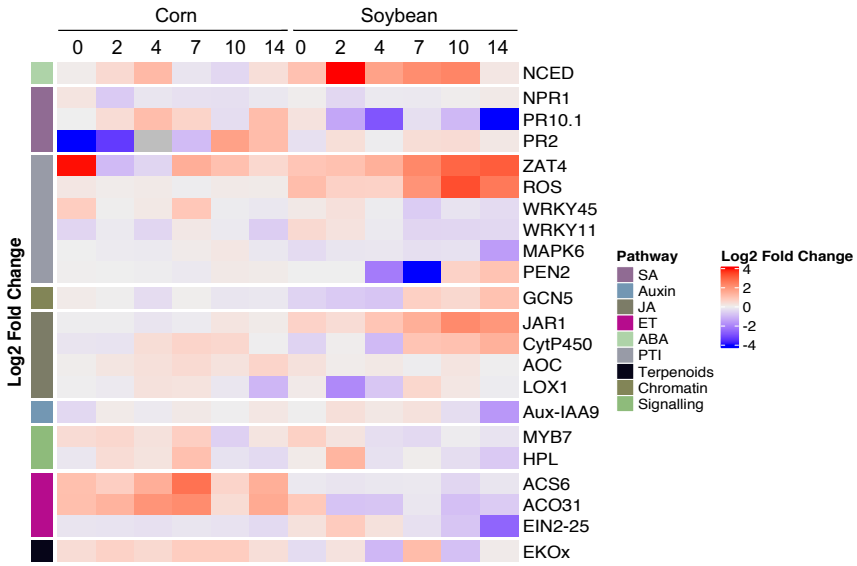

Figure 18. Expression of orthologous genes in defense relevant processes. Heatmap of gene expression $\log_2$-fold changes between *F. virguliforme* and mock treatment of corn and soybean hosts, for marker genes relevant to SA (salicylic acid), auxin, JA (jasmonic acid), ethylene, ABA (Abscisic Acid), PTI (Pattern Triggered Immunity), terpenoids, chromatin, and signaling.

A

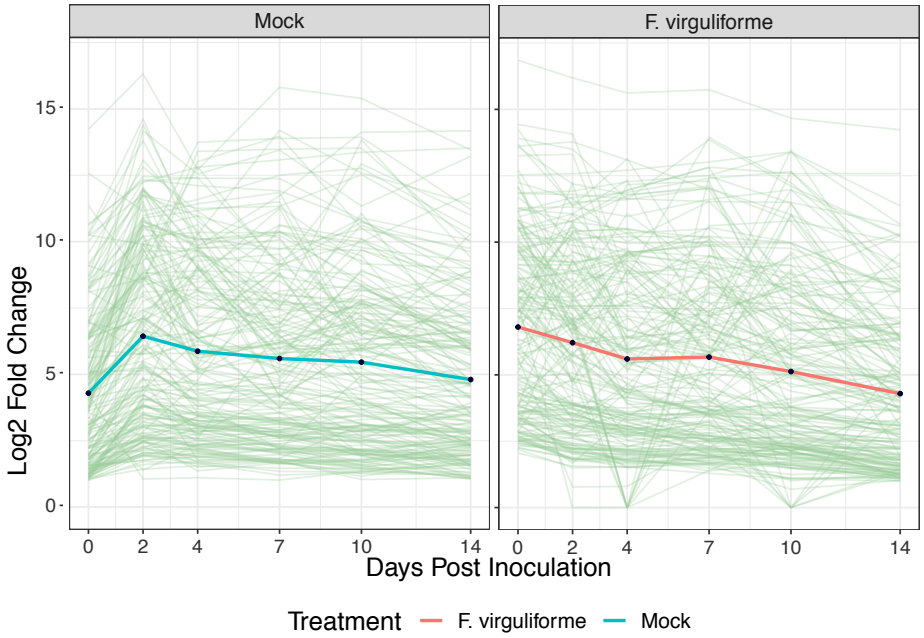

Figure 19. Conservation of innate defense gene expression preceding inoculation with *Fusarium virguliforme.* Line graph of expression patterns of orthogroups that are uniquely up regulated in corn when compared to soybean $\log_2(FC) > 1$, and corresponding regulation when corn and soybean are colonized by *F. virguliforme*.

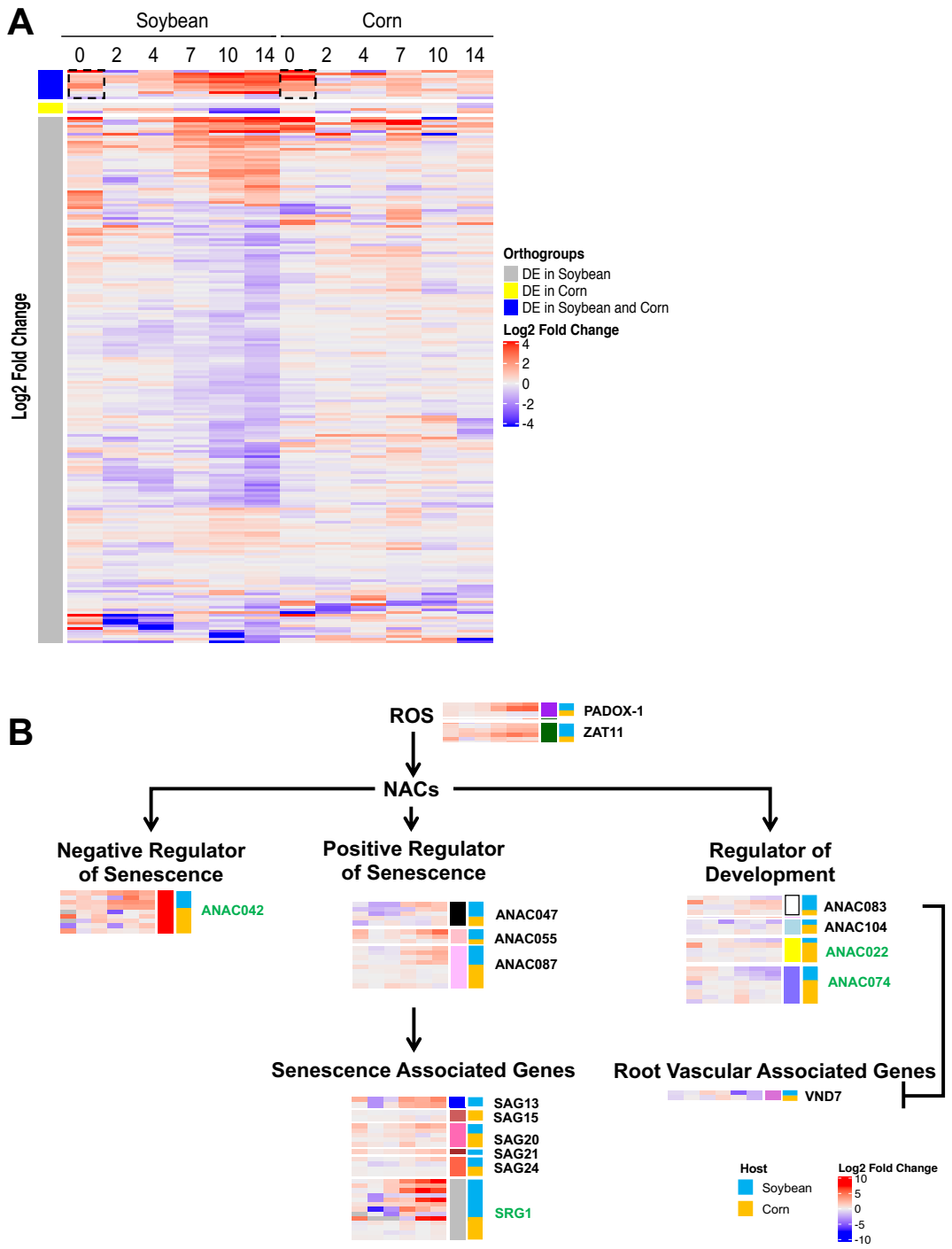

Figure 20. Divergence of defense expression patterns of orthologous transcription factors. (A) Heatmap of log2 fold change >1 of significantly upregulated genes at a single timepoint in at least one host between mock and inoculated (n=215). Blue indicates orthologous genes from soybean and corn were significant, grey indicates orthologous genes from soybean were significant, blue, that corn orthologous genes were significantly differential expressed (DE) (B). Representation of reactive oxygen species driven no apical meristem (NAM), ATAF1/2, cup-shaped cotyledon2 (CUC2) (NAC) pathways that exhibited

differential expression patterns of $\log_2$(FC) > 1 between mock and inoculated of soybean, and corresponding orthologous or homologs in corn, affecting senesce genes, root vascular development and senescence regulation. Each gene heatmap contains temporal expression from 0-14 DPI for soybean (bar color blue) and corn (bar color yellow). Green gene names indicates orthologous genes.

REFERENCES

REFERENCES

Abdelsamad, N.A., MacIntosh, G.C., and Leandro, L.F.S. (2019). Induction of ethylene inhibits development of soybean sudden death syndrome by inducing defense-related genes and reducing *Fusarium virguliforme* growth. PLoS ONE **14,** e0215653.

Alexa A and Rahnenfuhrer J. (2018). Topgo: Enrichment analysis for gene ontology. R package version 2.36.0.

Allardyce, J.A., Rookes, J.E., Hussain, H.I., and Cahill, D.M. (2013). Transcriptional profiling of *Zea mays* roots reveals roles for jasmonic acid and terpenoids in resistance against *Phytophthora cinnamomi*. Funct Integr Genom. **13,** 217-228.

Allen, T.W., Bradley, C.A., Sisson, A.J., Byamukama, E., Chilvers, M.I., Coker, C.M., Collins, A.A., Damicone, J.P., Dorrance, A.E., Dufault, N.S., Esker, P.D., Faske, T.R., Giesler, L.J., Grybauskas, A.P., Hershman, D.E., Hollier, C.A., Isakeit, T., Jardine, D.J., Kelly, H.M., Kemerait, R.C., Kleczewski, N.M., Koenning, S.R., Kurle, J.E., Malvick, D.K., Markell, S.G., Mehl, H.L., Mueller, D.S., Mueller, J.D., Mulrooney, R.P., Nelson, B.D., Newman, M.A., Osborne, L., Overstreet, C., Padgett, G.B., Phipps, P.M., Price, P.P., Sikora, E.J., Smith, D.L., Spurlock, T.N., Tande, C.A., Tenuta, A.U., Wise, K.A., and Wrather, J.A. (2017). Soybean yield loss estimates due to diseases in the united states and Ontario, Canada, from 2010 to 2014. Plant Health Prog. **18,** 19-27.

Anders, S., Pyl, P.T., and Huber, W. (2014). Htseq—a python framework to work with high-throughput sequencing data. Bioinform. **31,** 166-169.

Bagnaresi, P., Biselli, C., Orrù, L., Urso, S., Crispino, L., Abbruscato, P., Piffanelli, P., Lupotto, E., Cattivelli, L., and Valè, G. (2012). Comparative transcriptome profiling of the early response to *Magnaporthe oryzae* in durable resistant vs susceptible rice (*Oryza sativa* l.) genotypes. PLoS ONE **7,** e51609.

Balmer, D., Planchamp, C., and Mauch-Mani, B. (2012). On the move: Induced resistance in monocots. J. Exp. Bot. **64,** 1249-1261.

Balmer, D., de Papajewski, D.V., Planchamp, C., Glauser, G., and Mauch-Mani, B. (2013). Induced resistance in maize is based on organ-specific defence responses. Plant J **74,** 213-225.

Banerjee, S., Walder, F., Büchi, L., Meyer, M., Held, A.Y., Gattinger, A., Keller, T., Charles, R., and van der Heijden, M.G.A. (2019). Agricultural intensification reduces microbial network complexity and the abundance of keystone taxa in roots. ISME J**,** 1751-7370.

Bates, D., Machler, M., Bolker, B., Walker, S. (2015). Fitting linear mixed-effects models using {lme4}. J. Stat. Soft. **67,** 1-48.

Bolger, A.M., Lohse, M., and Usadel, B. (2014). Trimmomatic: A flexible trimmer for illumina sequence data. Bioinform. (Oxford, England) **30,** 2114-2120.

Bolt, S., Zuther, E., Zintl, S., Hincha, D.K., and Schmülling, T. (2017). Erf105 is a transcription factor gene of *Arabidopsis thaliana* required for freezing tolerance and cold acclimation. Plant, Cell Environ. **40,** 108-120.

Bu, Q., Jiang, H., Li, C.-B., Zhai, Q., Zhang, J., Wu, X., Sun, J., Xie, Q., and Li, C. (2008). Role of the *Arabidopsis thaliana* NAC transcription factors ANAC019 and ANAC055 in regulating jasmonic acid-signaled defense responses. Cell Res. **18,** 756-767.

Burkhardt, A., and Day, B. (2016). Transcriptome and small RNAome dynamics during a resistant and susceptible interaction between cucumber and downy mildew. Plant Gen. **9,** 10.3835/plantgenome2015.3808.0069.

Chang, H.X., Domier, L.L., Radwan, O., Yendrek, C.R., Hudson, M.E., and Hartman, G.L. (2016). Identification of multiple phytotoxins produced by *Fusarium virguliforme* including a phytotoxic effector (FVNIS1) associated with sudden death syndrome foliar symptoms. Mol Plant-Microbe Interact. **29,** 96-108.

Chen, C.-Y.A., Ezzeddine, N., and Shyu, A.-B. (2008). Messenger RNA half-life measurements in mammalian cells. Meth. Enzymol **448,** 335-357.

Chen, Y., Yin, H., Gao, M., Zhu, H., Zhang, Q., and Wang, Y. (2016). Comparative transcriptomics atlases reveals different gene expression pattern related to *Fusarium* wilt disease resistance and susceptibility in two *Vernicia* species. Front. Plant Sci. **7,** 1974-1974.

Chowdhury, S., Basu, A., and Kundu, S. (2017). Biotrophy-necrotrophy switch in pathogen evoke differential response in resistant and susceptible sesame involving multiple signaling pathways at different phases. Sci. Rep. **7,** 17251.

Chuberre, C., Plancot, B., Driouich, A., Moore, J.P., Bardor, M., Gügi, B., and Vicré, M. (2018). Plant immunity is compartmentalized and specialized in roots. Front. Plant Sci. **9,** 10.3389/fpls.2018.01692.

De Coninck, B., Timmermans, P., Vos, C., Cammue, B.P., and Kazan, K. (2015). What lies beneath: Belowground defense strategies in plants. Trends Plant Sci. **20,** 91-101.

Dupont, P.-Y., Eaton, C.J., Wargent, J.J., Fechtner, S., Solomon, P., Schmid, J., Day, R.C., Scott, B., and Cox, M.P. (2015). Fungal endophyte infection of ryegrass reprograms host metabolism and alters development. New Phytol. **208,** 1227-1240.

Etalo, D.W., Stulemeijer, I.J.E., Peter van Esse, H., de Vos, R.C.H., Bouwmeester, H.J., and Joosten, M.H.A.J. (2013). System-wide hypersensitive response-associated transcriptome and metabolome reprogramming in tomato. Plant Physiol. **162,** 1599-1617.

Fox, J., Weisberg, S. (2011). An {r} companion to applied regression. (Thousand Oaks {CA}: Sage).

Gdanetz, K., and Trail, F. (2017). The wheat microbiome under four management strategies, and potential for endophytes in disease protection. Phytobiomes J **1,** 158-168.

Haffner, E., Konietzki, S., and Diederichsen, E. (2015). Keeping control: The role of senescence and development in plant pathogenesis and defense. Plants (Basel) **4,** 449-488.

Häffner, E., Karlovsky, P., and Diederichsen, E. (2010). Genetic and environmental control of the verticillium syndrome in *Arabidopsis thaliana*. BMC Plant Biol. **10,** 235-235.

Hartman, G.L., Chang, H.X., and Leandro, L.F. (2015). Research advances and management of soybean sudden death syndrome. Crop Prot. **73,** 60-66.

Hothorn, T., Bretz, F., Westfall P. (2008). Simultaneous inference in general parametric models. Biom J. **50,** 346-363.

Huysmans, M., Buono, R.A., Skorzinski, N., Radio, M.C., De Winter, F., Parizot, B., Mertens, J., Karimi, M., Fendrych, M., and Nowack, M.K. (2018). NAC transcription factors ANAC087 and ANAC046 control distinct aspects of programmed cell death in the Arabidopsis columella and lateral root cap. Plant Cell **30,** 2197-2213.

Katan, J. (2017). Diseases caused by soilborne pathogens: Biology, management and challenges. J. Plant Path. **99,** 305-315.

Kim, D., Langmead, B., and Salzberg, S.L. (2015). Hisat: A fast spliced aligner with low memory requirements. Nature Meth **12,** 357-360.

Koenning, S.R., and Wrather, J.A. (2010). Suppression of soybean yield potential in the continental united states by plant diseases from 2006 to 2009. Plant Health Prog. **11,** 10.1094/php-2010-1122-1001-rs.

Kolander, T.M., Bienapfl, J.E., Kurle, J.E., and Malvick, D.K. (2012). Symptomatic and asymptomatic host range of *Fusarium virguliforme*, the causal agent of soybean sudden death syndrome. Plant Dis. **96,** 1148-1153.

Kong, W., Chen, N., Liu, T., Zhu, J., Wang, J., He, X., and Jin, Y. (2015). Large-scale transcriptome analysis of cucumber and *Botrytis cinerea* during infection. PLoS ONE **10,** e0142221.

Kuhar, K., Kansal, R., Subrahmanyam, B., Koundal, K.R., Miglani, K., and Gupta, V.K. (2013). A bowman–birk protease inhibitor with antifeedant and antifungal activity from dolichos biflorus. Acta Physiologiae Plantarum **35,** 1887-1903.

Laluk, K., and Mengiste, T. (2010). Necrotroph attacks on plants: Wanton destruction or covert extortion? (BIOONE).

Lanubile, A., Muppirala, U.K., Severin, A.J., Marocco, A., and Munkvold, G.P. (2015). Transcriptome profiling of soybean (*Glycine max*) roots challenged with pathogenic and non-pathogenic isolates of *Fusarium oxysporum*. BMC Genom. **16,** 1089.

Leandro, L.F.S., Eggenberger, S., Chen, C., Williams, J., Beattie, G.A., and Liebman, M. (2018). Cropping system diversification reduces severity and incidence of soybean sudden death syndrome caused by *Fusarium virguliforme*. Plant Dis. **102,** 1748-1758.

Liu, M.-J., Sugimoto, K., Uygun, S., Panchy, N., Campbell, M.S., Yandell, M., Howe, G.A., and Shiu, S.-H. (2018). Regulatory divergence in wound-responsive gene expression between domesticated and wild tomato. Plant Cell **30,** 1445-1460.

Lofgren, L.A., LeBlanc, N.R., Certano, A.K., Nachtigall, J., LaBine, K.M., Riddle, J., Broz, K., Dong, Y., Bethan, B., Kafer, C.W., and Kistler, H.C. (2018). *Fusarium graminearum*: Pathogen or endophyte of North American grasses? New Phytol. **217,** 1203-1212.

Lorrain, C., Marchal, C., Hacquard, S., Delaruelle, C., Pétrowski, J., Petre, B., Hecker, A., Frey, P., and Duplessis, S. (2018). The rust fungus *Melampsora larici-populina* expresses a conserved genetic program and distinct sets of secreted protein genes during infection of its two host plants, larch and poplar. Mol. Plant-Microbe Interact. **31,** 695-706.

Love, M.I., Huber, W., and Anders, S. (2014). Moderated estimation of fold change and dispersion for RNA-seq data with DE-seq. Genom Biol. **15,** 550-550.

Lu, S., Friesen, T.L., and Faris, J.D. (2011). Molecular characterization and genomic mapping of the pathogenesis-related protein 1 (PR-1) gene family in hexaploid wheat (*Triticum aestivum* l.*)*. Mol. Genet. Genom. **285,** 485-503.

Majid, I., and Abbas, N. (2019). Signal transduction in leaf senescence: An overview. In Senescence Signalling and Control in Plants, pp. 41-59.

Majumdar, R., Rajasekaran, K., Sickler, C., Lebar, M., Musungu, B.M., Fakhoury, A.M., Payne, G.A., Geisler, M., Carter-Wientjes, C., Wei, Q., Bhatnagar, D., and Cary, J.W. (2017). The pathogenesis-related maize seed (prms) gene plays a role in resistance

to *Aspergillus flavus* infection and aflatoxin contamination. Front. Plant Sci. **8,** 10.3389/fpls.2017.01758.

Malcolm, G.M., Kuldau, G.A., Gugino , B.K., and del Mar Jimenez-Gasco, M. (2013). Hidden host plant associations of soilborne fungal pathogens: An ecological perspective. Phytopathol. **103,** 538-544.

McKenzie, A.T., Katsyv, I., Song, W.M., Wang, M., and Zhang, B. (2016). Dgca: A comprehensive r package for differential gene correlation analysis. BMC Sys. Biol. **10,** 106.

Michielse, C.B., and Rep, M. (2009). Pathogen profile update: *Fusarium oxysporum*. Mol. Plant Pathol. **10,** 311-324.

Mittler, R., Kim, Y., Song, L., Coutu, J., Coutu, A., Ciftci-Yilmaz, S., Lee, H., Stevenson, B., and Zhu, J.-K. (2006). Gain- and loss-of-function mutations in zat10 enhance the tolerance of plants to abiotic stress. FEBS Lett. **580,** 6537-6542.

Ngaki, M.N., Wang, B., Sahu, B.B., Srivastava, S.K., Farooqi, M.S., Kambakam, S., Swaminathan, S., and Bhattacharyya, M.K. (2016). Tanscriptomic study of the soybean-*Fusarium virguliforme* interaction revealed a novel ankyrin-repeat containing defense gene, expression of whose during infection led to enhanced resistance to the fungal pathogen in transgenic soybean plants. PLoS ONE **11,** e0163106.

Njiti, V.N., Shenaut, M.A., Suttner, R.J., Schmidt, M.E., and Gibson, P.T. (1996). Soybean response to sudden death syndrome: Inheritance influenced by cyst nematode resistance in pyramid × douglas progenies. Crop Sci. **36,** 1165-1170.

O'Connell, R.J., Thon, M.R., Hacquard, S., Amyotte, S.G., Kleemann, J., Torres, M.F., Damm, U., Buiate, E.A., Epstein, L., Alkan, N., Altmüller, J., Alvarado-Balderrama, L., Bauser, C.A., Becker, C., Birren, B.W., Chen, Z., Choi, J., Crouch, J.A., Duvick, J.P., Farman, M.A., Gan, P., Heiman, D., Henrissat, B., Howard, R.J., Kabbage, M., Koch, C., Kracher, B., Kubo, Y., Law, A.D., Lebrun, M.-H., Lee, Y.-H., Miyara, I., Moore, N., Neumann, U., Nordström, K., Panaccione, D.G., Panstruga, R., Place, M., Proctor, R.H., Prusky, D., Rech, G., Reinhardt, R., Rollins, J.A., Rounsley, S., Schardl, C.L., Schwartz, D.C., Shenoy, N., Shirasu, K., Sikhakolli, U.R., Stüber, K., Sukno, S.A., Sweigard, J.A., Takano, Y., Takahara, H., Trail, F., van der Does, H.C., Voll, L.M., Will, I., Young, S., Zeng, Q., Zhang, J., Zhou, S., Dickman, M.B., Schulze-Lefert, P., Ver Loren van Themaat, E., Ma, L.-J., and Vaillancourt, L.J. (2012). Lifestyle transitions in plant pathogenic *Colletotrichum* fungi deciphered by genome and transcriptome analyses. Nat. Genet. **44,** 1060.

Pell, E.J., Miller, J.D., and Bielenberg, D.G. (2004). 20 - effects of airborne pollutants. In Plant cell death processes, L.D. Noodén, ed (San Diego: Academic Press), pp. 295-306.

Podzimska-Sroka, D., O'Shea, C., Gregersen, P.L., and Skriver, K. (2015). NAC transcription factors in senescence: From molecular structure to function in crops. Plants (Basel) **4,** 412-448.

Pusztahelyi, T., Holb, I.J., and Pócsi, I. (2016). Plant-fungal interactions: Special secondary metabolites of the biotrophic, necrotrophic, and other specific interactions. In Fung. Metabol. pp. 1-58.

R Development Core Team. (2010). R: A language and environment for statistical computing. In Vienna, Austria: R Foundation for Statistical Computing.

Saga, H., Ogawa, T., Kai, K., Suzuki, H., Ogata, Y., Sakurai, N., Shibata, D., and Ohta, D. (2012). Identification and characterization of ANAC042, a transcription factor family gene involved in the regulation of camalexin biosynthesis in Arabidopsis. Mol. Plant-Microbe Interact. **25,** 684-696.

Salleh, F.M., Evans, K., Goodall, B., Machin, H., Mowla, S.B., Mur, L.A.J., Runions, J., Theodoulou, F.L., Foyer, C.H., and Rogers, H.J. (2012). A novel function for a redox-related lea protein (SAG21/AtLEA5) in root development and biotic stress responses. Plant, Cell Environ. **35,** 418-429.

Savory, E.A., Adhikari, B.N., Hamilton, J.P., Vaillancourt, B., Buell, C.R., and Day, B. (2012). Mrna-seq analysis of the *Pseudoperonospora cubensis* transcriptome during cucumber (*Cucumis sativus* l.) infection. PLoS ONE **7,** e35796.

Šišić, A., Baćanović-Šišić, J., Al-Hatmi, A.M.S., Karlovsky, P., Ahmed, S.A., Maier, W., de Hoog, G.S., and Finckh, M.R. (2018). The 'forma specialis' issue in *Fusarium*: A case study in *Fusarium solani* f. Sp. *Pisi*. Sci Rep. **8,** 1252-1252.

Song, W.M., and Zhang, B. (2015). Multiscale embedded gene co-expression network analysis. PLoS Comput. Biol. **11,** e1004574.

Tang, N., Shahzad, Z., Lonjon, F., Loudet, O., Vailleau, F., and Maurel, C. (2018). Natural variation at xnd1 impacts root hydraulics and trade-off for stress responses in arabidopsis. Nat Commun. **9,** 3884.

Thatcher, L.F., Manners, J.M., and Kazan, K. (2009). *Fusarium oxysporum* hijacks COI1-mediated jasmonate signaling to promote disease development in Arabidopsis. Plant J. **58,** 927-939.

Thirumalaikumar, V.P., Devkar, V., Mehterov, N., Ali, S., Ozgur, R., Turkan, I., Mueller-Roeber, B., and Balazadeh, S. (2018). NAC transcription factor jungbrunnen1 enhances drought tolerance in tomato. Plant Biotechnol. J. **16,** 354-366.

Tian, T., Liu, Y., Yan, H., You, Q., Yi, X., Du, Z., Xu, W., and Su, Z. (2017). Agrigo v2.0: A go analysis toolkit for the agricultural community, 2017 update. Nuc Acid Res. **45,** W122-W129.

Wang, J., Jacobs, J.L., Byrne, J.M., and Chilvers, M.I. (2015). Improved diagnoses and quantification of *Fusarium virguliforme*, causal agent of soybean sudden death syndrome. Phytopathol. **105,** 378-387.

Wickham, H. (2016). Ggplot2: Elegant graphics for data analysis. (Springer-Verlag New York).

Williams, B., Kabbage, M., Kim, H.-J., Britt, R., and Dickman, M.B. (2011). Tipping the balance: *Sclerotinia sclerotiorum* secreted oxalic acid suppresses host defenses by manipulating the host redox environment. PLoS Pathog. **7,** e1002107.

Wimalanathan, K., Friedberg, I., Andorf, C.M., and Lawrence-Dill, C.J. (2018). Maize go annotation—methods, evaluation, and review (maize-gamer). Plant Direct **2,** e00052.

Wong, K.H., Tan, W.L., Kini, S.G., Xiao, T., Serra, A., Sze, S.K., and Tam, J.P. (2017). Vaccatides: Antifungal glutamine-rich hevein-like peptides from *Vaccaria hispanica*. Front. Plant Sci. **8**, 10.3389/fpls.2017.01100.

Wu, A., Allu, A.D., Garapati, P., Siddiqui, H., Dortay, H., Zanor, M.I., Asensi-Fabado, M.A., Munne-Bosch, S., Antonio, C., Tohge, T., Fernie, A.R., Kaufmann, K., Xue, G.P., Mueller-Roeber, B., and Balazadeh, S. (2012). Jungbrunnen1, a reactive oxygen species-responsive NAC transcription factor, regulates longevity in arabidopsis. Plant Cell **24,** 482-506.

Xia, J., Zhao, Y., Burks, P., Pauly, M., and Brown, P.J. (2018). A sorghum nac gene is associated with variation in biomass properties and yield potential. Plant Direct **2,** 10.1002/pld3.70.

Xie, Q., Frugis, G., Colgan, D., and Chua, N.-H. (2000). Arabidopsis NAC1 transduces auxin signal downstream of TIR1 to promote lateral root development. Genes Develop. **14,** 3024-3036.

Xiong, L., and Zhu, J.-K. (2003). Regulation of abscisic acid biosynthesis. Plant Physiol. **133,** 29-36.

Yamaguchi, M., Ohtani, M., Mitsuda, N., Kubo, M., Ohme-Takagi, M., Fukuda, H., and Demura, T. (2010). Vnd-interacting2, a NAC domain transcription factor, negatively regulates xylem vessel formation in Arabidopsis. Plant Cell **22,** 1249-1263.

Yuan, X., Wang, H., Cai, J., Li, D., and Song, F. (2019). Nac transcription factors in plant immunity. Phytopathology Research **1,** 2524-4167.

Zhang, J., Singh, A., Mueller, D.S., and Singh, A.K. (2015). Genome-wide association and epistasis studies unravel the genetic architecture of sudden death syndrome resistance in soybean. Plant J. **84,** 1124-1136.

Zhang, X., Valdes-Lopez, O., Arellano, C., Stacey, G., and Balint-Kurti, P. (2017). Genetic dissection of the maize (*Zea mays* l.) MAMP response. Theor. Appl. Genet. **130,** 1155-1168.

Zhang, Y., Tian, L., Yan, D.-H., and He, W. (2018). Genome-wide transcriptome analysis reveals the comprehensive response of two susceptible poplar sections to *Marssonina brunnea* infection. Genes **9,** 154.

Zhao, C., Avci, U., Grant, E.H., Haigler, C.H., and Beers, E.P. (2008). XND1, a member of the NAC domain family in *Arabidopsis thaliana*, negatively regulates lignocellulose synthesis and programmed cell death in xylem. Plant J. **53,** 425-436.

CHAPTER 5

Fusarium virguliforme Transcriptional Plasticity Revealed by Diverged Host Colonization

This chapter is unpublished, with intention to submit to Plant Cell

Baetsen-Young, A.M., Wai, C.M., VanBuren, R., Day, B. 20XX. *Fusarium virguliforme* transcriptional plasticity revealed by diverged host colonization. Plant Cell. XX: XX-XX

Abstract

Comparative transcriptomics of fungal colonization of hosts have indicated infection programs vary by fungal lifestyle. However, individual fungi can colonize a broad range of hosts, and must contain and manipulate its genetic repertoire to enable colonization of hosts with distinct phenotypic outcomes. In the current study, we exploited the broad host range of *Fusarium virguliforme* as a comparative model to identify differentially fungal responses leading to an endophytic or pathogenic lifestyle when colonizing two different hosts, highlighting gene expression critical to pathogenicity upon soybean. A comparison of *F. virguliforme* transcriptomes colonizing soybean and corn *in planta* over a 14-day time course, uncovered a nearly complete network rewiring, with less than 8% average gene co-expression module overlap upon colonizing the different hosts. Divergence of transcriptomes originated from host specific temporal induction genes central to infection and colonization, including CAZymes and necrosis inducing effectors. Upregulation of Zn(2)-Cys6 transcription factors were uniquely induced in soybean, potentially aiding in virulence to soybean. Fungal regulation of host immune processes was unveiled by *in planta* induction of milRNAs targeting stress, defense and senescence process. Overall, this suggests that *F. virguliforme* modulates the infection program in at least two hosts through transcriptional plasticity.

Introduction

Plant pathogens produce distinct phenotypes on susceptible hosts through molecular cross-talk enabling a compatible interaction. Fungal plant pathogens produce an array of symptoms during host colonization revealing diversity of infection programs through comparative exploration (Oliver and Ipcho, 2004; Horbach et al., 2011; Cordovez et al., 2017). While several studies have highlighted key processes and pathways critical to pathogenesis of fungi upon plants through single trait interactions (Derntl et al., 2017; Fang et al., 2017), genomic and transcriptomic exploration have revealed the elaborate infection program many fungi contain (Brown et al., 2017; Chowdhury et al., 2017). Comparative transcriptomics of fungal colonization have indicated infection programs vary by fungal lifestyle, suggesting induced pathways diverge within biotrophic, hemibiotrophic or necrotrophic interactions. The application of similar fungi yielding phenotypically diverse symptoms have also uncovered distinct processes employed to subvert host defenses (O'Connell et al., 2012; Haueisen et al., 2018). Transcriptomic approaches have highlighted that fungi regulate developmental programs to penetrate plants (Soanes et al., 2012; Vollmeister et al., 2012), secreted effectors (Yang et al., 2013; Haueisen et al., 2018), and express small RNAs (sRNAs) to modulate host defense response (Jiang et al., 2017; Lee Marzano et al., 2018). Yet these studies have often focused upon pinpointing candidates for virulence or aggressiveness upon single hosts by employing differences of the isolates genetic background. This approach has left gaps within our understanding of how individual pathogens regulate infection programs for successful colonization of different hosts.

Fungal plant pathogens can entail broad host ranges, causing substantial economic damage to agricultural crops. While most plant plants pathogens only colonize specific hosts, several fungi have broad pathogenic and non-pathogenic host ranges (Derbyshire et al., 2017). *Verticillium dahliae* causes diseases on more than 400 hosts, and while this fungus is considered adapted to specific hosts to cause disease, the broader question of the ecology of *V. dahlia* in agroecosystems has highlighted that this fungus has a much larger endophytic host range (Malcolm et al., 2013). This asymptomatic endophytic host range was more recently discovered for the causal agent of soybean sudden death syndrome, *Fusarium virguliforme* (Kolander et al., 2012). Therefore, individual fungi must contain and manipulate its genetic repertoire to enable colonization of hosts with distinct phenotypic outcomes. The application of single fungal species colonizing hosts with symptomatic and asymptomatic phenotypes provides an opportunity to understand transcriptional reprogramming to promote fungal colonization of hosts and disease development.

Comparative systems have provided resolution distinguishing plant pathogen interactions in specific classifications of pathogenetic and endophytic (Laluk and Mengiste, 2010; Lofgren et al., 2018). Yet, fungal ecology often suggests that the host fungal interactions exhibit a continuum of molecular cross talk, presenting a gradation of pathogenic to mutualistic outcomes when interacting with diverse hosts, such as *Botrytis* spp., *Verticillium* spp., and *Fusarium* spp. (Malcolm et al., 2013; Demers et al., 2015; Shaw et al., 2016). Furthermore, this indicates these fungi are able to fulfill two unique ecological niches, potentially within the same community (Selosse et al., 2018). Exploring the genomes of fungi with broad host ranges has uncovered the genetic potential substantiating diverse ecological and pathogenic

niches (Ma et al., 2010; Seidl et al., 2014; Derbyshire et al., 2017). Comparing the underlying transcriptional processes regulating a pathogenic organism to exhibit an endophytic lifestyle, could yield novel genetic signatures promoting virulence within a susceptible host.

To explore the fungal plant interaction continuum, *Fusarium virguliforme,* the causal agent for soybean sudden death syndrome, provides an exceptional model. This disease is a key limitation in reaching soybean yield potential, with an estimated annual economic impact of $330 million dollars in the United States, stemming from limited effective disease management practices (Koenning and Wrather, 2010; Hartman et al., 2015). This ascomycete fungus can colonize the roots of an array of leguminous dicots, stimulating the chlorosis, necrosis and eventual loss of above ground biomass (Kolander et al., 2012). However, on many monocots and weed species, this fungus colonizes roots without any observable negative implications to the host (Kolander et al., 2012; Kobayashi-Leonel et al., 2017). Within this array of *F. virguliforme* asymptomatic hosts is corn, a common rotational crop with soybean, indicating that this soybean pathogen is enacting as a potential endophyte in association with corn in the same agroecosystem. With the incomplete understanding of how *F. virguliforme* initializes molecular crosstalk with soybean and corn to enable distinct ecological niches, and with the limited exploration of genetic regulation of individual fungal colonization programs upon diverse hosts, we applied a systems comparison to resolve transcriptomic reprogramming aiding in pathogenic colonization of soybean, and asymptomatic interactions with corn roots. To highlight divergence in genetic pathways underlying fungal lifestyle, we investigated (1) early colonization strategies between *F. virguliforme* and soybean or corn through *in planta* assays, (2) what early

transcriptional responses of *F. virguliforme* colonizing corn or soybean are induced, (3) how distinct are fungal asymptomatic transcriptomes from symptomatic transcriptomes, and (4) does *F. virguliforme* modulate soybean defense responses through micro like RNA secretion.

Material and Methods

Genome Sequencing, Assembly, and Annotation of *Fusarium virguliforme*

PacBio and Illumina sequencing were performed on high molecular weight DNA extracted from lyophilized (FreeZone 2.5, Labconco) *F. virguliforme* Mont-1 mycelia grown for four weeks in potato dextrose broth using a modified Ctab procedure to include 1% polyvinylpyrrolidone (Lade et al., 2014). A PacBio library was constructed at the University of Georgia Genomics and Bioinformatics Core and size selected for 15-20 KB fragments by the BluePippen system (Sage Scientific). The library was sequenced on a Sequel Platform. The single smart cell yielded 6.5 GB. For error correction, Illumina TruSeq Nano DNA Libraries were prepared and sequenced on an Illumina MiSeq v3 in a 2x300bp paired end format and HiSeq 4000 in a 2x150 bp format at Michigan State University Research Technology Support Facility. PacBio reads were assembled and error corrected by Canu (v1.8) (Koren et al., 2017) in default parameters. Genome size for assembly was taken from the previous *F. virguliforme* assembly at 50.9 MB (Srivastava et al., 2014). Bacterial DNA was present in the assembly, thus daft contigs were compared to the previous genome assembly with LAST (v912) (Kiełbasa et al., 2011), and novel contigs were validated of fungal origin by BLAST+ (v2.2.30) (Camacho et al., 2009) against the non-redundant NCBI database. The

parsed genome assembly was graphed in Bandage (Holt et al., 2015). Assembled contigs were error corrected by Pilon (v1.22) (Walker et al., 2014) under default settings, using 50x coverage of Illumina paired end 300 bp and 150 bp data for *F. virguliforme*. Paired end reads were adaptor and quality trimmed using Trimmomatic (v0.33) (Bolger et al., 2014), and then were aligned to the draft contigs by Bowtie2 (v2.2.6) (Langmead and Salzberg, 2012) in default settings. Pilon was run five times sequentially, till limited corrections were found. The new genome assembly was compared to the previous genome assembly by QUAST (v3.0) (Gurevich et al., 2013).

Transcript evidence for gene predictions was acquired from the National Center for Biotechnology Information (NCBI) (SRA SRR1382101) and germinating macroconidia from the *F. virguliforme* RNA-Seq time course (see below). Single end reads were adaptor and quality trimmed using Trimmomatic (v0.33) (Bolger et al., 2014). These reads were then provided to FunGAP (v1.0) (Min et al., 2017) as transcript evidence. The parameters for running FunGAP were set as: --sister_proteome: Fusarium, --augustus_species fusarium_graminearum, with transcript reads provided as --trans_read_single. The final gene models from FunGAP contained 16,050. Single copy fungal orthologs from BUSCO (v3) (Kriventseva et al., 2015) assessed the completeness of the genome annotation.

Functional annotation was completed using Trinotate (v3.1.1) (Bryant et al., 2017). Trinotate annotated gene models with evidence from several databases (NCBI non-redundant protein database, Swissprot-Uniprot database, Gene Ontology (GO) and InterpoScan) with BlastX finding single hit at an E-value threshold of $1E^{-5}$ (Altschul et al.,

1990). This information was applied to predict protein domains with Hmmer (v3.1) (Clements et al., 2011), transmembrane proteins with TMHMM (v2.0) (Krogh et al., 2001), ribosomal RNA with RNAmmer (v1.2) (Lagesen et al., 2007), secreted proteins with SignalP (v4.1) (Petersen et al., 2011) and gene ontology with GOseq (Young et al., 2010). Additionally, EffectorP (v2.0) (Sperschneider et al., 2016) was used to predict fungal effectors within the secreted proteins, and dbCAN (Yin et al., 2012) found CAZymes and secondary metabolism genes.

Comparative Genomics with *Fusarium virguliforme*

MCSCAN toolkit (v1.1) (Wang et al., 2012) was used to find syntenic gene pairs between second version (v2) compared to the first version (v1) of the *F. virguliforme* genome. Conserved gene blocks were discovered through LAST alignment. Plots of macro and micro-synteny were created by the MCScan in python.

To discover novel and retained genes within the v2 genome was compared to the v1 genome of the *F. virguliforme* genome. Coding sequences for gene models were extracted from the v1 genome by gffread (Trapnell et al., 2010). Then genes were reciprocally compared by BLAST (v2.2.26) (Altschul et al., 1990). Genes with an e-value below $1E^{-5}$, greater than 70% gene alignment, and 95% gene identity were classified as retained. If a gene was matched with 95% identity and an e-value below $1E^{-5}$, but less than 70% gene alignment, it was denoted as mis-assembled.

Plant and *Fusarium virguliforme* Assay

Soybean c.v. Sloan (provided by Martin Chilvers, Michigan State University), and corn hybrid E13022S (Epley Brothers Hybrids Inc, Shell Rock, IA, provided by Martin Chilvers) were surface sterilized in 70% ethanol for 30 sec, 10% bleach solution for 20 min, and then triple rinsed in sterile water for 1 min. Soybeans seeds were placed between two sheets of sterile 100 mm Whatman filter paper with 5 mL of sterile water inside a petri dish. Seeds were incubated for five days in total darkness at 21°C. Corn seeds were incubated in sterile water for 24 hours in darkness and placed between two sheets of sterile 100 mm Whatman filter paper with 5 mL of sterile water inside a petri dish. Seeds were incubated for five days in total darkness at 21°C.

Fusarium virguliforme Mont-1 isolate was propagated on potato dextrose agar (Difco, Fisher Scientific) for seven weeks. Asexual macroconidia spores were collected, diluted to 1 x 10^5 macroconidia mL^{-1} and sprayed onto five-day old corn or soybean seedlings with a 3 oz travel spray bottle. Twenty-five sprays were applied to the seedlings at angles of 0°, 90°, 180°, and 270° to ensure seeds were properly covered. For mock inoculated samples, water was sprayed onto the seedlings. Seedlings were incubated for 30 min with the inoculum, then excess inoculum was removed, and seedlings were incubated for an additional hour. Following incubation, three corn or soybean seedlings were placed into seed germination pouches (Mega International), containing 25 mL of sterile distilled water. Pouches containing seedlings were placed in a BioChambers Bigfoot Series Model AC-60 growth chamber with 140 μE m^{-2} sec^{-1} and 14:10 h light/dark cycle at 12°C for seven days and then

25°C for seven days. Plants were watered as needed with sterile water. Tap root from soybean or radical from corn root samples were taken at the same time (16:00 h) of day from the original 4 cm inoculation site throughout the time course. The two-week time course was repeated three independent times in the same growth chamber, with sampling of six plants for RNA isolation and three plants for DNA isolation at 0, 2, 4, 7, 10, and 14 days post inoculation (DPI) in each biological repeat. Time point 0 was sampled after completion of fungal or mock inoculation. Plant growth and disease symptomology was recorded at each timepoint by photography with a Nikon D50 camera. canon camera.

Fungal Colonization Analysis

To visualize fungal growth on samples, microscopic analyses of corn and soybean roots were conducted at each time point for all treatments. Roots were cleared in 100% ethanol, followed by staining in a 0.05% trypan blue solution containing equal parts of water, glycerol and lactic acid (Savory et al., 2012). Fungal structures were observed using MZ16 dissecting scope (Leica).

DNA Extraction and Real Time PCR for *Fusarium virguliforme*

DNA for real-time quantitative polymerase chain reaction (qPCR) was extracted from flash-frozen root tissue to determine the amount of fungal biomass present in samples throughout the time course. A total of 60 mg of ground root tissue from individual corn or soybean plants from each time point were extracted with a NucleoSpin Plant II Kit (Macherey-Nagel), with

an additional incubation on 1 hour at 65°C during lysis. Samples were prepared for *F. virguliforme* DNA detection by qPCR following (Wang et al., 2015). Analysis of variance (ANOVA) was calculated for DNA quantities using the "lme4" (Bates, 2015) and "Car" (Fox, 2011) package in R v3.4.1(R Development Core Team, 2010). Means were separated at $P \leq 0.05$ using Tukey's least significant different test using the "multicomp" package (Hothorn, 2008).

RNA Extraction

Total RNA was isolated from 200 mg of ground flash frozen germinating macroconidia and plant root samples for small RNA (sRNA) and messenger RNA (mRNA) sequencing with a miRNeasy Mini Kit (Qiagen). Contaminating DNA was removed with TURBO DNase Free (Invitrogen). RNA quality was determined by gel electrophoresis and the 2100 Bioanalyzer (Agilent) with the Agilent RNA 6000 Pico kit.

Library Preparation and Sequencing

The same extraction for each sample was used for mRNA and sRNA library preparation. Libraries were prepared using the Illumina TruSeq mRNA Library Preparation Kit from three biological repeats of each time point of *F. virguliforme* or mock inoculated corn or soybean or germinating macroconidia samples by the Michigan State Research Technology and Support Facility. Samples were pooled and sequenced on the Illumina HiSeq 4000 under single end 50 bp mode. Base calling was done by Illumina Real Time Analysis (RTA) v2.7.7

and output of RTA was demultiplexed and converted to FastQ format with Illumina Bcl2fastq v2.19.1 Samples for sRNA were prepared using the NEB Next Small RNA Sample Prep Kit at University of Illinois at Urbana-Champaign W.M Keck Center. Samples were pooled and sequenced on the Illumina HiSeq 4000 under single end 50 bp mode. Fastq files were generated and demultiplexed with the bcl2fastq v2.20 Conversion Software (Illumina).

mRNA-Sequencing Processing and Differential Analysis

Reads were trimmed for adapter presence and quality score by Trimmomatic (v0.33) (Bolger et al., 2014). The trimmed reads were uniquely mapped to the corresponding reference genome of *F. virguliforme* (Fv_v2) with HISAT2 (v 2.1.0) (Kim et al., 2015) with the following parameters --dta --rna-strandness F. Hits from HISAT2 were converted from SAM to BAM format by Picard (v 2.18.1) (http://broadinstitute.github.io/picard/). Alignments were then counted by HTSeq (v0.6.1) (Anders et al., 2014) with the following options: --minaqual 50 -m intersection-strict -s reverse --idattr=gene_id. Gene counts were imported into DESeq2 (v1.22.2) (Love et al., 2014) conducted in R, normalized for library size and log2 transformed to determine correlation of biological replicates at each time point.

To determine differential gene expression DESeq2 (v1.22.2) executed in R (R Development Core Team, 2010) with raw HTSeq counts. Counts were filtered for 90% of genes with less than 10 across all samples. DESeq2 was applied to determine significant genes with an adjusted p-valued ≤ 0.05. Pairwise comparison between each time point of corn or soybean *F. virguliforme in planta* samples and germinating *F. virguliforme* germinating macroconidia.

Within each host, pairwise comparisons were completed across the time course. Additionally, *F. virguliforme* was compared at each time point across hosts.

Gene Co-Expression Network Analysis

Genes were also filtered for weighted gene correlation network analysis (WGCNA) (Langfelder and Horvath, 2008) implemented in R (R Development Core Team, 2010) for 90% of genes with less than 10 across all samples. These 11,112 genes were variance stabilized transformed for importation and *F. virguliforme* expression on corn or soybean signed co-expression networks were constructed separately. A soft threshold power of 7 and tree cut height of 0.15 were applied to these analyses, with all other parameters unchanged. Overall gene expression was clustered into 22 modules for *F. virguliforme* colonization of corn and 20 modules when colonizing soybean. Modules were visualized in ggplot2 (v3.1.1) package (Wickham, 2016) in R.

Gene Ontology Enrichment Analysis

For each predicted protein from the *F. virguliforme* v2 genome, unique GO terms from InterPro Scan (Jones et al., 2014) were extracted with a custom script. Gene lists from either differential analysis or clusters from co-expression analysis were analyzed by TopGO (2.34.0) conducted (Alexa A and Rahnenfuhrer J, 2018) in R. Fishers Exact Test was conducted on each gene set with an adjusted *P-value* ≤ 0.05 to determine significance of enrichment.

Small RNA Read Processing and Identification

Single end reads from *F. virguliforme* colonized soybean roots and germinating macroconidia were adaptor and quality trimmed by cutadapt (Martin, 2011) for reads 15-35 bp. Trimmed reads were aligned to the *F. virguliforme* v2 genome with the following parameters -v 0 -S -a -m 50 --best –strata with Bowtie (v1.1.2). Reads aligned to the *F. virguliforme* v2 genome were realigned with Bowtie to the soybean genome with the same parameters, and these reads that did not align to the soybean (Wm82.a2.v1) genome were utilized for downstream analysis. Reads that perfectly matched the *F. virguliforme* and did not align to soybean were collapsed and mapped in mirDeep2 (Friedländer et al., 2012). Next, mirDeep2 was employed to discover novel micro-like RNAs (milRNAs) and to quantify their abundance within each sample throughout the time course. milRNAs were identified through a BLASTn (Altschul et al., 1990) search with an E-value less than 1.0 against the miRBase database. A milRNA was considered expressed if present in two of three biological replicates and had a prediction score greater than one.

Target Prediction and Differential Accumulation of milRNAs

Targets of milRNAs were revealed by applying psRNATarget (Dai et al., 2018) with a minimum and maximum expectation value of 3 and 5, respectively. To validate targets were expressed within the *in planta* dataset, TAPIR was conducted to discover targets within the soybean transcripts. A gene considered a target of predicted milRNAs, if present in both

target prediction programs. The predicted milRNA targets were filtered for disease associated traits. Data were visualized by ggplot2 (Wickham, 2016) implemented in R.

Results

Generation of a Long-read *Fusarium virguliforme* Reference Genome

To define and characterize the transcriptional landscape of the *F. virguliforme*-host interaction, we first sought to improve the pathogen reference genome using third generation sequencing technologies. To do this, we generated a high-quality PacBio single-molecule derived genome, based on 6.5 Gb of sequencing data, yield an approximate 17X coverage of the *F. virguliforme* genome. Filtered reads were assembled using the long-read optimized assembler Canu (Koren et al., 2017), and resultant contigs were error-corrected using 50x Illumina data by Pilon (Walker et al., 2014). In total the assembled *F. virguliforme* genome encompassed 52 mb with 96 contigs, with a N50 of 1.54 mb (Figure 21 and 22, Table 16). The resulting overall genome size was slightly larger than the first genome assembly version (Srivastava et al., 2014), which we posit stems from a more robust assembly of longer reads; indeed, the N50 was exponentially larger in this version of the genome from larger contigs (Table 16). Synteny of the two genome versions was highly fragmented (Figure 22A), an observation that stems from the over 3,000 contigs in the first version of the genome, which are further assembled together herein, version 2. Within these syntenic regions, micro-collinearity between the two genomes was observed to be very consistent (Figure 22B).

The *F. virguliforme* genome generated in this study was annotated using FunGAP (Min et al., 2017), incorporating Breaker, MAKER, and Augustus gene model prediction algorithms. A total of 16,050 genes were identified in this version, representing an increase in 1,205 genes. Comparisons of the coding sequences between genome versions revealed 12,306 genes were conserved with a minimum 70% gene alignment rate and a 95% identity. However, 1,421 genes, including 564 genes that contained coding sequences of conserved genes, did not meet the threshold of similarity and thus were considered misassembled in one of the genomes. We suggest that this result arises from mis-assemblies generated using short read sequencing and repeat collapsing (Ardui et al., 2018). Overall, 2,889 genes did not have an alignment to the previous genome (Supplemental Dataset 2-1), and this gene set contained enrichments in protein ubiquitination, organic compound breakdown, and porphyrin compound biosynthesis (Table 17). Genome completion was assessed using Benchmarking Universal Single-Copy Orthologs, and from this, we observed an approximate 98% completion of the 1,438 groups searched. Through functional annotation, 10,162 of the 16,050 genes were found to have protein evidence. Further exploration of the genome found 232 genes were candidate effectors (Supplemental Dataset 2-2). As a hemibiotrophic pathogen, we also search the *F. virguliforme* genome for carbohydrate active enzymes (CAZymes) and discovered 365 genes with potential functions in this process. In total, these datasets provided a resource to explore the transcriptomic landscape of *F. virguliforme* across hosts.

Fungal Growth and Development Produced Differing Plant Root Phenotypes

To understand *F. virguliforme* interactions with corn (asymptomatic) and soybean (symptomatic), we profiled *F. virguliforme* roots over a two-week time course and collected samples for RNA-seq analysis. In short, this time-frame (i.e., 2-to 14-days-post-inoculation) was selected as it enabled the discovery of time frames critical to fungal attachment, growth, penetration, differentiation, and symptom development. As illustrated in Figure 23A, by the end of the two-week time course, soybean roots showed signs of necrotrophy in both the tap and hypocotyl regions. Additionally, fungal-induced necrosis had also spread to developing lateral roots adjoining the tap root. This symptom development is consent with root disease progression of SDS, initializing as an asymptomatic biotroph, with the fungus depending on living plant tissue, then turning necrotrophic and killing host tissue (Ma et al., 2013). In the asymptomatic host, corn, we did not observe any striking evidence of fungal infection over the time-course of the experiment.

To verify fungal growth, we used trypan blue staining to visualize fungal growth on both soybean and corn roots throughout the time-course. Fungal growth and colonization were apparent on both hosts, but developmental stage varied according to the host (Figure 23B). For example, following inoculation, fungal spore germination was apparent on roots of both hosts, and by 2 days post inoculation (DPI), fungal mycelia had expanded across the root surface. Interestingly, mycelia on corn roots parallel root epidermis cells, while mycelia growth on soybean roots did not have any apparent pattern of colonization. Also by 2 DPI, round and swollen mycelia structures were observed; these appear to be similar to

penetration structures (e.g., appressoria). Support for this classification comes from documented observations in *Fusarium graminearum* and *F. virguliforme* infection assays (Navi and Yang, 2008). Interestingly, these infection-like structures were observed, but not until ca. 7 DPI, indicating a slower infection process in corn. From 7 to 14 DPI, we continued to record fungal growth and development at the site of inoculation and observed an increase in mycelia colonization on both hosts. By 14 DPI however, masses of developing macroconidia were apparent on soybean roots, indicating asexual reproduction had initialized in the time course. The transition to necrotrophy was indicated by chlorosis on soybean roots at 7 DPI, followed by necrosis at 10 DPI (Figure 23B). On corn, no visible symptoms were observed throughout the time-course of the experiment.

Once we confirmed the *in planta* growth of the pathogen on both hosts, we next conducted RNA-Seq at six-time points over the course of the inoculation experiment; we also included additional sampling of germinating (*in vitro*) *F. virguliforme* macroconidia spores. After trimming of lower quality reads and adaptors, resultant reads were mapped to the *F. virguliforme* genome. In our initial analysis, we identified low levels of fungal mRNA reads, representing 0.04-0.13% of total reads across 0-2 DPI (Figure 23C). While this was not unexpected, we generated a minimum of 200 million reads per sample (at 0-4 DPI) to generate read numbers greater than 80,000 reads per biological repeat (Table 18). As expected, the percent of mRNA reads aligning varied by host over the time course. For example, fungal reads from corn (non-host) increased in a linear fashion over the time course; ranging from 1.11-2.53% of the sample at 7-14 DPI. However, fungal reads from soybean (symptomatic host) did not increase substantially until 7 DPI (Figure 23C),

following which time the percent of fungal reads approached those observed from corn-inoculated samples. In soybean, this increase coincided with symptom development and potential shift from biotrophy to necrotrophy.

Host-induced Gene Expression Profiles in *Fusarium virguliforme*

To assess if the colonization program of *F. virguliforme* diverged in a manner consistent with the differing hosts, we next employed a comparative transcriptomic-based approach. We hypothesized this design would highlight transcriptional reprogramming specific to each host, and as a function of a single, common pathogen interaction, would yield insight into the influence of host of fungal gene expression. To ensure biological reproducibility, we compared gene expression across biological replicates. From this, we found a greater than 90% reproducibility of the fungal gene expression profiles for the last timepoint of the infection time course, indicating the biological response of the fungus within another organism was highly consistent (Figure 24). To understand if our treatments were globally distinct from one another, we next preformed principle coordinate analysis of all 39 samples across corn and soybean colonization, as well as from germinating macroconidia. Using this approach, we discovered that fungal response was primarily correlated with treatment (Figure 25), and that the germinating macroconidia formed a distinct cluster from samples colonizing hosts. While *F. virguliforme* response on hosts did form a single, large, cluster, all samples were distinctly separate within this cluster as a function of host. Intriguingly, gene expression from both hosts were separated by time as well, with the greatest separation identified at timepoints between 4 and 14 DPI. Additionally, a separation from the plant

samples was apparent in reads derived from 7-14 DPI samples from *F. virguliforme* colonizing soybean. This grouping of samples suggests hosts interactions greatly shape gene expression, and moreover, the temporal expression of those gene expression interactions.

From the analysis above, we identified 11,112 *F. virguliforme* genes were expressed on corn, soybean, and germinating macroconidia that were expressed in at least one timepoint across the time course. To discover genes that were induced by host interaction, we next compared gene expression of *F. virguliforme* from soybean or corn with germinating (e.g., *in vitro*) macroconidia. Using this approach, we identified 4,192 and 4,072 unique genes that were upregulated ($\log_2$ fold change > 1) in fungal samples from soybean or corn, respectively, throughout the time course. As many genes were induced, we filtered the differentially expressed genes by $|\log_2$ fold change > 2| to discover processes relevant to host colonization. Of the significantly up-regulated genes from *F. virguliforme* on soybean, the vast majority of genes were induced at 0 and 7-14 DPI (Figure 26A). Similarly, the majority of induced *F. virguliforme* genes within corn roots were observed from samples derived at 7-14 DPI (Figure 26B). Surprisingly, while the read depth was less in corn samples at 0 DPI than soybean samples, an additional 127 gene were detected as significantly upregulated at $\log_2$ fold change > 2, highlighting an elevated response in *F. virguliforme* to corn than to soybean. The greatest changes of unique gene upregulation occurred between 4-7 DPI on corn, and at 10-14 DPI on soybean (Table 19). Only three genes were conserved as a function of expression between both hosts and timepoint.

To explore the function of the induced genes in *F. virguliforme* as they relate to host interactions, we undertook a functional gene ontology (GO) enrichment analysis of genes; the threshold for analysis was those genes that were upregulated greater than log_2-fold > 2. Of the more than 50 biological process categories that were found to be enriched, several processes were consistent between both soybean and corn, among which included carboxylic acid, lipid or co-factor biosynthesis, as well as polysaccharide metabolism, protein dephosphorylation, and small molecule biosynthesis (Figure 26C and D, Supplemental Dataset 2-4 and 5). Overall expression patterns on both hosts were similar for lipid and co-factor biosynthesis, which is not surprising, as these processes are critical for fungal growth and signaling pathways (Schrettl et al., 2007; Lysøe et al., 2008). Carboxylic acid biosynthesis was induced across the colonization time course, which we hypothesize would a critical process for secondary metabolite production in support of fungal colonization, regardless of the host (Brown and Proctor, 2016). Interestingly, protein dephosphorylation and small molecule biosynthesis were enriched in fungal transcriptomic programs and elevated in expression when colonizing soybean roots at 7-10 DPI. The protein dephosphorylation of plant plasma membranes by fungi have been documented to prevent signaling cascades that normally simulate host defense responses (Yang et al., 2015). Also, small molecules secreted by plant pathogens may target host defense machinery and/or processes to module immune responses to the fungus (Jennings et al., 2000; Chang et al., 2016b). The upregulation of these processes in *F. virguliforme* during soybean colonization suggests an infection strategy to reduce host immune responses, more so, than when *F. virguliforme* colonizes corn roots.

Temporal Divergence of *F. virguliforme in planta* Gene Co-expression upon Host Colonization

As specific genes related to broad processes of *F. virguliforme* colonization and development were differentially induced at distinct temporal stages during the time course, we were curious if global genes co-expression patterns had diverged during colonization of corn and soybean. To address this, we applied a weighted gene correlation network analysis (WGCNA) across the time course. As the results above suggest that *F. virguliforme* induces the expression of a large number of genetic processes during the shift from biotrophy to necrotrophy over the time course, we hypothesized this approach would allow us to separate the biotrophic from necrotrophic patterns. Gene co-expression networks have previously revealed induced developmental changes in *Ustilago maydis* (Lanver et al., 2018). Genes were filtered to remove low expression before co-expression network construction, leaving 11,112 genes remaining. Next, these genes were clustered into 22 modules for *F. virguliforme* colonization of corn and 20 modules for *F. virguliforme* colonization of soybean (Figure 27 Supplemental Datasets 2-6 and 7). As apparent temporal patterns existed within each co-expression network, we separated the modules into four large groups: 1) early induced expression at 2 DPI, but down regulated at 4DPI, 2) elevated expression at 4-7 DPI, 3) induced expression at 7-10 DPI and 4) down regulation of expression from 2-4 DPI, but induced at 10 DPI (Figure 27). While these temporal patterns of co-expression modules across *F. virguliforme* colonization of both hosts appear similar when placed in these four large groups, the gene enrichment of modules contained within these groups varied by host colonization by *F. virguliforme*.

Gene co-expressing modules in group one while *F. virguliforme* was colonizing corn roots, were enriched for negative regulation of many functional processes, inducing cellular metabolism, macromolecule production, and expression of primary metabolism. Indicating *F. virguliforme* was repressing secondary metabolism and utilizing self-derived energy at early interactions with corn roots. However, processes upregulated in *F. virguliforme* colonizing soybean roots at 2 DPI, were enriched for reactive oxygen species (ROS) generation and oxalic acid production. Both of these processes are associated with early hemibiotrophic and necrotrophic plant fungal interactions at early time points in colonization. Reactive oxygen species in fungal hyphae supports the differentiation of cells for infection structures like appressoria (Heller and Tudzynski, 2011). We observed the develop of appressoria like structures at 2 DPI (Figure 23B), suggesting that this fungal as already penetrating host tissues within 48 hours of contact. Also, oxalic acid biosynthesis enrichment indicates a potential down regulation of host cell death through autophagy processes, prevent a massive necrotic response to kill the fungus by the host, as with *Sclerotinia sclerotium* (Veloso and van Kan, 2018). Together, the processes suggest that *F. virguliforme* is infecting and manipulation soybean host responses by 2 DPI.

It is not surprising that numerous co-expression modules were upregulated from 2-4 DPI in *F. virguliforme* within corn and 2-7 DPI within soybean. Most of these modules were highly expressed for the remainder of the colonization time course. Modules generated from *F. virguliforme* derived from corn (Figure 27A and 28) also contained processes enriched for primary metabolism, similar to group 1; however, processes associated with response to the defenses were also enriched. For example, at 4 DPI, carboxylic acid biosynthesis-associated

genes and related processes were upregulated, suggesting that toxin production was occurring (Supplemental Dataset 2-6). Conversely, the same processes from *F. virguliforme*-associated soybean highlighted a faster colonization program; indeed, processes were enriched for cellular catabolic processes of cellulose, pectin and polysaccharides in soybean. Of interest to the nature of the host-association and symptomatic nature of *F. virguliforme*-soybean, we also observe an enrichment in small molecule biosynthesis following soybean colonization at ca; 4 DPI (Supplemental Dataset 2-7). These processes highlight the initial transition from a biotrophic to necrotrophic lifestyle of modifying and breaking down host tissue for further proliferation (Laluk and Mengiste, 2010).

One striking observation of this analysis is that numerous diverse processes were enriched during module upregulation at 7-10 DPI in *F. virguliforme*-corn samples. Of these, the upregulation of NADP stood out, as this process has been previously associated with hyphal differentiation initiation for infection structures (Heller and Tudzynski, 2011); this is consistent with our phenotypic observations shown in Figure 23B, 7 DPI. The upregulation of gene process in *F. virguliforme* associated with amino acid sugar catabolism also suggests access to plant derived compounds, likely via direct penetration of the host tissue by the fungus. Concomitant with this, upregulation of processes associated with chemical and stimulus likely indicates *F. virguliforme* was sensing host defense response to the production and secretion of anti-microbial compounds. During this same timeframe, while *F. virguliforme* from corn was activating nutrient access-associated processes, *F. virguliforme* interaction with soybean revealed an upregulation of protection-associated mechanisms,

among which included antibiotic catabolism, response to ROS and chemical to host defense activation.

By 14 DPI, processes that are associated with group-4 (Figure 27) were found to be expressed as a function of host colonization. Also at 14 DPI, primarily amino sugar and nitrate acquisition were induced in samples derived from corn, while at the same timepoint in samples from soybean, necrotrophic processes had ensued, and we observed an enrichment in functions associated with cell killing, organic acid transport, and self-protection form host induced ROS by cell redox homeostasis. This process enrichment is supported by the necrotrophic envelopment of the soybean tap root at 14 DPI (Figure 23B).

In total, the enrichment of biological processes during the colonization of corn and soybean roots suggest two distinct infection programs are occurring within the same fungal organism. For example, the infection program during the colonization of corn appears to be delayed, with fungal penetration of host cells occurring at a time much later than observed in soybean. This slower rate of infection and pathogen progress may stem either from the activation of host defenses, an absence of the appropriate host signals which are required to simulate the initiation of rapid infection-associated processes, or both (Elliott, 2016). Additionally, toxin related processes were enriched throughout the sampled timepoints during soybean colonization, a process that we hypothesize may further assist colonization, nutrient acquisition, and eventual host cell death (Chang et al., 2016b; Chang et al., 2016a; Ngaki et al., 2016). The lack of temporal conservation of enriched processes between colonization of these two hosts highlights plasticity of the *F. virguliforme* transcriptome.

Overall only few genes were co-expressed in a similar manner upon these two hosts (Figure 29). On average, only 8% of genes were conserved within module gene co-expression between *F. virguliforme* expression on soybean and corn. Comparison of gene overlap highlights that processes enriched in group three of co-expression in corn contain more genes from the temporal of *F. virguliforme* across all soybean co-expression groups. This indicates that enrichment of processes related to nutrient access and host infection from 7-10 DPI in corn were expressed across a much longer timeframe in soybean. Interestingly, module 14 in group 2 *of F. virguliforme* within soybean contained the greatest overlap with several early (2-4 DPI) induced corn modules. Module 14 was the largest co-expression module, with 3,503 genes, which may contain many genes relevant to basic cellular functions needed for viability and growth (Figure 30 and Supplemental Dataset 2-7).

Host-specific Gene Expression Patterns during Root Colonization

As noted above, we observed a temporal divergence of biological processes enriched by respective host colonization. To further explore this, we next asked if these induction responses were host specific. Previous work comparing the infection programs of phytopathogenic *Zymoseptoria tritici* discovered temporal variation of isolate infection (Haueisen et al., 2018). To determine if this is also the case in *F. virguliforme*, we directly compared *F. virguliforme* gene expression from each host at each time point (Figure 31A). The majority of genes in the *F. virguliforme* transcriptome were not differentially regulated by cross species colonization; this analysis represented 81% of the genes expressed. Of the proportion of genes that were differentially induced, 43% were uniquely upregulated during

corn root colonization, 56% were upregulated upon colonization of soybean only and 0.1% were conserved in upregulation at different time points, during the infection time course. Of these differentially induced genes at $|\log_2$ fold change > 1|, the vast majority were induced at 10 and 14 DPI (Table 21, Supplemental Dataset 2-8). While fewer genes were differentially upregulated at early time points, these genes highlight specific processes underlying fungal temporal colonization. Interestingly, genes highly (>20 $\log_2$) upregulated at 0 DPI within *F. virguliforme* colonizing soybean roots, were related to DNA methylation, suggesting this process did not occur during early interactions on corn roots. No processes were uniquely induced to corn root colonization at 0 DPI. *Fusarium virguliforme* began to respond to host induced anti-microbial metabolites at 2 DPI by upregulating ABC transporters (Gupta and Chattoo, 2008), and initializing toxin secretion with terpene synthases, as the fungus grew on the corn roots. Based on the unique upregulated genes during soybean colonization at 2 DPI, *F. virguliforme* was penetrating roots through reactive oxygen species production, and regulation through Zn(II)-Cys6 fungal transcription factors (Brown et al., 2007).

Fusarium virguliforme colonization of soybean roots resulted in the activation of marked defense signals, ca. 4 DPI, as indicated by the rapid upregulation (>10 log2) of various cytochrome oxidase genes. Interestingly, these genes were not upregulated at the same time in samples derived from *F. virguliforme*-corn colonization, suggesting that either the fungus had not penetrated the root, and/or a lack of anti-microbial metabolite accumulation. However, at 7 DPI, cytochrome oxidases and NDAP was upregulated in *F. virguliforme* corn interactions, thus indicating cellular differentiation of hyphal penetration structures (Heller and Tudzynski, 2011). At the same time, cellular degradation and nutrient access-associated

processes were highly (>10 $\log_2$) upregulated in *F. virguliforme*-colonized soybean samples, as indicated by the expression of glycoside hydrolases and pectinases, as well as various nutrient transporters. A larger set of genes were differentially induced within *F. virguliforme* across hosts at 10 and 14 DPI. At these timepoints, samples from corn showed induced genes enriched in secretion catabolic processes (Supplemental Dataset 2-9), while those from soybean revealed a shift to processes indicative of fungal growth (e.g., glycerolipid and lipoprotein biosynthesis; (Takahashi et al., 2009). This is in support of our observation of asexual production at 14 DPI (i.e., Figure 23B).

Toxin and secreted proteins were induced in a temporally-dependent manner, as well as in differential quantities, when compared across hosts (Figure 31B and C). While nearly triple the number of predicted effector-encoding mRNAs were upregulated at 0-2 DPI in soybean, none of the effector-encoding mRNAs were differentially induced between hosts at these time points. By 4 DPI, almost four times as many effectors were upregulated in soybean roots (Figure 32), including those with predicted functional domains associated with pectin lyases, glycoside hydrolases, and necrosis-inducing proteins. However, similar to the above, all but three genes were not considered differentially expressed when compared to *F. virguliforme* colonization of corn (Supplemental Dataset 2-10). Until this timepoint in the infection process, CAZymes expression was observed to be induced in similar patterns (i.e., no DE genes) (Figure 33). However, at 4 DPI pectin lyases and glycoside hydrolases were expressed much higher (>10 $\log_2$) by *F. virguliforme* in soybean roots (Supplemental Dataset 2-11). This trend was exacerbated by 7 DPI with many CAZymes and effectors related to pectin lysates being uniquely upregulated in *F. virguliforme* colonization of soybean roots. This suggests

divergence in fungal colonization programs between corn and soybean at 7 DPI, potentially stemming from the shift of biotrophic to necrotrophic, as visible symptoms started to initialize at 7 DPI. A necrotrophic lifestyle was evident by 10 and 14 DPI with 14 and 28 effectors, and 37 and 114 CAZymes, respectively targeting cellular breakdown of soybean roots by *F. virguliforme*. Across the time course, few pectin lyases were expressed while *F. virguliforme* was colonizing corn roots. This may stem from the differential physiology of monocot roots containing only 10% pectin, whereas dicots contain up to 30% pectin (Caffall and Mohnen, 2009). The effectors that were uniquely induced between 7-10 DPI in corn roots are currently putative candidates with no known function.

Regulation of Soybean Defenses by milRNAs

Modulation of fungal pathogenesis has recently expanded to include micro-like RNAs (milRNAs). These small regulatory RNA modules of 18-22 nt in length were first observed in *Neurospora crassa* (Romano and Macino, 1992). Since initial discovery, milRNA have been observed to be involved in processes related to fungal development (Shao et al., 2019), including in *S. sclerotiorum* (Zhou et al., 2012) and *F. oxysporum* (Chen et al., 2014). To build upon the demonstrated roles for milRNAs in fungi, we next asked if plant pathogenic fungal milRNAs regulate the expression of host targets, as previously observed with small RNAs (Weiberg et al., 2013). To test this, we conducted a comprehensive microRNA sequencing analysis of our time-course of infection to 1) inventory the suite of *F. virguliforme*-derived milRNAs, and 2) determine with these molecules affect the expression of host target transcripts. Reads from *F. virguliforme*-infected soybean samples, as well as from *in vitro*

germinating macroconidia, were aligned to both *F. virguliforme* and soybean genomes to remove reads that matched both genomes (Weiberg et al., 2013). Following this, samples of germinating macroconidia were found to contain approximately 74% mapped reads (Table 21). Mixed samples of soybean root and *F. virguliforme* ranged from 1.5-5.6% for 0-7 DPI, and 7.5-13.5% for 10 and 14 DPI read alignment after filtering. We posit that the increase in read alignment corresponds to increased fungal growth (Figure 23B). These unique reads shared a similar read length distribution to other fungi, with two peaks of read alignment at 21-23 nt and 26 nt (Figure 34A) (Zhou et al., 2012; Chen et al., 2014).

milRNA derived from *F. virguliforme* were predicted using mirDEEP2 (Friedländer et al., 2012), with no reference option to form pooled and collapsed *F. virguliforme* uniquely aligned reads. In total, 22 candidate milRNA were annotated, and of these, 20 passed the randfold p-value test. Of these 20 candidates, two putative milRNA were consistently induced (expressed in all 3 biological replicates) *in planta* (Supplemental Dataset 2-12). One candidate, *Fvm1-novel-1*, was highly expressed from 0-4 DPI only *in planta*. The second candidate was expressed from 10-14 DPI, at an elevated level from germinating macroconidia.

Using *Fvm1-novel-1* and *Fvm1-novel-2*, we next predicted soybean targets of these two candidates using psRNATraget (Dai et al., 2018) and TAPIR (Bonnet et al., 2010). The individual resultant target lists were filtered to only include candidates that were cross-validated in both programs. While no targets were repressed in their expression by *Fvm1-novel-2*, six soybean target genes were repressed in expression by *Fvm1-novel-1*; identified

targets all were associated with processes corresponding to defense and susceptibility pathways (Figure 34B). In brief, Fvm1-novel-1 was predicted to target root (Glyma.02g181500), cytochrome P450s (*CYP94C1*, Glyma.11g185700 an Glyma.12g087200), which are known to be induced by jasmonate acid and wounding (Heitz et al., 2012). *Fvm1-novel-1* also was predicted to target a regulator of stress responsive alternative splicing (Glyma.08g334100, Glyma.18g067300) (Gulledge et al., 2012). Intriguingly, one target (Glyma.14g022100) of *Fvm1-novel-1* was a dihydrolipoamide succinyltransferase, a component of oxoglutarate dehydrogenase complex. Previous work demonstrated that a knock-down of this pathway leads to enhanced senescence in tomato (Araújo et al., 2012). Based on this, we hypothesize that *F. virguliforme* may promote senescence in host tissue to advance necrotrophy and nutrient acquisition. In total, the repression in expression of these soybean targets suggests *F. virguliforme* regulates host immunity through milRNAs.

Discussion

Comparative systems-based approaches of pathogenic and nonpathogenic fungal isolates have led to the identification of genetic signatures relevant to pathogenicity and compatible host interactions on a single host. This approach can be manipulated to explore the continuum of pathogenic and endophytic niches of two hosts from the genetic repertoire of a single fungal organism. Herein, we applied a similar design of two distinct phenotypic outcomes generated by a single isolate to explore how fungal pathogens transcriptionally rewire infection programs to promote a symptomatic or asymptomatic host reaction. To

accomplish this goal, we *de novo* assembled an annotated the *F. virguliforme* genome, generated 39 mRNA transcriptomes across *in vitro* and *in planta* conditions to identify infection program modulation across two hosts, and assessed the soybean in planta milRNAome of *F. virguliforme* over a two-week time course.

Fusarium virguliforme colonization yields distinct changes in root phenotype, dependent upon host. Corn roots when colonized by *F. virguliforme* remain asymptomatic and soybean roots turn chlorotic and eventually necrotic. Underlying these phenotypic developments are host dependent transcriptional programs. Temporal shifts within the transcriptome of *F. virguliforme* colonizing corn roots were gradual during the infection time course. Whereas, *F. virguliforme* colonization program drastically shifted from 4-7 DPI. These large shifts in the *in planta* transcriptome of hemibiotrophic plant pathogens has been observed within single hosts (O'Connell et al., 2012).

Interestingly, the identified differences in transcriptomes appears to not be solely derived by gene content, but rather the temporal induction of genes with respect to host colonization. Gene co-expression networks highlighted temporal processes unique to each host through varying stages of fungal growth, infection and proliferation through nutrient access. The quick growth and infection of *F. virguliforme* on soybean roots by 2 DPI, indicates a rapid recognition of the host surface and initiation of the early infection program (Elliott, 2016). However, *F. virguliforme* gene expression on corn roots through the early time course were enriched for negative regulation of biological processes and primary metabolism, suggesting that this fungal was not immediately stimulated to infect the corn host. Upregulation of

processes indicative of host infection did not occur till 7 DPI, suggesting a delaying in fungal-host recognition (Giovannetti et al., 1994). By the timeframe *F.* virguliforme had penetrated corn roots, the same fungus on soybean roots had started to transition in lifestyle form biotrophic to necrotrophic. Upregulation of small protein secretion and fungal derived toxins signaled that *F. virguliforme* was promoting cell modification of host tissues for nutrient access (Sahu et al., 2017). As *F. virguliforme* within soybean roots induced process for cell killing and pathogenicity through the remainder of the time course, gene activity on corn highlighted fewer catabolic processes to acquire nutrients.

These host derived temporal shifts in the *F. virguliforme* transcriptome reveals gene expression plasticity. While the vast majority of the transcriptome was expressed during colonization of corn and soybean roots, the induction of genes enabling the processes were temporally diverged. Temporal changes of gene expression have been observed between colonization of hosts of the same fungus exhibiting different lifestyles (Lahrmann et al., 2013; Lorrain et al., 2018), and may suggest the shift to necrotrophy on corn was limited.

The transcriptomic plasticity of *F. virguliforme* between soybean and corn colonization provides a unique angle to view processes critical to necrotrophy on soybean. For example, the upregulation of effectors and CAZymes initializing at 4 DPI, highlights the start of the transition from biotrophic activity to necrotrophic (Ngaki et al., 2016). CAZymes expressed within soybean roots had a greater upregulation of pectin lyase expression, more than corn roots. Also the Necrosis Inducing Protein, was highly upregulated during soybean colonization across the time course, suggesting dicot specific upregulation (Bae et al., 2006).

Effectors and CAZymes within soybean roots were secreted in temporal waves at 2, 4 and 7 DPI. Each temporal wave increased in intensity of gene expression as well as diversity of enzymatic activity. This upregulation of diverse array of cell degrading and necrosis inducing peptides, demonstrates the shift to necrotrophy (Kleemann et al., 2012; Haueisen et al., 2018).

While a hemibiotrophic infection program ensued in soybean roots, infection was delayed, and catabolic activities were lower in corn by *F. virguliforme*. A lack of host recognition (Giovannetti et al., 1994) or an upregulation of host defenses from pattern triggered immunity (Bagnaresi et al., 2012; Zhang et al., 2018), could slow fungal growth and down regulate development. Once inside the host fewer effectors and CAZymes were uniquely expressed in corn roots and were, more often than not, down-regulated after induction. The lower level of expression along with the decrease in CAZyme diversity, suggest that the cellular environment within corn roots did not stimulate prolific upregulation of necrotic inducing peptides. This may stem from the physiological differences in cell structure between monocots and dicots (Caffall and Mohnen, 2009). Additionally, as the primary hosts for *F. virguliforme* is legumes, potentially *F. virguliforme* may not be as adapted to colonization of monocots (Zhao et al., 2013).

Regulation of biotrophy to necrotrophy during the hemibiotrophic lifestyle of fungi has intrigued many plant pathologists (Rai and Agarkar, 2016; Chowdhury et al., 2017; Haueisen et al., 2018). Transcription factors may pay a critical role in shifting fungal gene expression from biotrophic to necrotrophic lifestyle. Several transcription factors from the Zn(II)-Cys6

and C2H2 Zinc Finger family alter pathogenicity and growth (Chen et al., 2017; Sang et al., 2019). We discovered several Zn(II)-Cys6 were uniquely upregulated during soybean colonization, which may initiate pathogenicity of this fungus to soybean. Additionally, we explored host defense regulation by *F. virguliforme* and discovered a putative milRNA targeting stress, defense and plant maturation pathways in soybean. Collectively these gene targets indicate *F. virguliforme* is secreting milRNAs to modulate host defenses, as discovered with other filamentous pathogens (Weiberg et al., 2013; Burkhardt and Day, 2016). The targeting of plant senescence by a milRNA secreted for a hemibiotrophic pathogen may indicate an induction of early senescence to promote tissue maturation and susceptibility (Haffner et al., 2015). In total, these milRNA targets should be further explored to understand their role in pathogenesis by *F. virguliforme.*

The transition from biotrophic to necrotrophic on soybean, while colonizing corn roots as a lower subdued infection program, highlights the transcriptional plasticity of a single fungal isolate. The diverse transcriptomic rewiring aids in the phenotypic development of an asymptomatic and symptomatic hosts over a two-week time course. The visual manifestation of these interactions suggests a potential endophytic role for *F. virguliforme* in corn roots, while also enacting as a pathogen on soybean (Rai and Agarkar, 2016), constituting two distinct roles *F. virguliforme* may play in agroecosystems. The ability of *F. virguliforme* to enact in these two distinct roles suggests the need to consider the genomic potential for plant pathogens to be expressing a gradation of transcriptional programs enabling lifestyle plasticity on a broad range of hosts.

Acknowledgments

We would like to recognize Michigan State University (MSU) project GREEEN and the C.S. Mott Foundation for funding of ABY and research. We would like to thank Kevin Childs and John Johnston for sever access and computational assistance, Marty Chilvers for providing the *Fusarium virguliforme* mont-1 isolate. We would also like to recognize the support staff at the MSU Institute for Cyber enabled Research High Performance Computing Cluster for assistance in software optimization. This research was supported by funding from the MSU Plant Resilience Institute.

Author Contributions

Designed framework: B.D., R.B., C.M.W, A.B.Y.; Conducted Experiments: A.B.Y; Analyzed data: A.B.Y. B.D., R.B., C.M.W, A.B.Y.; Wrote the manuscript: B.D., R.B., C.M.W, A.B.Y.;

Table 16. Genome assembly metrics of *Fusarium virguliforme* versions 1 and 2.

Metric	V1[Z]	V2
Number of Contigs	3,089	96
Contig N50 (bp)	72,747	1,547,076
GC %	49.38	49.21
Total Length (bp)	50,448,805	52,079,485
Total Coverage	20x	17x
Predicted Genes	14,845	16,050

[Z]Metrics were taken from Srivastava et al., 2014 for the first version of the *F. virguliforme* genome.

Table 17. GO enrichment of genes only contained in Fv_v2 genome.

GO.ID	Ontology	Term	Classic Fisher
GO:0006779	P	porphyrin-containing compound biosynthesis	0.0039
GO:0006821	P	chloride transport	0.0127
GO:0016567	P	protein ubiquitination	0.0166
GO:0006351	P	transcription, DNA-templated	0.0288
GO:0045116	P	protein neddylation	0.0409

Table 18. Number of quality trimmed reads uniquely aligning to the *Fusarium virguliforme* v2 genome.

				Days Post Inoculation					
				0	2	4	7	10	14
Sample ID	Biological Replicate	Plant Type	Inoculated	Number of Uniquely Aligned Reads					
EFv1	1	Corn	*F. virguliforme*	129,458	112,045	448,448	460,305	611,916	820,196
EFv2	2	Corn	*F. virguliforme*	84,485	195,637	2,059,296	1,026,275	2,232,654	1,549,577
EFv3	3	Corn	*F. virguliforme*	113,274	189,543	640,340	153,871	891,445	719,899
SFv1	1	Soybean	*F. virguliforme*	193,270	127,706	138,772	99,069	665,846	1,154,194
SFv2	2	Soybean	*F. virguliforme*	91,268	87,332	167,226	227,823	1,112,727	1,860,529
SFv3	3	Soybean	*F. virguliforme*	159,529	114,317	324,521	323,611	1,137,281	4,575,746

Table 19. Host specific differential gene expression across timepoints of *Fusarium virguliforme* colonization of soybean or corn.

			Soybean compared to corn		Corn compared to soybean		Shared expression	
Timepoint	Soybean total	Corn total	Uniquely up	Uniquely down	Uniquely up	Uniquely down	Matching direction change	Differing direction change
0 vs 2	22	27	13	7	26	1	0	0
2 vs 4	1	27	0	1	0	27	0	0
4 vs 7	1	94	0	1	94	0	0	0
7 vs 10	30	10	24	5	7	2	1	0
10 vs 14	128	13	95	19	8	3	1	1

Table 20. Host specific differential gene expression within timepoints of *Fusarium virguliforme* colonization of soybean or corn at log_2 fold change > 1.

	Number of Differentially Expressed Genes		
Timepoint	Total	Soybean	Corn
0	11	11	0
2	50	39	11
4	55	55	0
7	143	106	37
10	615	322	293
14	1858	1077	781

Table 21. Number of quality trimmed milRNA reads uniquely aligning to the *Fusarium virguliforme* v2 genome. SFv indicates *in planta* sample, and GM indicates geminating macroconidia.

				Days Post Inoculation					
				0	2	4	7	10	14
Sample ID	Biological Replicate	Plant Type	Inoculated	Number of Uniquely Aligned milRNA Reads					
SFv1	1	Soybean	*F. virguliforme*	428,635	482,138	453,556	542,446	2,456,820	1,705,182
SFv2	2	Soybean	*F. virguliforme*	273,748	371,088	445,743	844,800	2,078,877	3,268,441
SFv3	3	Soybean	*F. virguliforme*	352,295	527,232	567,939	937,109	1,654,041	3,031,727
GM-1	1	N/A	*F. virguliforme*	9,985,673					
GM-2	2	N/A	*F. virguliforme*	14,937,775					
GM-3	3	N/A	*F. virguliforme*	18,689,308					

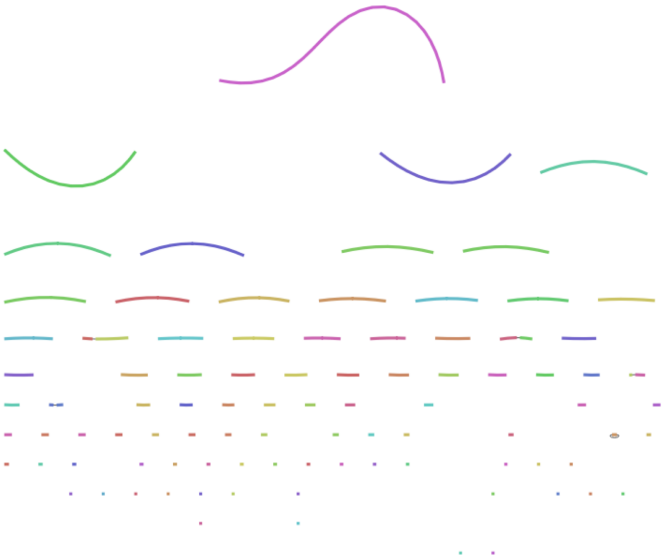

Figure 21. Genome assembly of *Fusarium virguliforme*. Individual lines represent a single contig and relative length. Color was assigned randomly, with lines connecting contigs indicating uncertainty in the genome assembly.

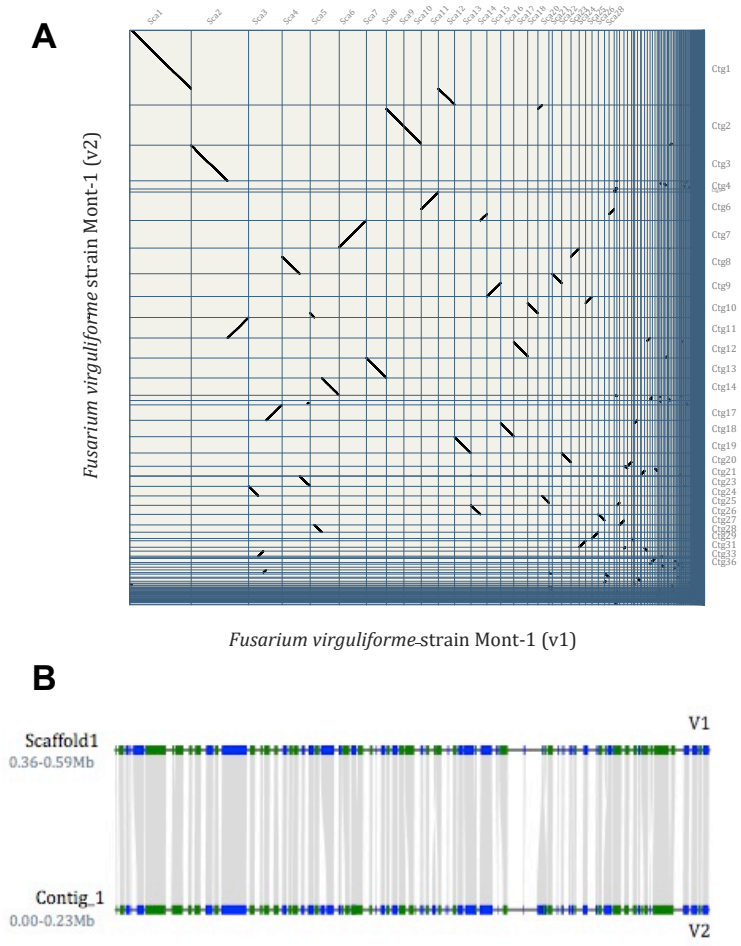

Figure 22. Syntenic regions between genome versions of *Fusarium virguliforme*. (A) Dot plot of syntenic regions retained between genome version 1 (v1) and genome version 2 (v2). (B) Micro-collinearity between scaffold 1 of v1 genome and contig 1 of v2 connected by shaded grey areas. Regions containing genes are highlighted in green or blue, for forward or reverse orientation, respectively.

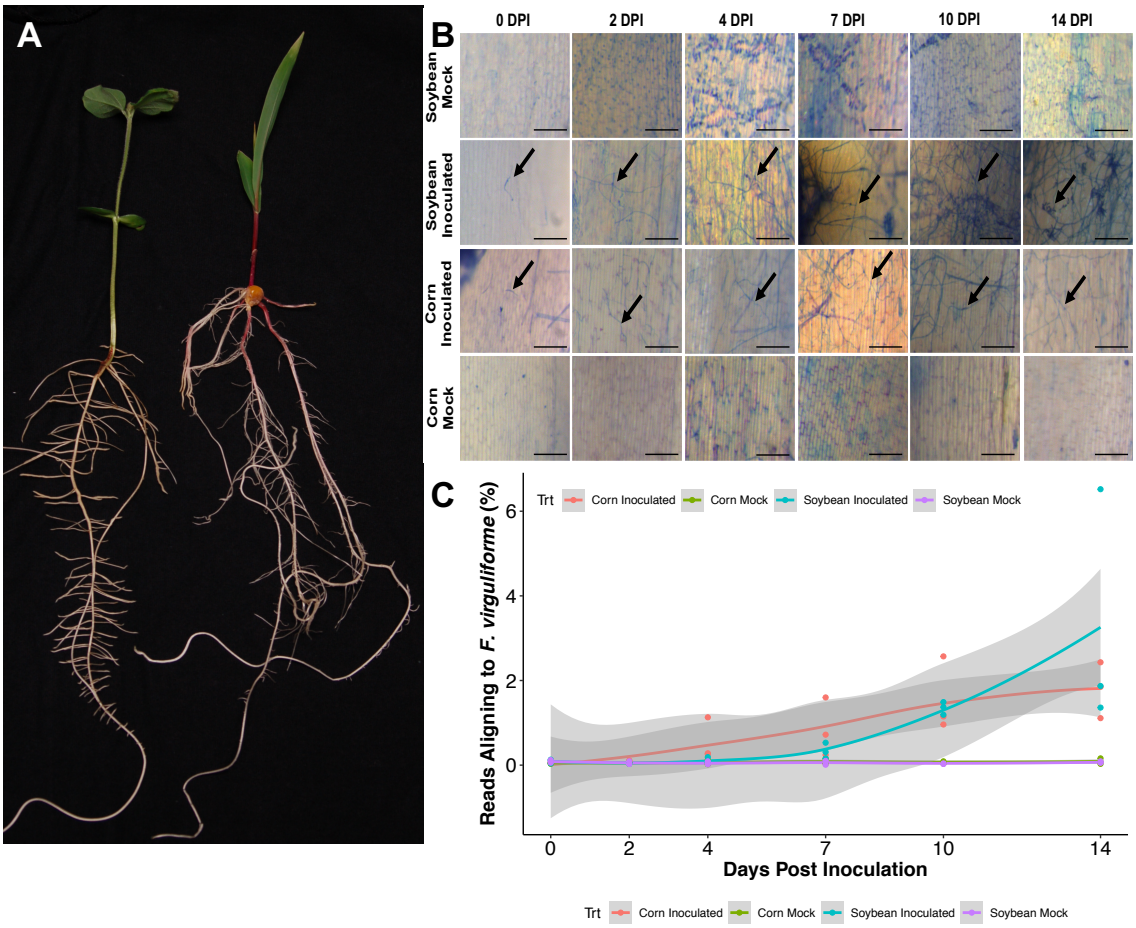

Figure 23. *Fusarium virguliforme* growth chamber assay of soybean and corn. (A) Plant growth and development after 14 days post inoculation with *F. virguliforme*. (B) Trypan blue staining of inoculation site on inoculated with *F. virguliforme* or mock inoculated soybean cv. Sloan and corn cv. E13022S roots. (DPI = Days post inoculation). Black bar represents 16 mm. (C) The percent of unique reads aligning *F. virguliforme* within corresponding treatments of corn or soybean inoculated with *F. virguliforme* or mock (water) inoculated soybean or corn, across 0-14 days post inoculation. Reads were trimmed by Trimmomatic/0.33, aligned to Fusarium_virguliforme_V2 genome assembly with HISAT2/2.1.0. Each sample is indicated by a colored dot and lines are the average of three biological repeats. Grey shade indicates SEM.

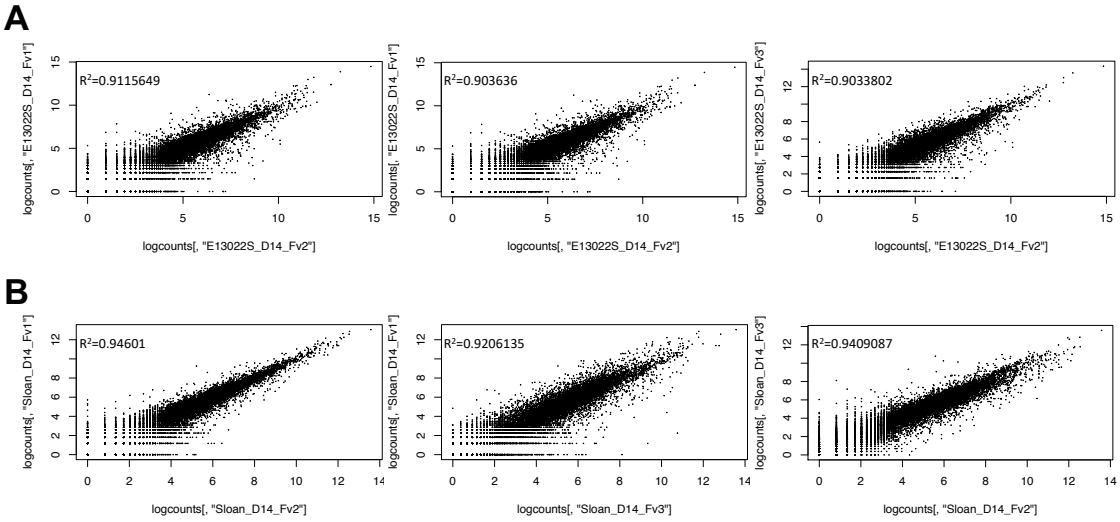

Figure 24. Biological consistency of samples from different time courses. Correlation of gene expression values in three biological replicates from 14 DPI samples of *Fusarium virguliforme* colonizing corn (A), and *Fusarium virguliforme* colonizing soybean (B).

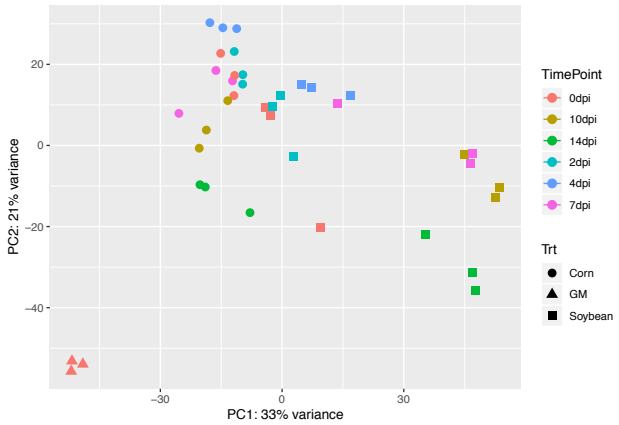

Figure 25. Samples of fungal plant colonization cluster by host. Principle component analysis (PCA) of gene expression values of *F. virguliforme* colonizing soybean or corn, or germinating macroconidia (GM).

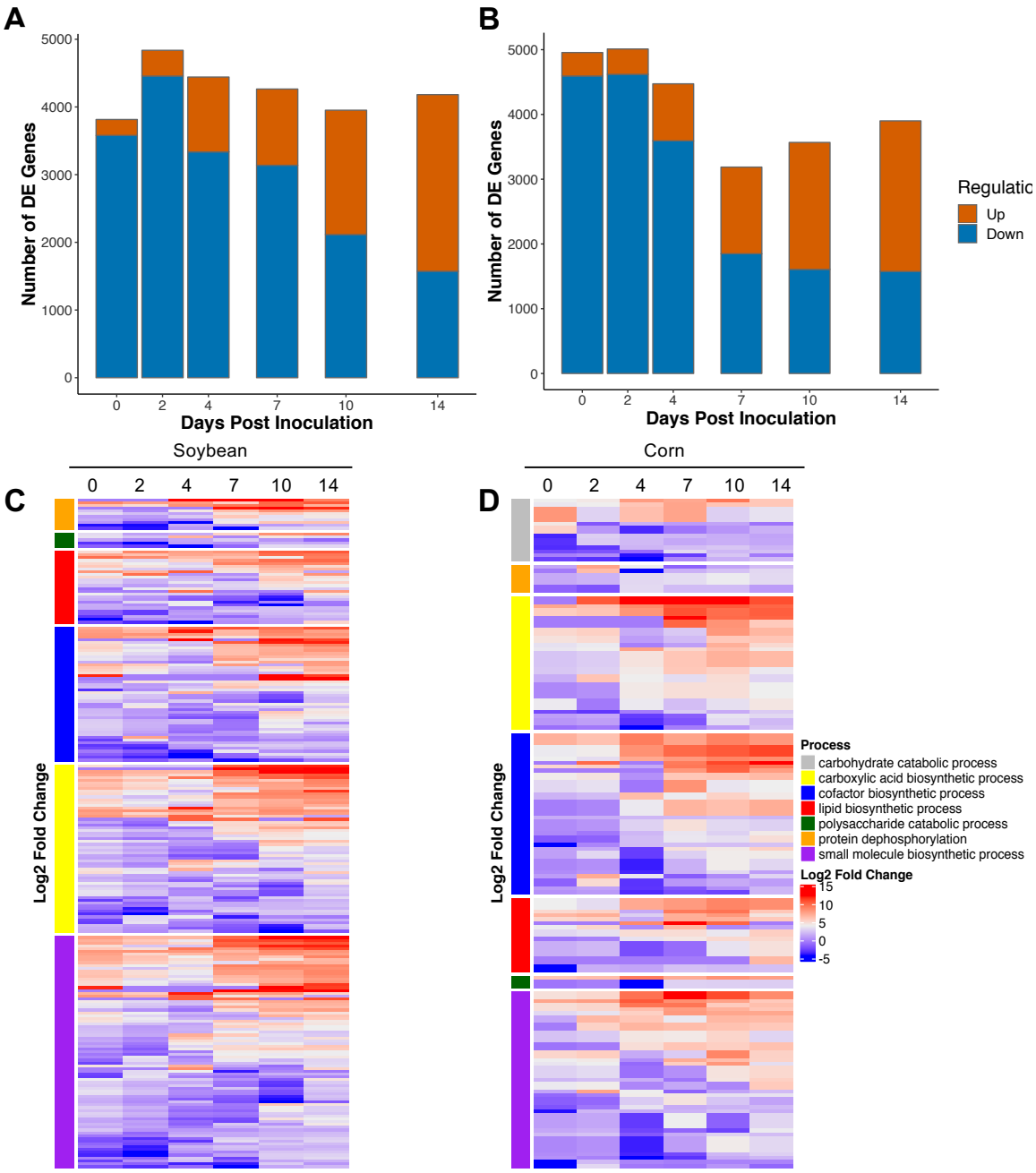

Figure 26. Temporal expression patterns of *Fusarium virguliforme* response genes within soybean and corn hosts in comparison to germinating macroconidia. (A) and (B) Number of significant differentially regulated genes with $|\log_2(FC) > 2|$ between *F. virguliforme* in planta compared to geminating macroconidia within corn or soybean roots over six timepoints. (C) and (D) Heatmap of significant gene ontology enrichment of $|\log_2(FC) > 2|$ upregulated genes across pooled time points for *F. virguliforme* colonization soybean (n=233) and corn (n=165).

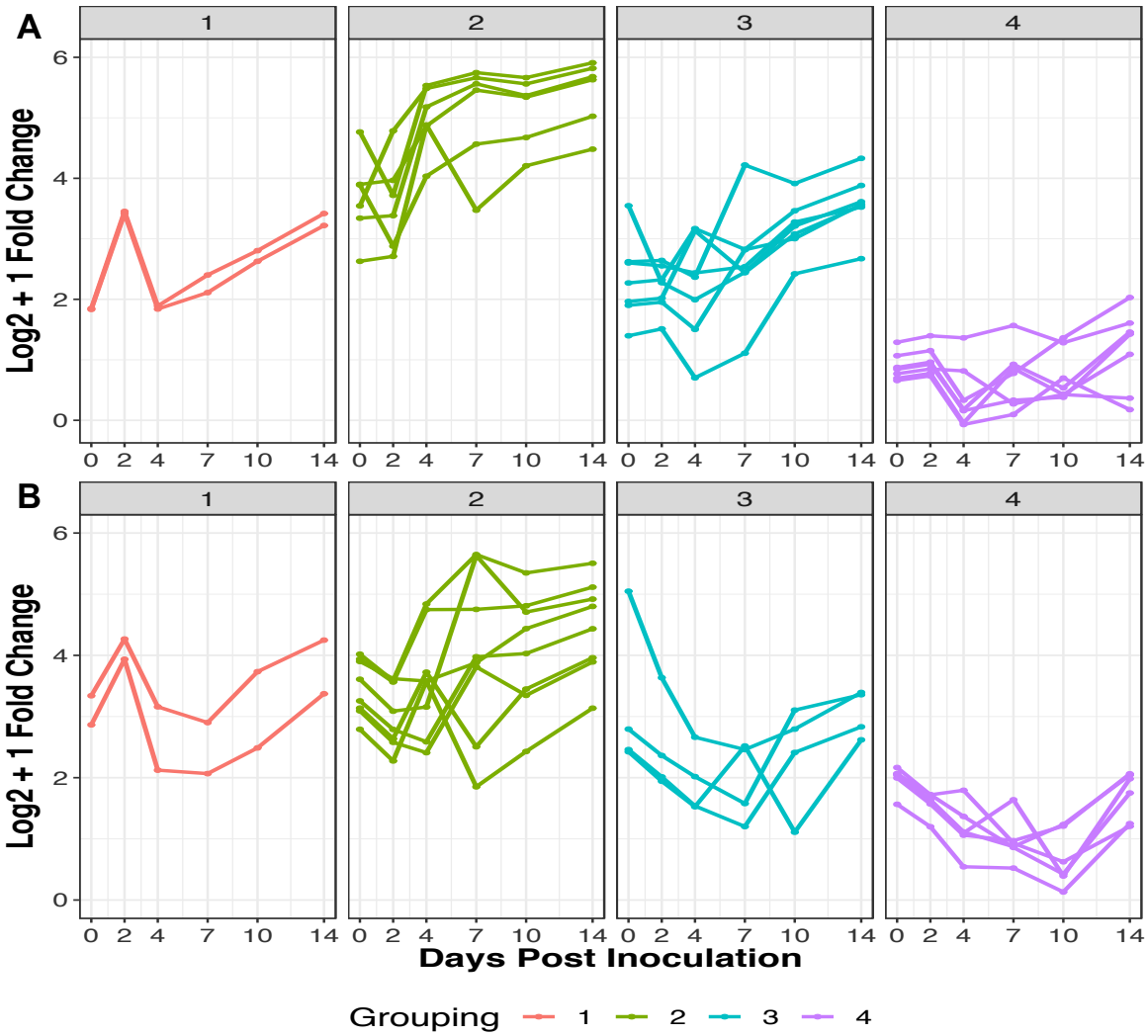

Figure 27. Distinct gene co-expression groups of host induced *Fusarium virguliforme* response. (A) and (B) Mean expression of genes within co-expression modules from *F. virguliforme* colonization of corn or soybean roots, respectively across the time course. Modules grouped into four distinct expression patterns of 1) upregulation at 2 DPI, 2) upregulation at 4-7 DPI, 3) induction at 7-10 DPI, and 4) increase in expression at 10-14 DPI.

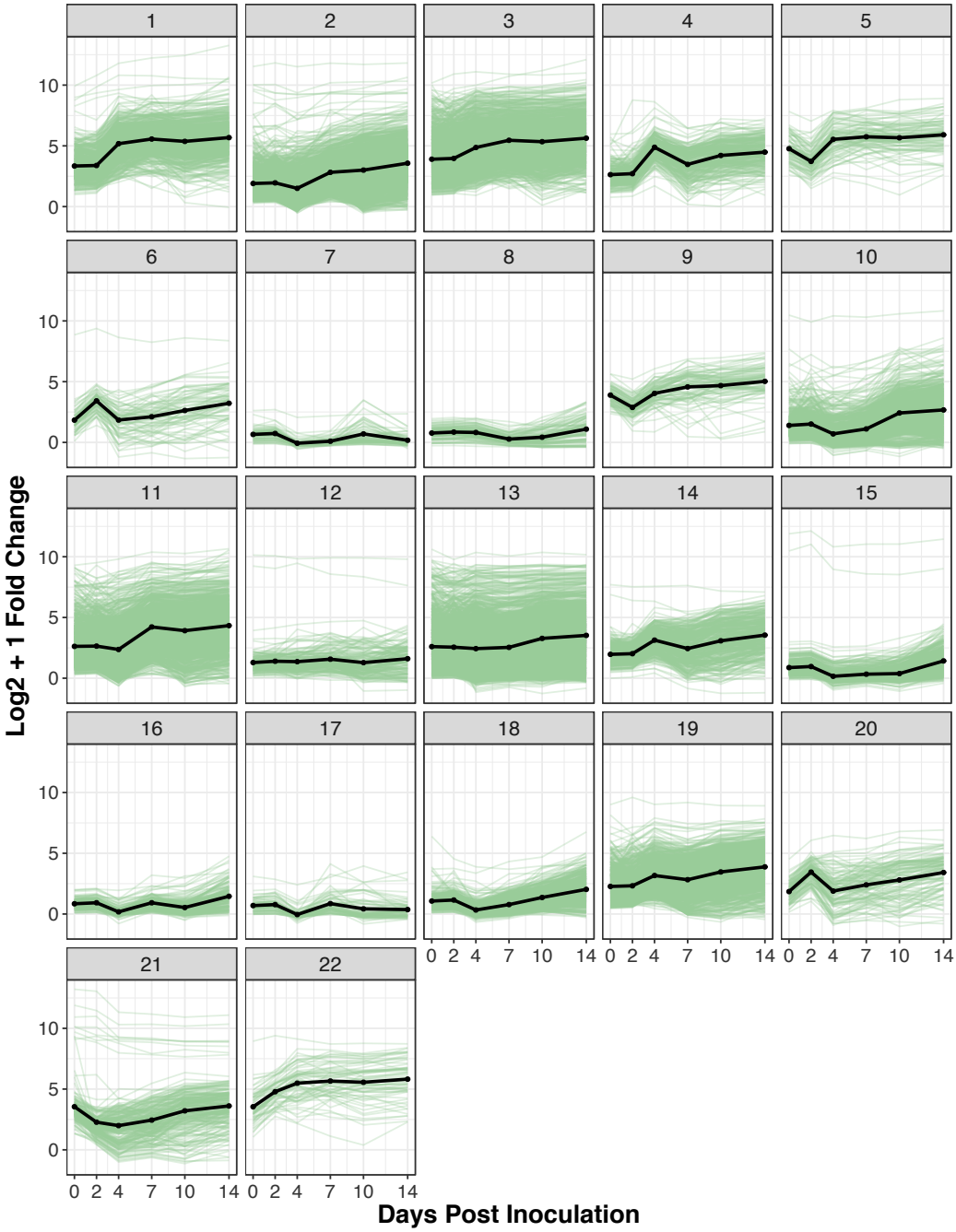

Figure 28. Weighted gene co-expression network modules from *F. virguliforme* temporal colonization of corn. Log_2 plus one transformed expression for all genes in the co-expression module is plotted in green over the time course. The mean expression for all genes in that modules is plotted in black.

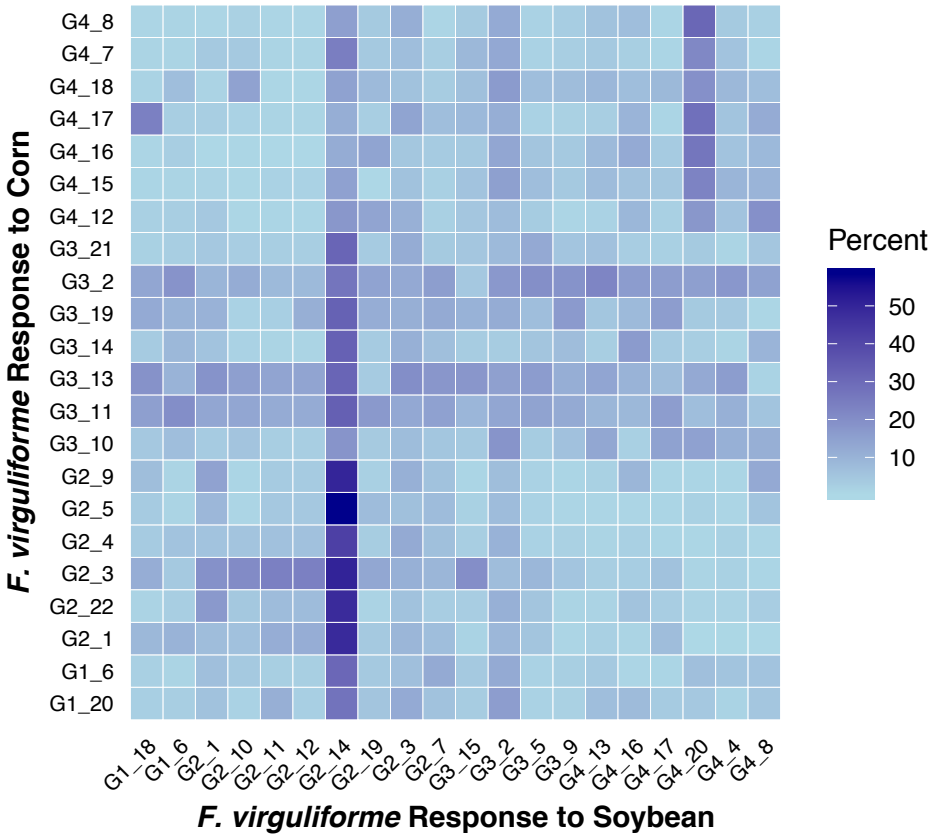

Figure 29. Symptomatic and asymptomatic hosts uncover *Fusarium virguliforme* transcriptome plasticity. Genes from weighted gene correlation network analysis modules were calculated for percent overlap from gene count shared divided by the smaller module between *F. virguliforme* expression on each host. Modules are annotated with grouping assignment from Figure 27.

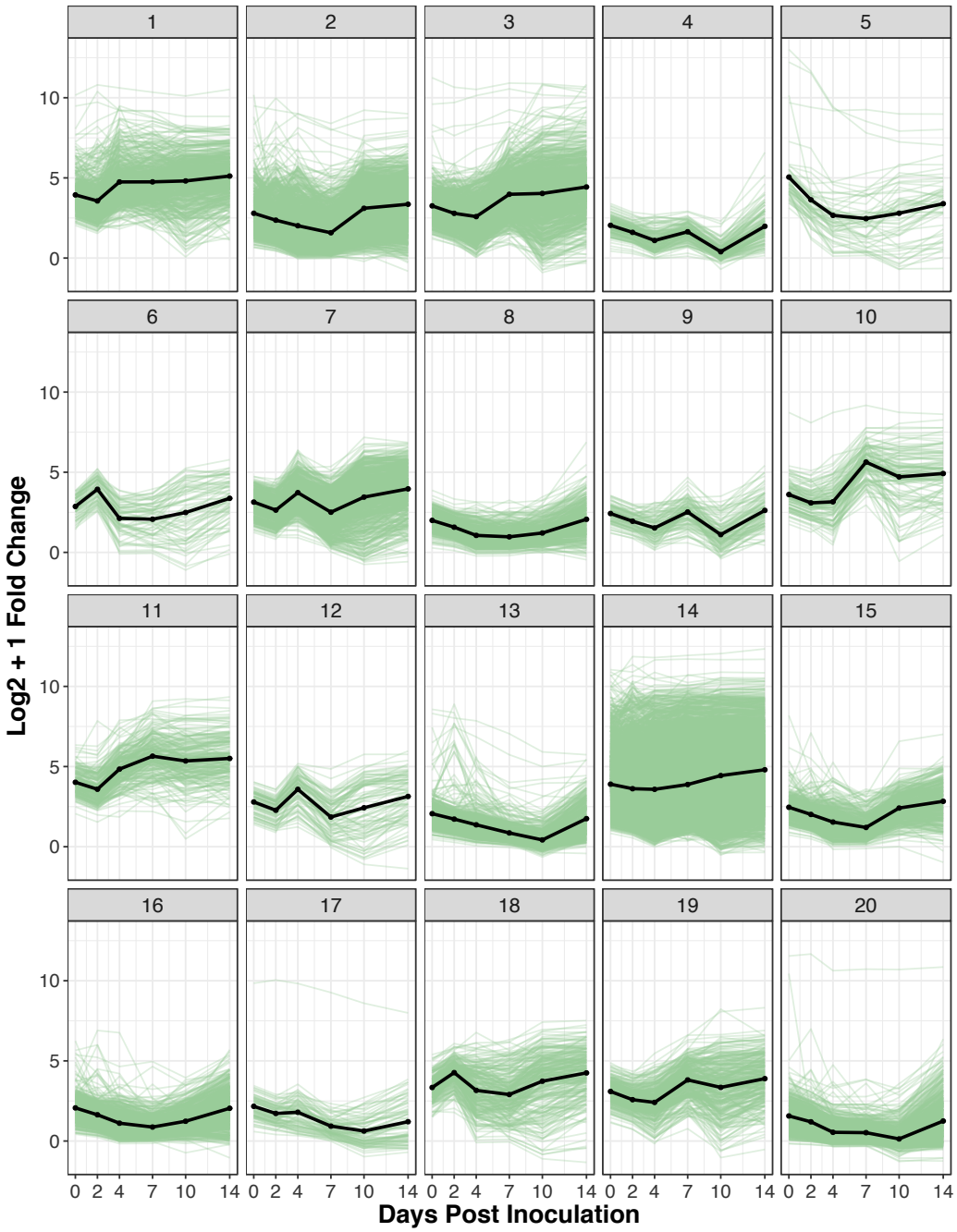

Figure 30. Weighted gene co-expression network modules from *F. virguliforme* temporal colonization of soybean. Log_2 plus one transformed expression for all genes in the co-expression module is plotted in green over the time course. The mean expression for all genes in that modules is plotted in black.

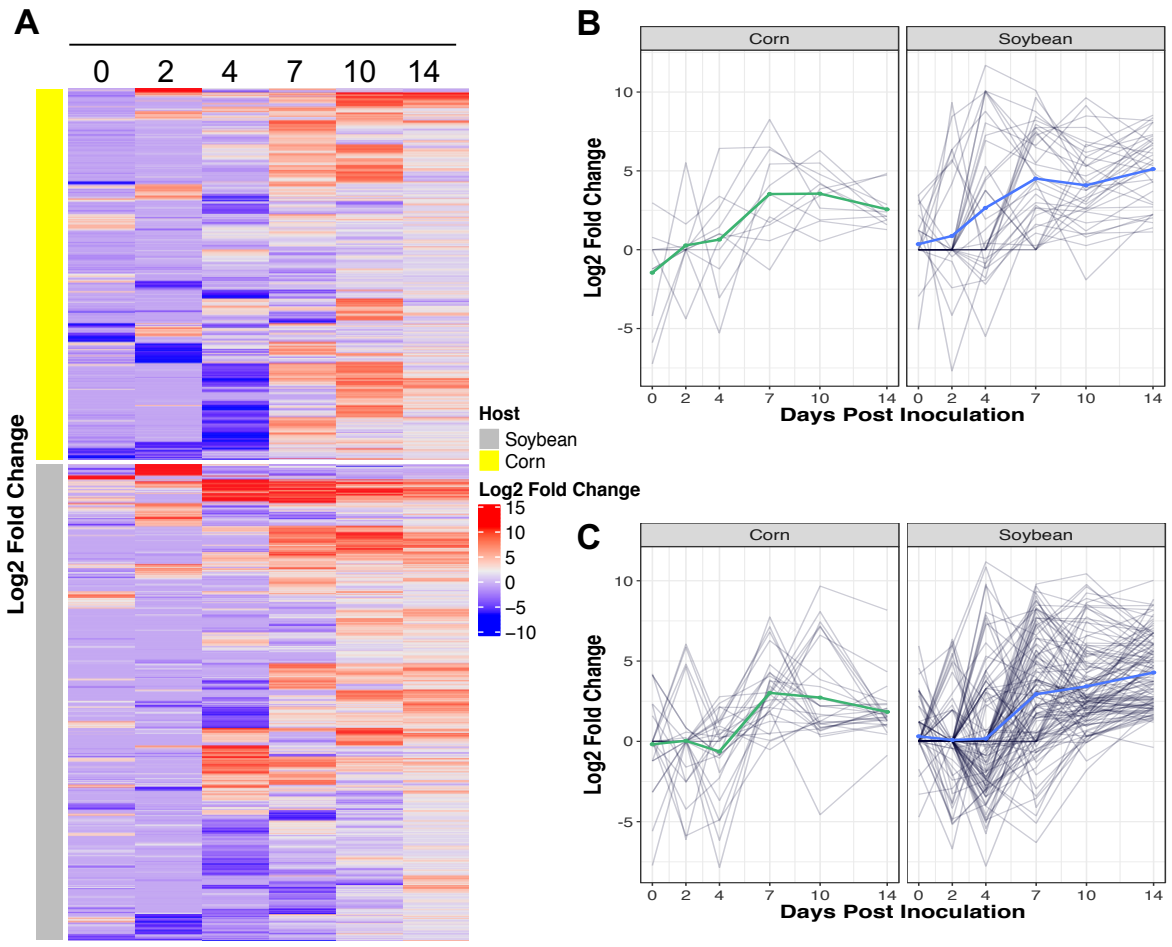

Figure 31. Host unique genes induced within *Fusarium virguliforme* highlight disease development. (A) Heatmap of $\log_2$(FC) > 1 of significantly upregulated genes at a single timepoint in *F. virguliforme* between soybean and corn (n=2,099). Yellow indicates differentially upregulated genes from *F. virguliforme* colonization of corn and blue indicates, grey indicates differentially upregulated genes from *F. virguliforme* colonization of soybean. (B) Expression patterns of $\log_2$(FC) > 1 comparing *F. virguliforme* host expression, of significantly upregulated candidate effector genes at a single timepoint in in corn or soybean over the infection time course. (C) Expression patterns of $\log_2$(FC) > 1 comparing *F. virguliforme* host expression, of significantly upregulated candidate carbohydrate active enzymes at a single timepoint in in corn or soybean over the infection time course. Color line indicates mean of all genes in the plot. Grey lines represent individual genes.

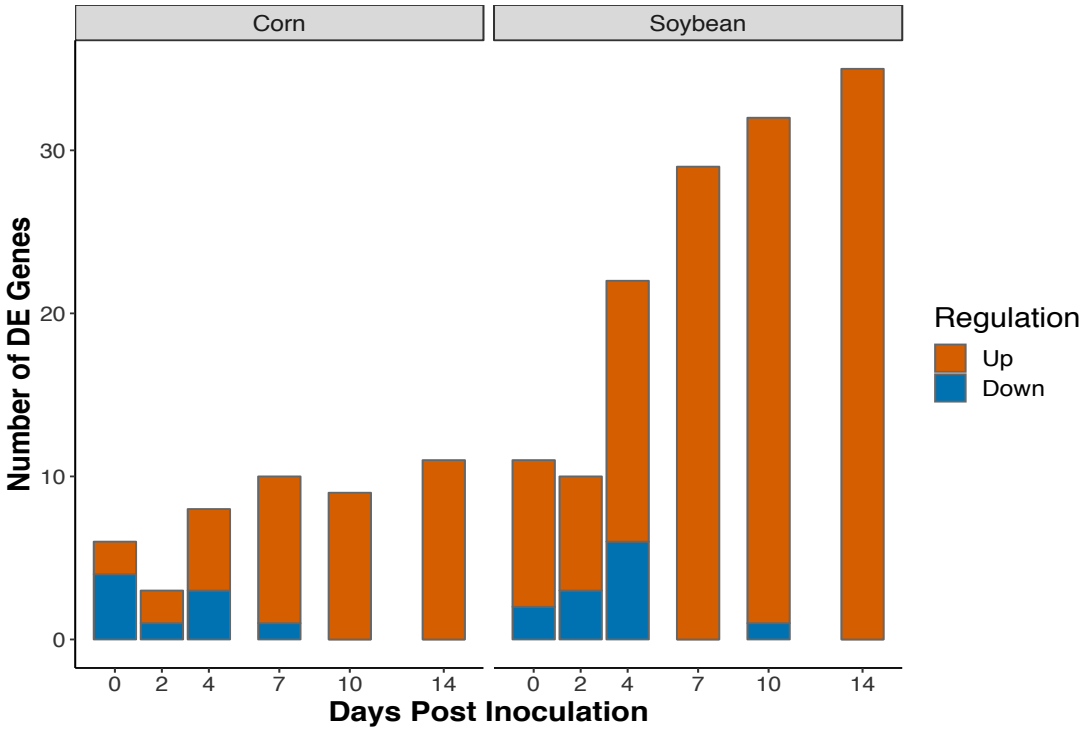

Figure 32. Temporal expression patterns of *Fusarium virguliforme* candidate effector genes within soybean and corn hosts. Number of significant differentially regulated effector genes with $|\log_2(FC) > 1|$ in at least a single timepoint between *F. virguliforme* in each corn or soybean compared soybean or corn, respectively over the time course.

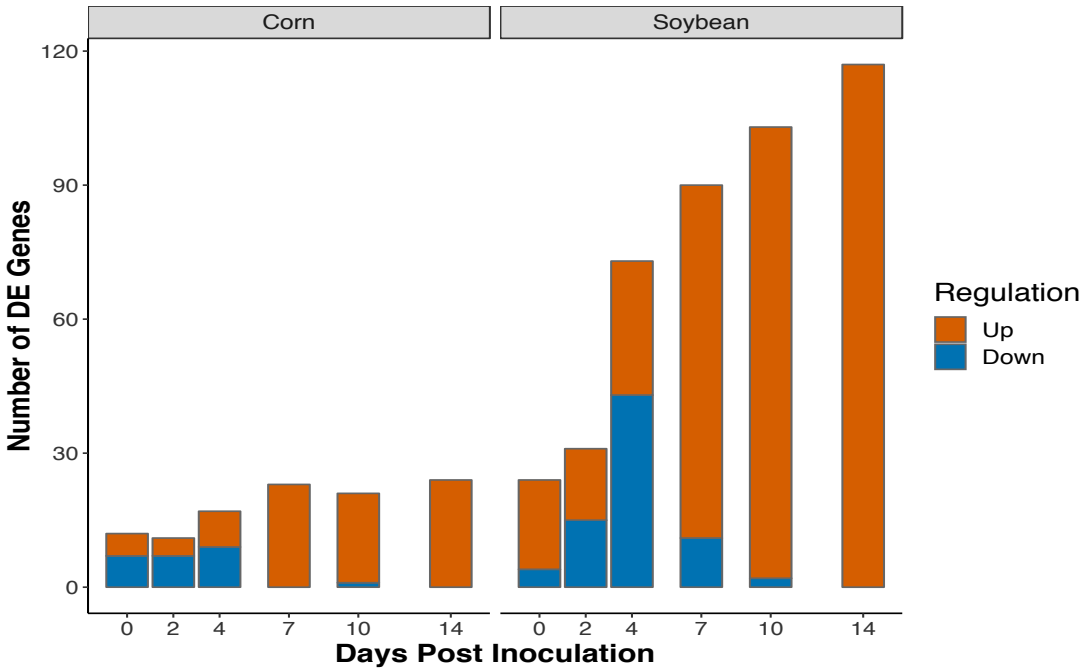

Figure 33. Temporal expression patterns of *Fusarium virguliforme* carbohydrate active enzyme related genes within soybean and corn hosts. Number of significant differentially regulated carbohydrate active enzyme related genes with $|\log_2(FC) > 1|$ in at a single timepoint between *F. virguliforme* in each corn or soybean compared soybean or corn, respectively over the time course.

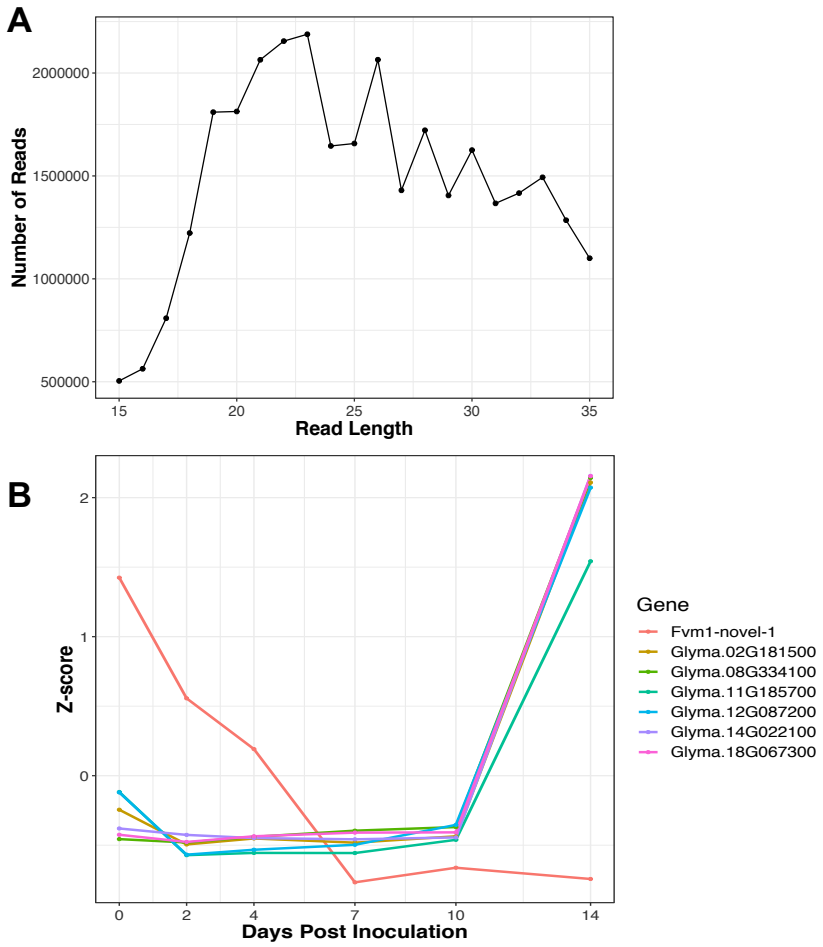

Figure 34. Expression of micro-like RNAs (milRNAs)in *Fusarium virguliforme* colonization of soybean host. (A) Read length distribution of reads mapping to *F. virguliforme*. (B) Z-score plots of transcripts per million (TPM) of fungal milRNA *Fvm1-novel-1* and targeted soybean genes across temporal time course.

REFERENCES

REFERENCES

Alexa A and Rahnenfuhrer J. (2018). Topgo: Enrichment analysis for gene ontology.

Altschul, S.F., Gish, W., Miller, W., Myers, E.W., and Lipman, D.J. (1990). Basic local alignment search tool. J. Mol. Biol. **215,** 403-410.

Anders, S., Pyl, P.T., and Huber, W. (2014). HTSEQ—a python framework to work with high-throughput sequencing data. Bioinform. **31,** 166-169.

Araújo, W.L., Tohge, T., Osorio, S., Lohse, M., Balbo, I., Krahnert, I., Sienkiewicz-Porzucek, A., Usadel, B., Nunes-Nesi, A., and Fernie, A.R. (2012). Antisense inhibition of the 2-oxoglutarate dehydrogenase complex in tomato demonstrates its importance for plant respiration and during leaf senescence and fruit maturation. Plant Cell **24,** 2328-2351.

Ardui, S., Ameur, A., Vermeesch, J.R., and Hestand, M.S. (2018). Single molecule real-time (smrt) sequencing comes of age: Applications and utilities for medical diagnostics. Nucl. Acids Res. **46,** 2159-2168.

Bae, H., Kim, M.S., Sicher, R.C., Bae, H.-J., and Bailey, B.A. (2006). Necrosis- and ethylene-inducing peptide from *Fusarium oxysporum* induces a complex cascade of transcripts associated with signal transduction and cell death in Arabidopsis. Plant Physiol. **141,** 1056-1067.

Bagnaresi, P., Biselli, C., Orrù, L., Urso, S., Crispino, L., Abbruscato, P., Piffanelli, P., Lupotto, E., Cattivelli, L., and Valè, G. (2012). Comparative transcriptome profiling of the early response to *Magnaporthe oryzae* in durable resistant vs susceptible rice (*Oryza sativa* l.) genotypes. PLoS ONE **7,** e51609.

Bates, D., Machler, M., Bolker, B., Walker, S. (2015). Fitting linear mixed-effects models using {lme4}. J. Stat. Soft **67,** 1-48.

Bolger, A.M., Lohse, M., and Usadel, B. (2014). Trimmomatic: A flexible trimmer for illumina sequence data. Bioinform. (Oxford, England) **30,** 2114-2120.

Bonnet, E., He, Y., Billiau, K., and Van de Peer, Y. (2010). Tapir, a web server for the prediction of plant microrna targets, including target mimics. Bioinform. **26,** 1566-1568.

Brown, D.W., and Proctor, R.H. (2016). Insights into natural products biosynthesis from analysis of 490 polyketide synthases from *Fusarium*. Fun. Gen. Biol. **89,** 37-51.

Brown, D.W., Butchko, R.A.E., Busman, M., and Proctor, R.H. (2007). The *Fusarium verticillioides* fum gene cluster encodes a zn(ii)2cys6 protein that affects fum gene expression and fumonisin production. Eukary. Cell **6,** 1210-1218.

Brown, N.A., Evans, J., Mead, A., and Hammond-Kosack, K.E. (2017). A spatial temporal analysis of the *Fusarium graminearum* transcriptome during symptomless and symptomatic wheat infection. Mol. Plant Pathol. **18,** 1295-1312.

Bryant, D.M., Johnson, K., DiTommaso, T., Tickle, T., Couger, M.B., Payzin-Dogru, D., Lee, T.J., Leigh, N.D., Kuo, T.-H., Davis, F.G., Bateman, J., Bryant, S., Guzikowski, A.R., Tsai, S.L., Coyne, S., Ye, W.W., Freeman, R.M., Jr., Peshkin, L., Tabin, C.J., Regev, A., Haas, B.J., and Whited, J.L. (2017). A tissue-mapped axolotl de novo transcriptome enables identification of limb regeneration factors. Cell Rep. **18,** 762-776.

Burkhardt, A., and Day, B. (2016). Transcriptome and small rnaome dynamics during a resistant and susceptible interaction between cucumber and downy mildew. Plant Genome **9,** 10.3835/plantgenome2015.3808.0069.

Caffall, K.H., and Mohnen, D. (2009). The structure, function, and biosynthesis of plant cell wall pectic polysaccharides. Carb. Res. **344,** 1879-1900.

Camacho, C., Coulouris, G., Avagyan, V., Ma, N., Papadopoulos, J., Bealer, K., and Madden, T.L. (2009). Blast+: Architecture and applications. BMC Bioinform **10,** 421.

Chang, H.X., Yendrek, C.R., Caetano-Anolles, G., and Hartman, G.L. (2016a). Genomic characterization of plant cell wall degrading enzymes and *in silico* analysis of xylanases and polygalacturonases of *Fusarium virguliforme*. BMC Microbiol. **16,** 147.

Chang, H.X., Domier, L.L., Radwan, O., Yendrek, C.R., Hudson, M.E., and Hartman, G.L. (2016b). Identification of multiple phytotoxins produced by *Fusarium virguliforme* including a phytotoxic effector (FvNIS1) associated with sudden death syndrome foliar symptoms. Mol. Plant-Microbe Interact. **29,** 96-108.

Chen, R., Jiang, N., Jiang, Q., Sun, X., Wang, Y., Zhang, H., and Hu, Z. (2014). Exploring microrna-like small RNAs in the filamentous fungus *Fusarium oxysporum*. PLoS One **9,** e104956.

Chen, Y., Le, X., Sun, Y., Li, M., Zhang, H., Tan, X., Zhang, D., Liu, Y., and Zhang, Z. (2017). Moycp4 is required for growth, conidiogenesis and pathogenicity in magnaporthe oryzae. Mol. Plant Pathol. **18,** 1001-1011.

Chowdhury, S., Basu, A., and Kundu, S. (2017). Biotrophy-necrotrophy switch in pathogen evoke differential response in resistant and susceptible sesame involving multiple signaling pathways at different phases. Sci. Rep. **7,** 17251.

Clements, J., Eddy, S.R., and Finn, R.D. (2011). Hmmer web server: Interactive sequence similarity searching. Nuc. Acids Res. **39,** W29-W37.

Cordovez, V., Mommer, L., Moisan, K., Lucas-Barbosa, D., Pierik, R., Mumm, R., Carrion, V.J., and Raaijmakers, J.M. (2017). Plant phenotypic and transcriptional changes induced by volatiles from the fungal root pathogen *Rhizoctonia solani*. Front. Plant Sci. **8,** 10.3389/fpls.2017.01262.

Dai, X., Zhuang, Z., and Zhao, P.X. (2018). psRNATarget: A plant small RNA target analysis server (2017 release). Nuc Acids Res **46,** W49-W54.

Demers, J.E., Gugino, B.K., and Jiménez-Gasco, M.d.M. (2015). Highly diverse endophytic and soil content genus-species *Fusarium oxysporum* populations associated with field-grown tomato plants. Appl. Environ. Microbiol. **81,** 81-90.

Derbyshire, M., Denton-Giles, M., Hegedus, D., Seifbarghy, S., Rollins, J., van Kan, J., Seidl, M.F., Faino, L., Mbengue, M., Navaud, O., Raffaele, S., Hammond-Kosack, K., Heard, S., and Oliver, R. (2017). The complete genome sequence of the phytopathogenic fungus *Sclerotinia sclerotiorum* reveals insights into the genome architecture of broad host range pathogens. Genom. Biol. Evol. **9,** 593-618.

Derntl, C., Kluger, B., Bueschl, C., Schuhmacher, R., Mach, R.L., and Mach-Aigner, A.R. (2017). Transcription factor XPP1 is a switch between primary and secondary fungal metabolism. Proc Natl Acad Sci U. S. A. **114,** E560-E569.

Elliott, C.E. (2016). 5 control of gene expression in phytopathogenic ascomycetes during early invasion of plant tissue. In Biochem. Mol. Bio., D. Hoffmeister, ed (Cham: Springer International Publishing), pp. 69-94.

Fang, Y.L., Peng, Y.L., and Fan, J. (2017). The NEP1-like protein family of *Magnaporthe oryzae* is dispensable for the infection of rice plants. Sci. Rep. **7,** 4372.

Fox, J., Weisberg, S. (2011). An {r} companion to applied regression. (Thousand Oaks {CA}: Sage).

Friedländer, M.R., Mackowiak, S.D., Li, N., Chen, W., and Rajewsky, N. (2012). Mirdeep2 accurately identifies known and hundreds of novel microrna genes in seven animal clades. Nuc. Acids. Res. **40,** 37-52.

Giovannetti, M., Sbrana, C., Citernesi, A.S., Avio, L., Gollotte, A., Gianinazzi-Pearson, V., and Gianinazzi, S. (1994). Recognition and infection process, basis for host specificity of arbuscular mycorrhizal fungi. In Impact of arbuscular mycorrhizas on sustainable agriculture and natural ecosystems, S. Gianinazzi and H. Schüepp, eds (Basel: Birkhäuser Basel), pp. 61-72.

Gulledge, A.A., Roberts, A.D., Vora, H., Patel, K., and Loraine, A.E. (2012). Mining arabidopsis thaliana rna-seq data with integrated genome browser reveals stress-induced alternative splicing of the putative splicing regulator sr45a. Am. J. Bot. **99,** 219-231.

Gupta, A., and Chattoo, B.B. (2008). Functional analysis of a novel ABC transporter ABC4 from *Magnaporthe grisea*. FEMS Microbiol. Lett. **278,** 22-28.

Gurevich, A., Tesler, G., Vyahhi, N., and Saveliev, V. (2013). Quast: Quality assessment tool for genome assemblies. Bioinform. **29,** 1072-1075.

Haffner, E., Konietzki, S., and Diederichsen, E. (2015). Keeping control: The role of senescence and development in plant pathogenesis and defense. Plants (Basel) **4,** 449-488.

Hartman, G.L., Chang, H.X., and Leandro, L.F. (2015). Research advances and management of soybean sudden death syndrome. Crop Prot. **73,** 60-66.

Haueisen, J., Möller, M., Eschenbrenner, C.J., Grandaubert, J., Seybold, H., Adamiak, H., and Stukenbrock, E.H. (2018). Highly flexible infection programs in a specialized wheat pathogen. Ecol. Evol. **9,** 275-294.

Heitz, T., Widemann, E., Lugan, R., Miesch, L., Ullmann, P., Désaubry, L., Holder, E., Grausem, B., Kandel, S., Miesch, M., Werck-Reichhart, D., and Pinot, F. (2012). Cytochromes P450, CYP94C1, and CYP94B3 catalyze two successive oxidation steps of plant hormone jasmonoyl-isoleucine for catabolic turnover. J. Biol. Chem. **287,** 6296-6306.

Heller, J., and Tudzynski, P. (2011). Reactive oxygen species in phytopathogenic fungi: Signaling, development, and disease. Ann. Rev. Phytopathol. **49,** 369-390.

Holt, K.E., Schultz, M.B., Wick, R.R., and Zobel, J. (2015). Bandage: Interactive visualization of *de novo* genome assemblies. Bioinform. **31,** 3350-3352.

Horbach, R., Navarro-Quesada, A.R., Knogge, W., and Deising, H.B. (2011). When and how to kill a plant cell: Infection strategies of plant pathogenic fungi. J. Plant Physiol. **168,** 51-62.

Hothorn, T., Bretz, F., Westfall P. (2008). Simultaneous inference in general parametric models. Biometrical J. **50,** 346-363.

Jennings, J.C., Apel-Birkhold, P.C., Bailey, B.A., and Anderson, J.D. (2000). Induction of ethylene biosynthesis and necrosis in weed leaves by a *Fusarium oxysporum* protein. Weed Sci. **48,** 7-14.

Jiang, X., Qiao, F., Long, Y., Cong, H., and Sun, H. (2017). Microrna-like rnas in plant pathogenic fungus *Fusarium oxysporum* f. sp. *Niveum* are involved in toxin gene expression fine tuning. 3 Biotech. **7,** 354.

Jones, P., Binns, D., Chang, H.-Y., Fraser, M., Li, W., McAnulla, C., McWilliam, H., Maslen, J., Mitchell, A., Nuka, G., Pesseat, S., Quinn, A.F., Sangrador-Vegas, A., Scheremetjew, M., Yong, S.-Y., Lopez, R., and Hunter, S. (2014). Interproscan 5: Genome-scale protein function classification. Bioinform. (Oxford, England) **30,** 1236-1240.

Kiełbasa, S.M., Wan, R., Sato, K., Horton, P., and Frith, M.C. (2011). Adaptive seeds tame genomic sequence comparison. Gen. Res. **21,** 487-493.

Kim, D., Langmead, B., and Salzberg, S.L. (2015). Hisat: A fast spliced aligner with low memory requirements. Nature Meth. **12,** 357-360.

Kleemann, J., Rincon-Rivera, L.J., Takahara, H., Neumann, U., van Themaat, E.V.L., van der Does, H.C., Hacquard, S., Stüber, K., Will, I., Schmalenbach, W., Schmelzer, E., and O'Connell, R.J. (2012). Sequential delivery of host-induced virulence effectors by appressoria and intracellular hyphae of the phytopathogen *Colletotrichum higginsianum*. PLoS Pathog. **8,** e1002643.

Kobayashi-Leonel, R., Mueller, D., Harbach, C., Tylka, G., and Leandro, L. (2017). Susceptibility of cover crop plants to *Fusarium virguliforme*, causal agent of soybean sudden death syndrome, and *Heterodera glycines*, the soybean cyst nematode. J. Soil Water Conserv. **72,** 575-583.

Koenning, S.R., and Wrather, J.A. (2010). Suppression of soybean yield potential in the continental united states by plant diseases from 2006 to 2009. Plant Health Prog. **11,** 10.1094/php-2010-1122-1001-rs.

Kolander, T.M., Bienapfl, J.E., Kurle, J.E., and Malvick, D.K. (2012). Symptomatic and asymptomatic host range of *Fusarium virguliforme*, the causal agent of soybean sudden death syndrome. Plant Dis. **96,** 1148-1153.

Koren, S., Walenz, B.P., Berlin, K., Miller, J.R., Bergman, N.H., and Phillippy, A.M. (2017). Canu: Scalable and accurate long-read assembly via adaptive k-mer weighting and repeat separation. Genome Res.**,** 10.1101/gr.215087.215116.

Kriventseva, E.V., Zdobnov, E.M., Simão, F.A., Ioannidis, P., and Waterhouse, R.M. (2015). Busco: Assessing genome assembly and annotation completeness with single-copy orthologs. Bioinform. **31,** 3210-3212.

Krogh, A., Larsson, B., von Heijne, G., and Sonnhammer, E.L.L. (2001). Predicting transmembrane protein topology with a hidden Markov model: Application to complete genomes. J. Mol. Biol. **305,** 567-580.

Lade, B.D., Patil, A.S., and Paikrao, H.M. (2014). Efficient genomic DNA extraction protocol from medicinal rich *Passiflora foetida* containing high level of polysaccharide and polyphenol. SpringerPlus **3,** 457-457.

Lagesen, K., Hallin, P., Rødland, E.A., Staerfeldt, H.-H., Rognes, T., and Ussery, D.W. (2007). RNAmmer: Consistent and rapid annotation of ribosomal RNAU*stilago maydis* studied by RNA-seq analysis. Plant Cell **30,** 300-323.

Lee Marzano, S.-Y., Neupane, A., and Domier, L. (2018). Transcriptional and small rna responses of the white mold fungus *Sclerotinia sclerotiorum* to infection by a virulence-attenuating hypovirus. Viruses **10,** 713.

Lofgren, L.A., LeBlanc, N.R., Certano, A.K., Nachtigall, J., LaBine, K.M., Riddle, J., Broz, K., Dong, Y., Bethan, B., Kafer, C.W., and Kistler, H.C. (2018). *Fusarium graminearum*: Pathogen or endophyte of North American grasses? New Phytol. **217,** 1203-1212.

Lorrain, C., Marchal, C., Hacquard, S., Delaruelle, C., Pétrowski, J., Petre, B., Hecker, A., Frey, P., and Duplessis, S. (2018). The rust fungus *Melampsora larici-populina* expresses a conserved genetic program and distinct sets of secreted protein genes during infection of its two host plants, larch and poplar. Mol. Plant-Microbe Interact. **31,** 695-706.

Love, M.I., Huber, W., and Anders, S. (2014). Moderated estimation of fold change and dispersion for rna-seq data with deseq2. Gen. Bio. **15,** 550-550.

Lysøe, E., Bone, K.R., and Klemsdal, S.S. (2008). Identification of up-regulated genes during zearalenone biosynthesis in *Fusarium*. Eur. J. Plant Pathol. **122,** 505-516.

Ma, L.J., van der Does, H.C., Borkovich, K.A., Coleman, J.J., Daboussi, M.J., Di Pietro, A., Dufresne, M., Freitag, M., Grabherr, M., Henrissat, B., Houterman, P.M., Kang, S., Shim, W.B., Woloshuk, C., Xie, X., Xu, J.R., Antoniw, J., Baker, S.E., Bluhm, B.H., Breakspear, A., Brown, D.W., Butchko, R.A., Chapman, S., Coulson, R., Coutinho, P.M., Danchin, E.G., Diener, A., Gale, L.R., Gardiner, D.M., Goff, S., Hammond-Kosack, K.E., Hilburn, K., Hua-Van, A., Jonkers, W., Kazan, K., Kodira, C.D., Koehrsen, M., Kumar, L., Lee, Y.H., Li, L., Manners, J.M., Miranda-Saavedra, D., Mukherjee, M., Park, G., Park, J., Park, S.Y., Proctor, R.H., Regev, A., Ruiz-Roldan, M.C., Sain, D., Sakthikumar, S., Sykes, S., Schwartz, D.C., Turgeon, B.G., Wapinski, I., Yoder, O., Young, S., Zeng, Q., Zhou, S., Galagan, J., Cuomo, C.A., Kistler, H.C., and Rep, M. (2010). Comparative genomics reveals mobile pathogenicity chromosomes in *Fusarium*. Nature **464,** 367-373.

Malcolm, G.M., Kuldau, G.A., Gugino , B.K., and del Mar Jimenez-Gasco, M. (2013). Hidden host plant associations of soilborne fungal pathogens: An ecological perspective. Phytopathol. **103,** 538-544.

Martin, M. (2011). Cutadapt removes adapter sequences from high-throughput sequencing reads. EMBnet J. **17,** 10.14806/ej.14817.14801.14200.

Min, B., Choi, I.-G., and Grigoriev, I.V. (2017). Fungap: Fungal genome annotation pipeline using evidence-based gene model evaluation. Bioinform. **33,** 2936-2937.

Navi, S.S., and Yang, X.B. (2008). Foliar symptom expression in association with early infection and xylem colonization by *Fusarium virguliforme* (formerly *f. Solani* f. Sp. *Glycines*), the causal agent of soybean sudden death syndrome. Plant Heal. Prog. 10.1094/PHP-2008-0222-01-RS.

Ngaki, M.N., Wang, B., Sahu, B.B., Srivastava, S.K., Farooqi, M.S., Kambakam, S., Swaminathan, S., and Bhattacharyya, M.K. (2016). Tanscriptomic study of the soybean-*Fusarium virguliforme* interaction revealed a novel ankyrin-repeat containing defense gene, expression of whose during infection led to enhanced resistance to the fungal pathogen in transgenic soybean plants. PLoS One **11,** e0163106.

O'Connell, R.J., Thon, M.R., Hacquard, S., Amyotte, S.G., Kleemann, J., Torres, M.F., Damm, U., Buiate, E.A., Epstein, L., Alkan, N., Altmüller, J., Alvarado-Balderrama, L., Bauser, C.A., Becker, C., Birren, B.W., Chen, Z., Choi, J., Crouch, J.A., Duvick, J.P., Farman, M.A., Gan, P., Heiman, D., Henrissat, B., Howard, R.J., Kabbage, M., Koch, C., Kracher, B., Kubo, Y., Law, A.D., Lebrun, M.-H., Lee, Y.-H., Miyara, I., Moore, N., Neumann, U., Nordström, K., Panaccione, D.G., Panstruga, R., Place, M., Proctor, R.H., Prusky, D., Rech, G., Reinhardt, R., Rollins, J.A., Rounsley, S., Schardl, C.L., Schwartz, D.C., Shenoy, N., Shirasu, K., Sikhakolli, U.R., Stüber, K., Sukno, S.A., Sweigard, J.A., Takano, Y., Takahara, H., Trail, F., van der Does, H.C., Voll, L.M., Will, I., Young, S., Zeng, Q., Zhang, J., Zhou, S., Dickman, M.B., Schulze-Lefert, P., Ver Loren van Themaat, E., Ma, L.-J., and Vaillancourt, L.J. (2012). Lifestyle transitions in plant pathogenic *Colletotrichum* fungi deciphered by genome and transcriptome analyses. Nature Genet. **44,** 1060.

Oliver, R.P., and Ipcho, S.V.S. (2004). Arabidopsis pathology breathes new life into the necrotrophs-vs.-biotrophs classification of fungal pathogens. Mol. Plant Pathol. **5,** 347-352.

Petersen, T.N., Brunak, S., von Heijne, G., and Nielsen, H. (2011). Signalp 4.0: Discriminating signal peptides from transmembrane regions. Nature Meth. **8,** 785.

R Development Core Team. (2010). R: A language and environment for statistical computing. In Vienna, Austria: R Foundation for Statistical Computing.

Rai, M., and Agarkar, G. (2016). Plant-fungal interactions: What triggers the fungi to switch among lifestyles? Crit. Rev. Microbiol. **42,** 428-438.

Romano, N., and Macino, G. (1992). Quelling: Transient inactivation of gene expression in *neurospora crassa* by transformation with homologous sequences. Mol. Microbiol. **6,** 3343-3353.

Sahu, B.B., Baumbach, J.L., Singh, P., Srivastava, S.K., Yi, X., and Bhattacharyya, M.K. (2017). Investigation of the *Fusarium virguliforme* transcriptomes induced during infection of soybean roots suggests that enzymes with hydrolytic activities could play a major role in root necrosis. PloS ONE **12,** e0169963-e0169963.

Sang, H., Chang, H.-X., and Chilvers, M.I. (2019). A *Sclerotinia sclerotiorum* transcription factor involved in sclerotial development and virulence on pea. mSphere **4,** e00615-00618.

Savory, E.A., Adhikari, B.N., Hamilton, J.P., Vaillancourt, B., Buell, C.R., and Day, B. (2012). Mrna-seq analysis of the *Pseudoperonospora cubensis* transcriptome during cucumber (*Cucumis sativus* l.) infection. PLoS ONE **7,** e35796.

Schrettl, M., Bignell, E., Kragl, C., Sabiha, Y., Loss, O., Eisendle, M., Wallner, A., Arst, H.N., Jr., Haynes, K., and Haas, H. (2007). Distinct roles for intra- and extracellular siderophores during *Aspergillus fumigatu*s infection. PLoS Pathog. **3,** e128.

Seidl, M.F., Faino, L., Shi-Kunne, X., van den Berg, G.C.M., Bolton, M.D., and Thomma, B.P.H.J. (2014). The genome of the saprophytic fungus *Verticillium tricorpus* reveals a complex effector repertoire resembling that of its pathogenic relatives. Mol. Plant-Microbe Interact. **28,** 362-373.

Selosse, M.-A., Schneider-Maunoury, L., and Martos, F. (2018). Time to re-think fungal ecology? Fungal ecological niches are often prejudged. New Phytol. **217,** 968-972.

Shao, Y., Tang, J., Chen, S., Wu, Y., Wang, K., Ma, B., Zhou, Q., Chen, A., and Wang, Y. (2019). Milr4 and milr16 mediated fruiting body development in the medicinal fungus *Cordyceps militaris*. Front. Microbiol. **10,** 10.3389/fmicb.2019.00083.

Shaw, M.W., Emmanuel, C.J., Emilda, D., Terhem, R.B., Shafia, A., Tsamaidi, D., Emblow, M., and van Kan, J.A.L. (2016). Analysis of cryptic, systemic *Botrytis* infections in symptomless hosts. Front. Plant Sci. **7,** 625-625.

Soanes, D.M., Chakrabarti, A., Paszkiewicz, K.H., Dawe, A.L., and Talbot, N.J. (2012). Genome-wide transcriptional profiling of appressorium development by the rice blast fungus *Magnaporthe oryzae*. PLoS Pathog. **8,** e1002514.

Sperschneider, J., Gardiner, D.M., Dodds, P.N., Tini, F., Covarelli, L., Singh, K.B., Manners, J.M., and Taylor, J.M. (2016). Effectorp: Predicting fungal effector proteins from secretomes using machine learning. New Phytol. **210,** 743-761.

Srivastava, S.K., Huang, X., Brar, H.K., Fakhoury, A.M., Bluhm, B.H., and Bhattacharyya, M.K. (2014). The genome sequence of the fungal pathogen *Fusarium virguliforme* that causes sudden death syndrome in soybean. PLoS One **9,** e81832.

Takahashi, H.K., Toledo, M.S., Suzuki, E., Tagliari, L., and Straus, A.H. (2009). Current relevance of fungal and trypanosomatid glycolipids and sphingolipids: Studies defining structures conspicuously absent in mammals. Anais da Academia Brasileira de Ciências **81,** 477-488.

Trapnell, C., Williams, B.A., Pertea, G., Mortazavi, A., Kwan, G., van Baren, M.J., Salzberg, S.L., Wold, B.J., and Pachter, L. (2010). Transcript assembly and quantification by rna-seq reveals unannotated transcripts and isoform switching during cell differentiation. Nature Biotech. **28,** 511.

Veloso, J., and van Kan, J.A.L. (2018). Many shades of grey in *Botrytis* host plant interactions. Trends Plant Sci. **23,** 613-622.

Vollmeister, E., Schipper, K., Baumann, S., Haag, C., Pohlmann, T., Stock, J., and Feldbrügge, M. (2012). Fungal development of the plant pathogen *Ustilago maydis*. FEMS Microbiol. Rev. **36,** 59-77.

Walker, B.J., Abeel, T., Shea, T., Priest, M., Abouelliel, A., Sakthikumar, S., Cuomo, C.A., Zeng, Q., Wortman, J., Young, S.K., and Earl, A.M. (2014). Pilon: An integrated tool for comprehensive microbial variant detection and genome assembly improvement. PLoS ONE **9,** e112963.

Wang, J., Jacobs, J.L., Byrne, J.M., and Chilvers, M.I. (2015). Improved diagnoses and quantification of *Fusarium virguliforme*, causal agent of soybean sudden death syndrome. Phytopathol. **105,** 378-387.

Wang, Y., Tang, H., DeBarry, J.D., Tan, X., Li, J., Wang, X., Lee, T.-h., Jin, H., Marler, B., Guo, H., Kissinger, J.C., and Paterson, A.H. (2012). Mcscanx: A toolkit for detection and evolutionary analysis of gene synteny and collinearity. Nuc. Acids Res. **40,** e49-e49.

Weiberg, A., Wang, M., Lin, F.M., Zhao, H., Zhang, Z., Kaloshian, I., Huang, H.D., and Jin, H. (2013). Fungal small RNAs suppress plant immunity by hijacking host RNA interference pathways. Science **342,** 118-123.

Wickham, H. (2016). Ggplot2: Elegant graphics for data analysis. (Springer-Verlag New York).

Yang, F., Li, W., and Jørgensen, H.J.L. (2013). Transcriptional reprogramming of wheat and the hemibiotrophic pathogen septoria tritici during two phases of the compatible interaction. PLoS ONE **8,** e81606.

Yang, L., Xie, L., Xue, B., Goodwin, P.H., Quan, X., Zheng, C., Liu, T., Lei, Z., Yang, X., Chao, Y., and Wu, C. (2015). Comparative transcriptome profiling of the early infection of wheat roots by *Gaeumannomyces graminis* var. *Tritici*. PLoS One **10,** e0120691.

Yin, Y., Mao, X., Yang, J., Chen, X., Mao, F., and Xu, Y. (2012). Dbcan: A web resource for automated carbohydrate-active enzyme annotation. Nuc. Acids Res. **40,** W445-W451.

Young, M.D., Wakefield, M.J., Smyth, G.K., and Oshlack, A. (2010). Gene ontology analysis for rna-seq: Accounting for selection bias. Genome Biol. **11,** R14-R14.

Zhang, Y., Tian, L., Yan, D.-H., and He, W. (2018). Genome-wide transcriptome analysis reveals the comprehensive response of two susceptible poplar sections to *Marssonina brunnea* infection. Genes **9,** 154.

Zhao, Z., Liu, H., Wang, C., and Xu, J.-R. (2013). Comparative analysis of fungal genomes reveals different plant cell wall degrading capacity in fungi. BMC Genom. **14,** 274.

Zhou, J., Fu, Y., Xie, J., Li, B., Jiang, D., Li, G., and Cheng, J. (2012). Identification of microrna-like rnas in a plant pathogenic fungus *Sclerotinia sclerotiorum* by high-throughput sequencing. Mol. Genet. Genom. **287,** 275-282.